

For Reference

NOT TO BE TAKEN FROM THIS ROOM

Ex LIBRIS
UNIVERSITATIS
ALBERTAENSIS





Digitized by the Internet Archive
in 2021 with funding from
University of Alberta Libraries

<https://archive.org/details/Fuhr1974>

T H E U N I V E R S I T Y O F A L B E R T A

RELEASE FORM

NAME OF AUTHOR: BRYAN JOHN FUHR

TITLE OF THESIS: NUCLEAR MAGNETIC RESONANCE STUDIES
 OF THE SOLUTION CHEMISTRY OF METAL
 COMPLEXES

DEGREE FOR WHICH THESIS WAS PRESENTED: DOCTOR OF
 PHILOSOPHY

YEAR THIS DEGREE GRANTED: 1974

Permission is hereby granted to THE UNIVERSITY OF ALBERTA LIBRARY to reproduce single copies of this thesis and to lend or sell such copies for private, scholarly or scientific research purposes only.

The author reserves other publication rights, and neither the thesis nor extensive abstracts from it may be printed or otherwise reproduced without the author's written permission.

4

(Signed) _____

Department of Medical Cell Biology
University of Alberta
Edmonton, Alberta T6G 2G4

DATED _____, 1974

THE UNIVERSITY OF ALBERTA

NUCLEAR MAGNETIC RESONANCE STUDIES OF
THE SOLUTION CHEMISTRY OF METAL COMPLEXES

BY

 BRYAN JOHN FUHR

A THESIS

SUBMITTED TO THE FACULTY OF GRADUATE STUDIES
AND RESEARCH IN PARTIAL FULFILMENT OF
THE REQUIREMENTS FOR THE DEGREE OF
DOCTOR OF PHILOSOPHY

DEPARTMENT OF CHEMISTRY

EDMONTON, ALBERTA

SPRING, 1974

THE UNIVERSITY OF ALBERTA
FACULTY OF GRADUATE STUDIES AND RESEARCH

The undersigned certify that they have read,
and recommend to the Faculty of Graduate Studies
and Research, for acceptance, a thesis entitled
NUCLEAR MAGNETIC RESONANCE STUDIES OF THE SOLUTION
CHEMISTRY OF METAL COMPLEXES
submitted by BRYAN JOHN FUHR
in partial fulfilment of the requirements for the
degree of DOCTOR OF PHILOSOPHY.

Part I

Proton magnetic resonance (PMR) methods have been used to determine the average structure of the nonequivalent acetate methylene protons before and after the change in the cadmium and zinc complexes of 1,4-propylenediaminetetracarboxylic acid (1,4-PDTA) and 1,4-butylenediaminetetracarboxylic acid (1,4-BDTA). Nonequivalence is indicated by the appearance of two signals in the PMR spectra of these complexes, which were determined over a range of temperatures. The extent of splitting of the signals in the experimental spectra with temperature was calculated as a function of the average lifetimes before and after the interchange. The lifetimes are a measure of the rates of partial dissociation of these complexes. The splitting patterns in the PMR spectra of the cadmium and zinc and lead complexes of ethylenediamine-N,N'-diacetic acid (EDDA) were also investigated as a function of temperature.

TO MY WIFE, ARLENE

ABSTRACT

Part I

Proton magnetic resonance (pmr) methods have been used to determine the average lifetimes of the nonequivalent acetate methylenic protons before interchange in the cadmium and zinc complexes of 1,3-propylenediaminetetraacetic acid (1,3-PDTA) and of 1,4-butylenediaminetetraacetic acid (1,4-BDTA). Nonequivalence is indicated by AB multiplet patterns in the pmr spectra of these complexes. The lifetimes were determined over a range of temperatures from the extent of collapse of the AB patterns by matching experimental spectra with theoretical spectra which were calculated as a function of the average lifetime before AB interchange. It is proposed that these lifetimes are a measure of the rates of partial dissociation of these complexes. The AB multiplet patterns in the pmr spectra of the cadmium, zinc and lead complexes of ethylenediamine-N-N'-diacetic-N-N'-dipropionic acid (EDDDA) were also investigated as a function of temperature.

The kinetics of the ligand exchange reactions of the cadmium, zinc, and lead complexes of 1,3-PDTA and EDDDA have been studied using pmr line-broadening

methods. Rate constants were obtained for the proton-assisted dissociation of each of these complexes and for the displacement of complexed ligand by free ligand for several of the complexes. The rates of first order dissociation of all the complexes are too slow to measure by the pmr technique. Rate constants for the reaction of cadmium and zinc with monoprotonated 1,3-PDTA are approximately equal to those of the analogous reactions with monoprotonated ethylenediaminetetraacetic acid, while the rate constants for reaction of cadmium, zinc and lead with monoprotonated EDDDA are from 2.5 to 10 times slower than the rate constants for reaction with monoprotonated 1,3-PDTA. Mechanisms are proposed for the formation reactions of the monoprotonated ligands.

Part II

The binding of zinc, cadmium, lead and mercury by the tripeptide glutathione has been investigated by ^{13}C magnetic resonance spectroscopy. Binding to the potential coordination sites was monitored as a function of solution conditions by observing the chemical shifts of the carbon atoms of glutathione. The results indicate that each of these metal ions

binds to the potential coordination sites of glutathione with a high degree of specificity. Mercury binds only to the sulfhydryl group at mercury to glutathione ratios up to 0.5 and over the entire accessible pD range. At a metal to glutathione ratio of 0.5, zinc and cadmium bind to both the sulfhydryl and amino groups, the extent of binding to the two different sites being a function of pD, while lead binds only to the sulfhydryl group. Some binding of the carboxylic acid groups to zinc, cadmium and lead was detected in certain pD regions. The chemical shift data also suggest that zinc-promoted ionization of the peptide protons with subsequent binding of zinc to the ionized peptide nitrogen takes place above pD 10.5. The results are discussed in terms of the possible structures of the complexes.

ACKNOWLEDGEMENTS

I should like to thank Dr. D. L. Rabenstein for his guidance and encouragement during the course of my research.

I am also grateful to my colleagues, especially Mary Fairhurst, for their helpful discussions, and to Arlene for her moral support.

Financial support from the National Research Council and the University of Alberta is gratefully acknowledged.

TABLE OF CONTENTS

CHAPTER		PAGE
	LIST OF TABLES	xii
	LIST OF FIGURES	xiv

Part I

KINETICS OF METAL COMPLEXES OF AMINO- CARBOXYLIC ACIDS

I.	INTRODUCTION	2
	A. DISSOCIATION KINETICS	2
	B. FORMATION KINETICS	10
II.	PARTIAL DISSOCIATION KINETICS OF METAL COMPLEXES OF AMINOCARBOXYLIC ACIDS	18
	A. RESULTS	18
	Analysis of AB Multiplet Patterns	18
	AB Interchange Rates for the 1,3- PDTA and 1,4-BDTA Complexes	27
	Temperature Dependence of the AB Multiplet Patterns for the EDDDA Complexes	39
	Pmr Spectra of the EDTA Complexes	40
	B. DISCUSSION	41
	Partial Dissociation Kinetics of the Complexes of 1,3-PDTA and 1,4-BDTA	41
	Temperature Dependence of the AB Multiplet Patterns of the EDDDA Complexes	49

CHAPTER	PAGE
III. LIGAND EXCHANGE KINETICS OF METAL	
COMPLEXES OF 1,3-PDTA AND EDDDA	54
A. RESULTS	54
pH Dependence of the Chemical Shifts	54
Ligand Exchange Kinetics of the 1,3-PDTA Complexes	62
Ligand Exchange Kinetics of the EDDDA Complexes	83
B. DISCUSSION	88
Mechanism of Formation of the $M(1,3-PDTA)^{2-}$ and $M(EDDDA)^{2-}$ Complexes ...	88
Second Order Ligand Displacement Reactions	96
IV. EXPERIMENTAL	98
A. CHEMICALS	98
B. SOLUTIONS	98
C. pH MEASUREMENTS	99
D. PMR MEASUREMENTS	100
E. KINETIC APPLICATIONS OF NUCLEAR MAGNETIC RESONANCE	101
BIBLIOGRAPHY	106

Part II

THE BINDING OF METAL IONS BY GLUTATHIONE

V. INTRODUCTION	112
VI. THE BINDING OF ZINC, CADMIUM, LEAD AND MERCURY BY GLUTATHIONE	116

CHAPTER	PAGE
A. RESULTS	118
Glutathione	118
Zinc-Glutathione	120
Cadmium-Glutathione	127
Lead-glutathione	133
Mercury-glutathione	135
B. DISCUSSION	135
Zinc and Cadmium Binding to the Sulfhydryl and Glutamyl Groups	138
Ionization of the Peptide Protons	145
Mercury and Lead Binding to the Sulfhydryl Group	146
Chemical Shift Differences	148
Conclusions	152
VII. EXPERIMENTAL	153
A. CHEMICALS AND SOLUTIONS	153
B. POTENTIOMETRIC AND CMR MEASUREMENTS ..	154
BIBLIOGRAPHY	155

LIST OF TABLES

Table		Page
I	Pmr Spectral Parameters for the Acetate Methylenic Protons of the Indicated Metal Complexes	21
II	Average Lifetimes of the Acetate Methylenic Protons of Cd(1,3-PDTA) ²⁻ and Cd(1,4-BDTA) ²⁻ Before AB Interchange	32
III	Comparison of Average Lifetimes of the Acetate Methylenic Protons of Cd(1,3-PDTA) ²⁻ Before AB Interchange Determined from 60 MHz and 100 MHz Spectra	34
IV	Average Lifetimes of the Acetate Methylenic Protons of Zn(1,3-PDTA) ²⁻ and Zn(1,4-BDTA) ²⁻ Before AB Interchange	36
V	Acid Ionization Constants of 1,3-PDTA and EDDDA	57
VI	Kinetic Data for the Cd-1,3-PDTA System at Constant pH Values as a Function of Free Ligand Concentration	67
VII	Experimentally Determined Ligand Exchange Rate Constants for 1,3-PDTA and EDDDA Complexes	72
VIII	Kinetic Data as a Function of pH for the Cd-1,3-PDTA System	73
IX	Kinetic Data as a Function of pH for the Zn-1,3-PDTA System	77
X	Kinetic Data for the Pb-1,3-PDTA System at Constant pH Values as a Function of Free Ligand Concentration	81
XI	Kinetic Data as a Function of pH for the Pb-1,3-PDTA System	82

Table		Page
XII	Kinetic Data for the Cd-EDDDA System at Constant pH Values as a Function of Free Ligand Concentration	84
XIII	Kinetic Data as a Function of pH for the Cd-EDDDA System	86
XIV	Kinetic Data for the Pb-EDDDA System at Constant pH Values as a Function of Free Ligand Concentration	87
XV	Kinetic Data as a Function of pH for the Pb-EDDDA System	89
XVI	Kinetic Data as a Function of pH for the Zn-EDDDA System	90
XVII	Fraction of Glutamyl Groups of Glutathione Complexed by Zn^{2+} and Cd^{2+} as a Function of pD	141
XVIII	^{13}C Chemical Shift Changes for Selected Carbon Resonances of Glutathione upon Complexation	149

LIST OF FIGURES

Figure	Page
1. Proposed stepwise reaction mechanism for the formation of ML^{2-} complexes from M^{2+} and HL^{3-} .	15
2. Representative experimental (left) and theoretical (right) 60 MHz pmr spectra of the acetate methylenic protons of an aqueous solution of $Zn(1,3-PDTA)^{2-}$.	19
3. The 100 MHz pmr spectrum of the acetate methylenic protons of a D_2O solution of $Cd(1,3-PDTA)^{2-}$.	22
4. 220 MHz spectra of the acetate methylenic protons of an aqueous solution of $Cd(1,4-BDTA)^{2-}$ at the indicated temperatures.	25
5. 220 MHz pmr spectra of the acetate methylenic protons of an aqueous solution of $Cd(EDDDA)^{2-}$ at the indicated temperatures.	26
6. Representative experimental (left) and theoretical (right) 60 MHz spectra of the acetate methylenic protons of an aqueous solution of $Cd(1,3-PDTA)^{2-}$.	28
7. 60 MHz pmr spectra of the acetate methylenic protons of an aqueous solution of $Zn(1,4-BDTA)^{2-}$ at the indicated temperatures.	38
8. Possible stepwise reactions that can lead to the A to B interchange observed by the pmr method for the acetate methylenic protons in complexes of EDTA and its homologs.	44
9. pH dependence of the chemical shift of the acetate methylenic protons of 1,3-PDTA.	56

Table		Page
10.	pH dependence of the chemical shift of the acetate methylenic protons of EDDDA.	59
11.	60 MHz pmr spectra showing the acetate methylenic resonances for an aqueous solution containing both free 1,3-PDTA and $\text{Cd}(1,3\text{-PDTA})^{2-}$ at the indicated pH values.	66
12.	Pmr rate data for the Cd-1,3-PDTA system at pH 6.51 as a function of the free 1,3-PDTA concentration.	70
13.	Pmr rate data for the Cd-1,3-PDTA system as a function of $[\text{H}^+]$.	76
14.	Representative experimental (left) and theoretical (right) 60 MHz pmr spectra of the acetate methylenic protons of an aqueous solution of $\text{Pb}(1,3\text{-PDTA})^{2-}$ containing the indicated concentrations of free 1,3-PDTA at pH 7.00.	79
15.	^{13}C magnetic resonance spectra of glutathione.	119
16.	pD dependence of the chemical shifts of the cysteinyl carbons for a D_2O solution containing 0.30 <u>M</u> glutathione and 0.15 <u>M</u> $\text{Zn}(\text{NO}_3)_2$.	121
17.	pD dependence of the chemical shifts of selected glutamyl and glycyl carbons for a D_2O solution containing 0.30 <u>M</u> glutathione and 0.15 <u>M</u> $\text{Zn}(\text{NO}_3)_2$.	123
18.	The chemical shifts of selected carbons as a function of the zinc to glutathione ratio for an aqueous solution at pH 5.51.	126
19.	pD dependence of the chemical shifts of the cysteinyl carbons for a D_2O solution containing 0.30 <u>M</u> glutathione and 0.15 <u>M</u> $\text{Cd}(\text{NO}_3)_2$.	128

Figure		Page
20.	pD dependence of the chemical shifts of selected glutamyl and glycyl carbons for a D ₂ O solution containing 0.30 M glutathione and 0.15 M Cd(NO ₃) ₂ .	129
21.	The chemical shifts of selected carbons as a function of the cadmium to glutathione ratio for an aqueous solution at pH 6.59.	132
22.	pD dependence of the chemical shifts of selected carbons for a D ₂ O solution containing 0.30 M glutathione and 0.15 M Pb(NO ₃) ₂ .	134
23.	pD dependence of the chemical shifts of the cysteinyl carbons for a D ₂ O solution containing 0.30 M glutathione and 0.15 M Hg(NO ₃) ₂ .	136
24.	The chemical shifts of selected carbons as a function of the mercury to glutathione ratio for an aqueous solution at pH 5.01.	137

INTRODUCTION

A. OBSERVATION

Formation and reaction of multidentate ligands is one of the most important fields in which one of the problems of the reaction is the order of the reaction. For example, (2) found that the reaction of the ligand with the metal ion is consistent with a

of the individual rate constants

workers (3), on

PART I

formation of some

A reaction KINETICS OF METAL COMPLEXES OF

individual AMINOCARBOXYLIC ACIDS

formation of the first complex

rate-determining step. The

workers have also determined the equilibrium constants from their

equilibrium constants from their

mechanisms have also been proposed for reactions involving the exchange of a multidentate ligand between two different metal ions or

between two multidentate ligands (4). For

is obtained from

CHAPTER I

INTRODUCTION

A. DISSOCIATION KINETICS

Formation and dissociation reactions involving multidentate ligands proceed via stepwise mechanisms in which one of the steps governs the overall rate of the reaction (1). For example, Ahmed and Wilkins (2) found that the kinetic results for the dissociation of the nickel complex of ethylenediamine were consistent with a mechanism involving stepwise rupture of the individual dentate bonds. Margerum and co-workers (3), on the basis of kinetic data for the formation of some nickel-polyamine complexes, proposed a mechanism involving the stepwise formation of the individual coordinate bonds and concluded that the formation of the first nickel-nitrogen bond was the rate-determining step. It was possible for these workers to estimate the values for the stepwise equilibrium constants from their kinetic data.

Stepwise mechanisms have also been proposed for reactions involving the exchange of a multidentate ligand between two different metal ions and of a metal ion between two multidentate ligands (4). For instance, such mechanisms have been inferred from

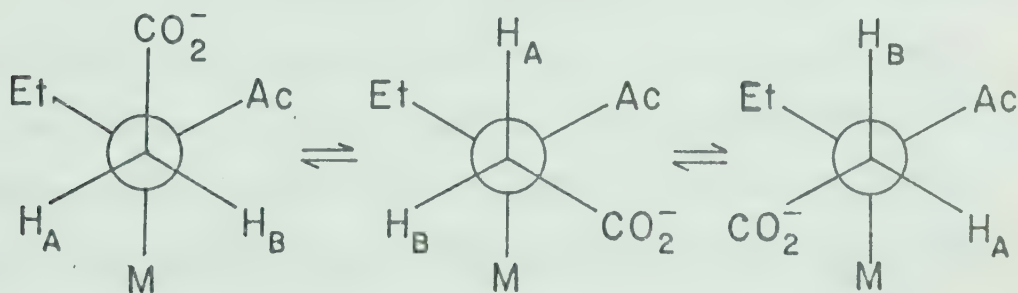
kinetic data for the reactions of zinc and copper with the nickel complex of ethylenediaminetetraacetic acid (EDTA) and analogs of EDTA (5,6,12,19) and for the reactions of EDTA with several nickel-polyamine complexes (7,8). In particular, the proposed mechanism for the reaction of copper with the nickel complex of EDTA (6) involves the unwrapping of an iminodiacetate fragment from the complex, followed by reaction with copper to give a dinuclear intermediate. For this case, the kinetic data yielded a rate constant for the half-unwrapping of EDTA from nickel.

The preceding work, in which such techniques as isotopic labelling, spectrophotometry and temperature jump relaxation were used, has shown that exchange reactions involving metal complexes of multidentate ligands take place in a stepwise fashion. However, it has only been possible in a few cases, such as in the work of Margerum and coworkers (6), to measure the rate constants for the individual steps.

Proton magnetic resonance (pmr) studies of metal complexes of EDTA (9-11,13-17) and analogs of EDTA (10,13,15-18,20-23) have shown that the complexity of the pmr spectrum of complexes of this type depends on the lability of the individual metal-ligand bonds. Hence pmr may provide a way to study

the kinetics of individual metal-ligand bonds. EDTA contains both oxygen and nitrogen donor groups and, depending on the lability of the various metal-ligand bonds, several situations may arise. The first is the one in which both the metal-oxygen and metal-nitrogen bonds are labile on the pmr time scale. In this case, because of rapid nitrogen inversion, the acetate methylenic protons are all equivalent, and the pmr spectrum for these protons consists of a single resonance peak. An example of a complex giving rise to this type of spectrum is $\text{Sr}(\text{EDTA})^{2-}$ (39).

The second case, in which the metal-oxygen bonds are labile but the metal-nitrogen bonds are inert on the pmr time scale, may be illustrated by the following rotational conformers.



The acetate group is free to rotate about the nitrogen-acetate methylenic carbon bond. Examination reveals that, regardless of the rate of rotation, leading to interchange of the above three conformations, H_A and H_B do

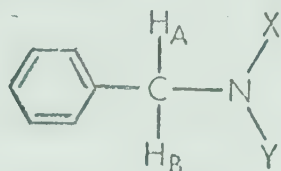
not necessarily experience equivalent environments because of the asymmetry of the quaternary nitrogen atom. Hence H_A and H_B may have different chemical shifts and if so, their pmr spectrum will consist of a single AB pattern. Interchange of H_A and H_B can occur only by inversion of the nitrogen atom, which presumably is possible only when the nitrogen atom is not metal coordinated. As long as the rate of interchange of H_A and H_B is less than the chemical shift difference $\Delta\delta_{AB}$ (in sec^{-1}) between H_A and H_B , an AB pattern will be observed. In other words, metal-nitrogen bonding is inert on the pmr time scale. The pmr spectrum of the acetate methylenic protons of $\text{Cd}(\text{EDTA})^{2-}$ consists of a single AB pattern such as that described above (24).

For the situation in which both the metal-oxygen and metal-nitrogen bonding is inert on the pmr time scale, rather complex spectra are expected because the acetate groups are no longer equivalent. In the case of an octahedral complex in which all the ligand atoms are bound, two of the acetate groups are in the plane formed by the metal and the two nitrogen atoms and two are out of the plane. Therefore the acetate groups may be expected to exhibit two different AB patterns in their pmr spectra. The inert bonding

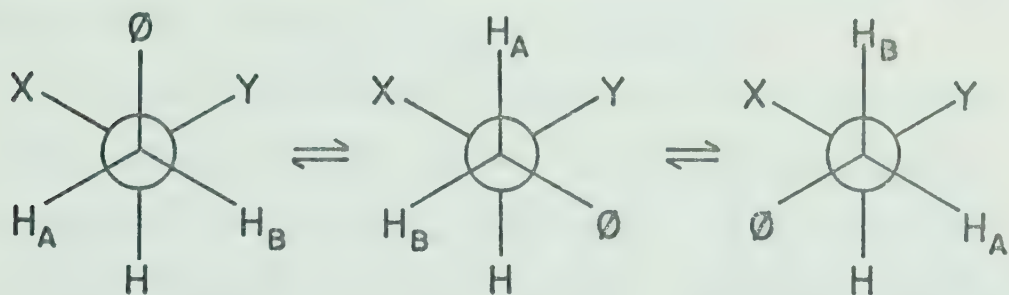
in Co(EDTA)^{2-} results in two different AB patterns in the pmr spectrum for the acetate methylenic protons of this complex (9).

Sudmeier and Reilley (24) obtained evidence for a stepwise mechanism for the reaction of EDTA with Cd(EDTA)^{2-} by monitoring the degree of collapse of the AB pattern in the pmr spectrum of the complex under changing solution conditions. In particular they studied the relative effectiveness of ligands which simulate fragments of EDTA in causing AB interchange. At some point in the overall displacement reaction, the first nitrogen of the complexed EDTA ligand is displaced. Dissociation of this metal-nitrogen bond was studied from the collapse of the AB pattern. It was found that ligands most effective in causing AB interchange contain at least three coordinating groups, a nitrogen and two carboxylate groups. On this basis, it was postulated that formation of the third bond is most effective in breaking the metal-nitrogen bond of the original complex. A stepwise mechanism was proposed with the rate-determining step being the breaking of the first metal-nitrogen bond of the originally complexed ligand and displacement by a carboxylate group of the incoming ligand.

Information about the kinetics of dissociation of the proton from the nitrogen in acidic solutions of tertiary amines of the structure



has been obtained from collapse of the AB pattern for the methylenic protons (25-28). When the nitrogen in these types of amines is protonated, it cannot undergo inversion. In this case, the following three rotational conformers are important, assuming rotation about the carbon-nitrogen bond.



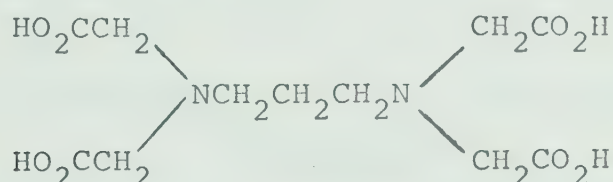
As in the case of the EDTA type complexes, when the rate of nitrogen inversion is slow on the pmr time scale, H_A and H_B will not necessarily experience equivalent environments regardless of the rate of interconversion of the above three conformers. Hence the pmr spectrum for the methylenic protons will

consist of an AB pattern. As the inversion rate is increased by increasing the pH of the solution, thus reducing the fraction of protonated amine in solution, the rate of interchange of H_A and H_B is increased resulting in a collapse of the AB pattern to a single peak. The rate of this AB interchange was determined for a series of tertiary amines by lineshape analysis of the pmr spectra (27). It was shown that if the rate of nitrogen inversion is very much less than the rate of reprotonation of a deprotonated amine, the observed AB interchange rate will be some fraction of the rate of nitrogen inversion. However, if the rate of inversion is very much greater than the rate of reprotonation, the observed AB interchange rate will be one-half the rate of proton exchange.

The work of Sudmeier and Reilley (24) and that on the tertiary amines (27,28) indicates that from a lineshape analysis of AB patterns it may be possible to obtain detailed information about the dissociation kinetics of complexes of multidentate ligands. By analogy with the work on tertiary amines, collapse of the AB pattern by inversion of a nitrogen atom in a complexed aminocarboxylic acid ligand may be governed by the rate of metal-nitrogen bond dissociation and/or the rate of inversion of the noncoordinated nitrogen

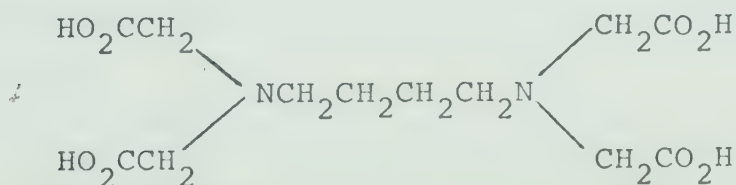
atom. If dissociation of the metal-nitrogen bond governs the rate of collapse, the presence of an AB pattern is an indication of inert metal-nitrogen bonding and potentially can provide information about the partial dissociation kinetics of the complex.

In Chapter II, the results of a pmr temperature study of the AB multiplet patterns arising from the acetate methylenic protons of the cadmium and zinc complexes of 1,3-propylenediaminetetraacetic acid (1,3-PDTA),



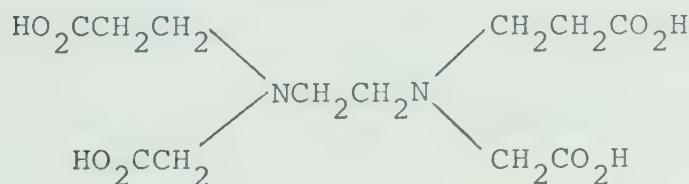
1,3-PDTA

and of 1,4-butylenediaminetetraacetic acid (1,4-BDTA) are presented and discussed (29,30). These particular



1,4-BDTA

ligands were chosen since they are structurally similar to EDTA whose cadmium complex, as noted above (24), exhibits an AB pattern in its pmr spectrum. It was thought that the different sizes of the nitrogen-metal-nitrogen chelate rings in the metal complexes of 1,3-PDTA and 1,4-BDTA might affect the lability of the metal-nitrogen bonds. The mutliplet patterns for the acetate methylenic protons of the cadmium, zinc and lead complexes of ethylenediamine-N,N'-diacetic-N,N'-dipropionic acid (EDDDA) were also studied as a function of temperature.



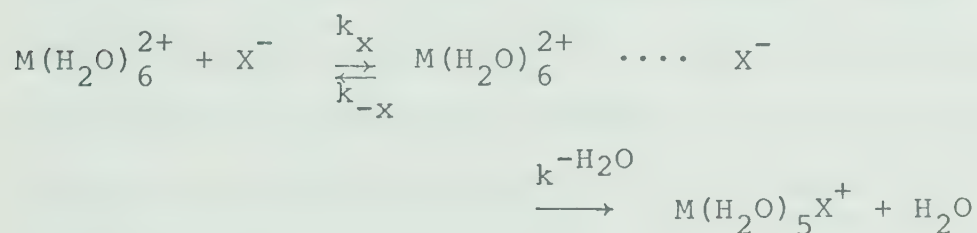
EDDDA

The main objective of this work was to determine what kinetic information can be obtained from the multiplet patterns of the methylenic protons in complexes of this type.

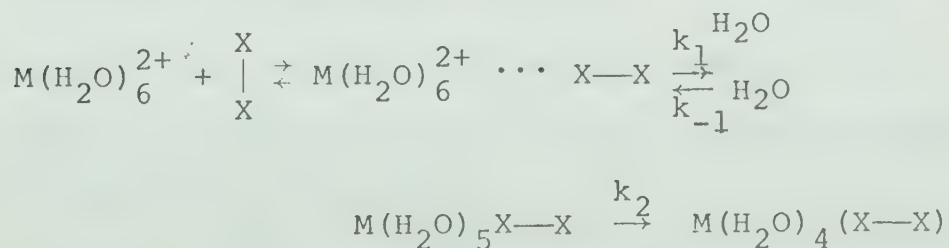
B. FORMATION KINETICS

According to the dissociative mechanism for the

reaction of an aquated metal ion with a ligand to form a metal complex (31-33,70), the metal ion and the ligand first diffuse together to form an outer-sphere complex. A water molecule then dissociates from the aquated metal ion and a donor group of the ligand coordinates with the metal ion at the vacated site. When steric and electrostatic effects are negligible, the rate-determining step in this reaction mechanism is water loss from the aquated metal ion. For a monodentate ligand this mechanism may be depicted as



For a multidentate ligand, this reaction scheme has to be modified to account for the stepwise nature of complex formation with multidentate ligands (2,7,8). This is illustrated by the reaction scheme for a bidentate ligand.



As in the case of a monodentate ligand, the bidentate ligand forms an outer-sphere complex with the metal ion, followed by water loss from the metal ion and formation of the first metal-ligand bond. A second water molecule then dissociates from the metal ion in a position cis to the first metal-ligand bond, and the second metal-ligand bond forms. The rate of this second bond formation process is represented by k_2 in the above reaction sequence. Depending upon the relative magnitudes of $k_{-1}^{\text{H}_2\text{O}}$ and k_2 , the formation of the first or second bond to the bidentate ligand determines the overall rate of complex formation. For multidentate ligands such as EDTA, the reaction sequence for complex formation would include steps for each successive bond formation.

It has been found for the majority of complex formation reactions involving multidentate ligands, that the formation of the first metal-ligand bond is rate-determining (70), its rate being governed by the rate of water dissociation from the aquated metal ion in the outer-sphere complex. For example, the rate of complexation of divalent cadmium, zinc, cobalt, copper and nickel by the monoprotonated form of EDTA (15,24,34,36-38).

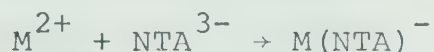


are all approximately equal to those predicted by the dissociative mechanism.

Other studies have shown, however, that the rates of complexation of calcium and strontium by the tetraanion of EDTA are factors of 2.5×10^2 and



1.6×10^3 greater than their rates of complexation by $HEDTA^{3-}$ (39,40). Similarly, the rates of complexation of nickel (41) and cadmium (42,44) by the trianion of nitrilotriacetic acid (NTA) are 7×10^4 times



greater than their rates with $HNTA^{2-}$, while the rates of reaction of zinc (44) and lead (43) with $HNTA^{2-}$ are three to four orders of magnitude less than the approximate values predicted by the dissociative mechanism.

In one of the mechanisms proposed to account for these decreased rates, a small amount of the mono-protonated ligand is considered to be present in the carboxylate-protonated form along with the nitrogen-protonated form. This carboxylate-protonated form is considered to be the reactive species due to the blocking of the nitrogen atom by the proton (44-46).

A second reaction mechanism to account for the decreased rates of reaction of M^{2+} with HL^{3-} for ligands of the EDTA type may be illustrated by reference to Figure 1. Reaction proceeds by dissociation of water molecules followed by metal-ligand bond formation to yield intermediate (III) in which the three dentates of one end of the ligand are metal coordinated while coordination of the other end is blocked by the proton on the nitrogen. For further coordination to occur, the proton must be transferred to a carboxylate oxygen or a solvent molecule before the intermediate dissociates to the reactants. A slow proton transfer step relative to dissociation of the intermediate back to reactants would account for the decreased rates mentioned above.

The size of a chelate ring formed in many complexation reactions may also affect the overall rate of the reaction. For instance, the rate of reaction of cobalt(II) with α -alanine, in which a five-membered ring is formed, is an order of magnitude greater than that for the similar reaction with β -alanine, in which a six-membered ring is formed (47). Similarly, the rates for the reactions of nickel and cobalt with α -aminobutyric acid were found to be about an order of magnitude greater than the corresponding

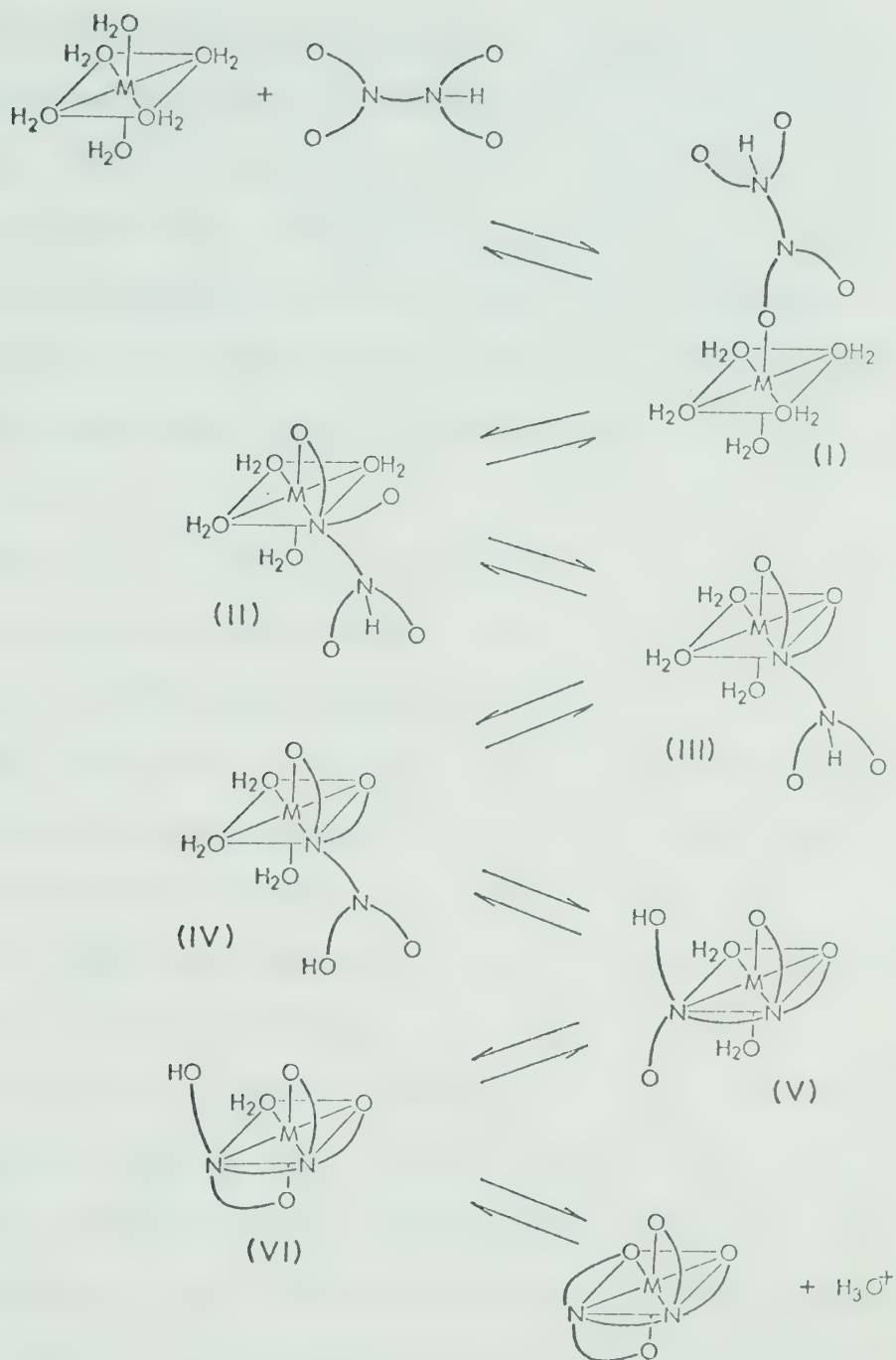


Figure 1: Proposed stepwise reaction mechanism for the formation of ML^{2-} complexes from M^{2+} and HL^{3-} . HL^{3-} is the monoprotonated form of EDTA type ligands.

rates with the β -amino acid (48). The results with the α -amino acids are consistent with the dissociative mechanism. With the β -amino acids, however, the results are consistent with a mechanism in which ring closure is the rate-determining step. The latter mechanism implies that the repossession of the vacated coordination site by a water molecule is a faster process than ring closure.

The size of chelate rings formed may also be an important factor governing the rates of the formation reactions of EDTA type complexes from the mono-protonated form of the ligand. For example, the larger the chelate ring which must be formed in going from intermediates (IV) to (V) in Figure 1, the more likely the vacated coordination site is to be reoccupied by a water molecule before ring closure can occur. The stability of certain intermediates may also affect the overall rates of these formation reactions. For instance, the less stable intermediate (III) is, the more likely it is to dissociate to reactants before proton transfer and bonding of the second nitrogen can occur. In order to see if these two factors do have an effect on the rates of certain complexation reactions, a pmr line-broadening study of the kinetics of the ligand exchange reactions of the cadmium, zinc

and lead complexes of 1,3-PDTA and EDDDA was undertaken (49). The results of this study are described in Chapter III. The predominant pathways by which the ligands exchange between free and complexed forms are established and their rate constants measured. The results are discussed with emphasis on the mechanism of formation of the complexes from the monoprotinated forms of the ligands.

CHAPTER II

PARTIAL DISSOCIATION KINETICS OF METAL COMPLEXES OF AMINOCARBOXYLIC ACIDS

In this chapter, the results of a study of the temperature dependence of the AB multiplet patterns in the pmr spectra of certain metal complexes of aminocarboxylic acids are presented and discussed. In particular, the cadmium and zinc complexes of both 1,3-PDTA and 1,4-BDTA and the cadmium, zinc and lead complexes of EDDDA were investigated. A central purpose of this work was to ascertain what kinetic information can be obtained from the nonequivalence of the acetate methylenic protons in complexes of this type.

A. RESULTS

Analysis of Multiplet Patterns

The 60 MHz pmr spectrum of the acetate methylenic protons of $\text{Zn}(1,3\text{-PDTA})^{2-}$ in aqueous solution at 25° is shown in the lower left hand side of Figure 2. The pH of the solution was 8.7 at 25°. The spectrum consists of an AB pattern, the upfield peak of which is obscured by a broad triplet due to the two methylene groups bonded to the nitrogen atoms in the

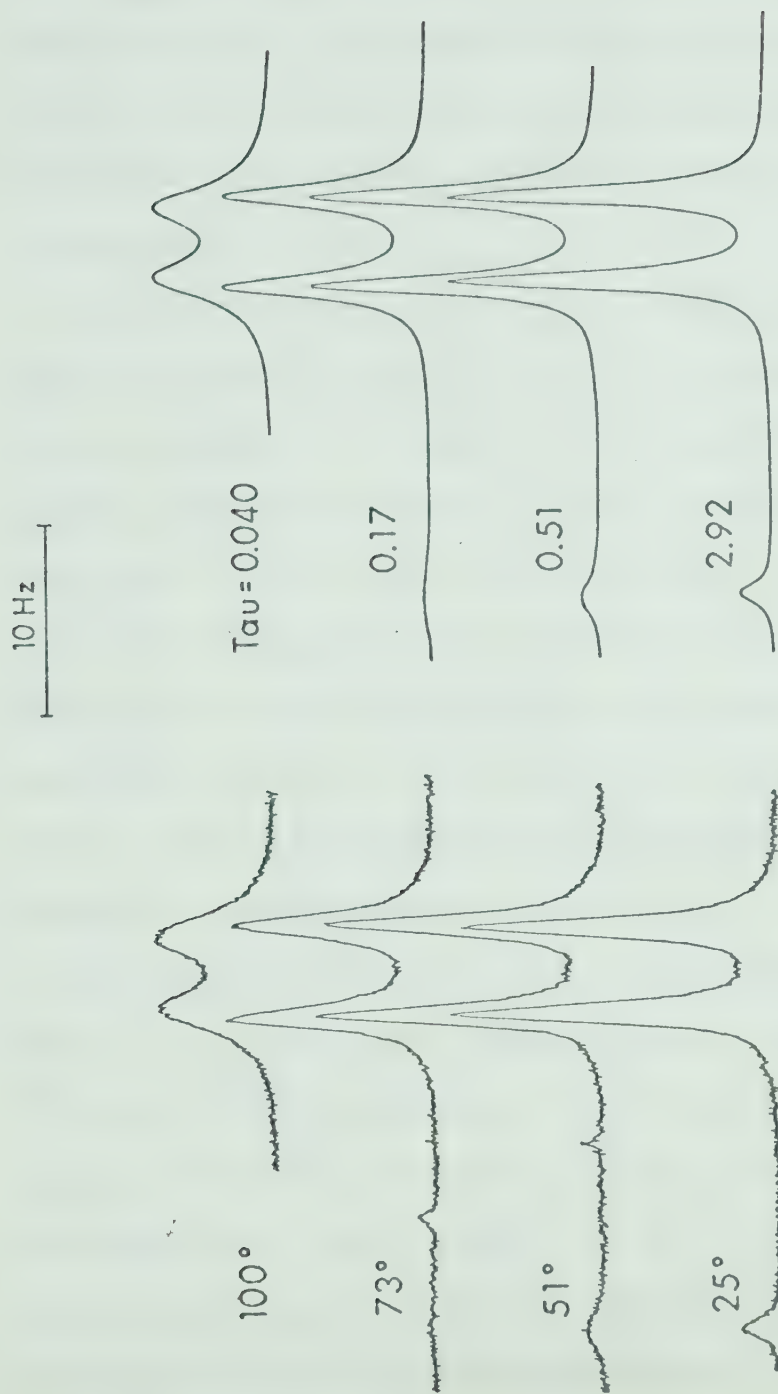


Figure 2: Representative experimental (left) and theoretical (right) 60 MHz pmr spectra of the acetate methylenic protons of an aqueous solution of $\text{Zn}(1,3\text{-PDTPA})^{2-}$.

propylene part of the ligand. Analysis of this AB pattern by standard methods (35) yielded the values for $\Delta\delta_{AB}$ and J_{AB} listed in Table I. $\Delta\delta_{AB}$ is the chemical shift difference between the A and B protons and J_{AB} is the spin-spin coupling constant. The value for this geminal coupling constant was assumed to be negative (17).

The 100 MHz pmr spectrum of the acetate methylenic protons of $\text{Cd}(1,3\text{-PDTA})^{2-}$ in D_2O solution at 10° is shown in Figure 3. The pD of the solution was 7.5 at 25° . This multiplet pattern is more complicated than that for the zinc system because of the ^{111}Cd and ^{113}Cd isotopes which have a nuclear spin quantum number of $1/2$ and are present at a combined natural abundance of 25.0%. The multiplet consists of the AB part of an ABX pattern superimposed on an AB pattern. The AB pattern arises from the complexes of the cadmium isotopes whose spin numbers are zero, while the AB part of an ABX pattern is due to the ^{111}Cd and ^{113}Cd complexes. The broad triplet just upfield from the multiplet pattern arises from the two methylene groups bonded to the nitrogen atoms in the propylene part of the ligand. Analysis of the AB pattern from slow exchange spectra of the type shown in Figure 3 at several temperatures in the range

Table I

Pmr Spectral Parameters for the Acetate Methylenic
Protons of the Indicated Metal Complexes

	$\Delta\delta_{AB}$ (ppm)	J_{AB} (Hz)	$ J_{AX} $	$ J_{BX} $
$\text{Cd}(1,3\text{-PDTA})^{2-}$	0.192	-16.3	11.8	15.0
$\text{Zn}(1,3\text{-PDTA})^{2-}$	0.220	-16.3		
$\text{Pb}(1,3\text{-PDTA})^{2-}$			19.2	
$\text{Cd}(1,4\text{-BDTA})^{2-}$	0.141	-16.2	17.3	17.7
$\text{Zn}(1,4\text{-BDTA})^{2-a}$	0.204	-16.3		
$\text{Cd}(\text{EDDDA})^{2-}$	b	b	13.5	12.5
$\text{Zn}(\text{EDDDA})^{2-}$	0.453	-18.3		
$\text{Pb}(\text{EDDDA})^{2-}$	0.221	-16.7	22.6	17.5

(a) From reference 30.

(b) Could not be determined from the spectrum.

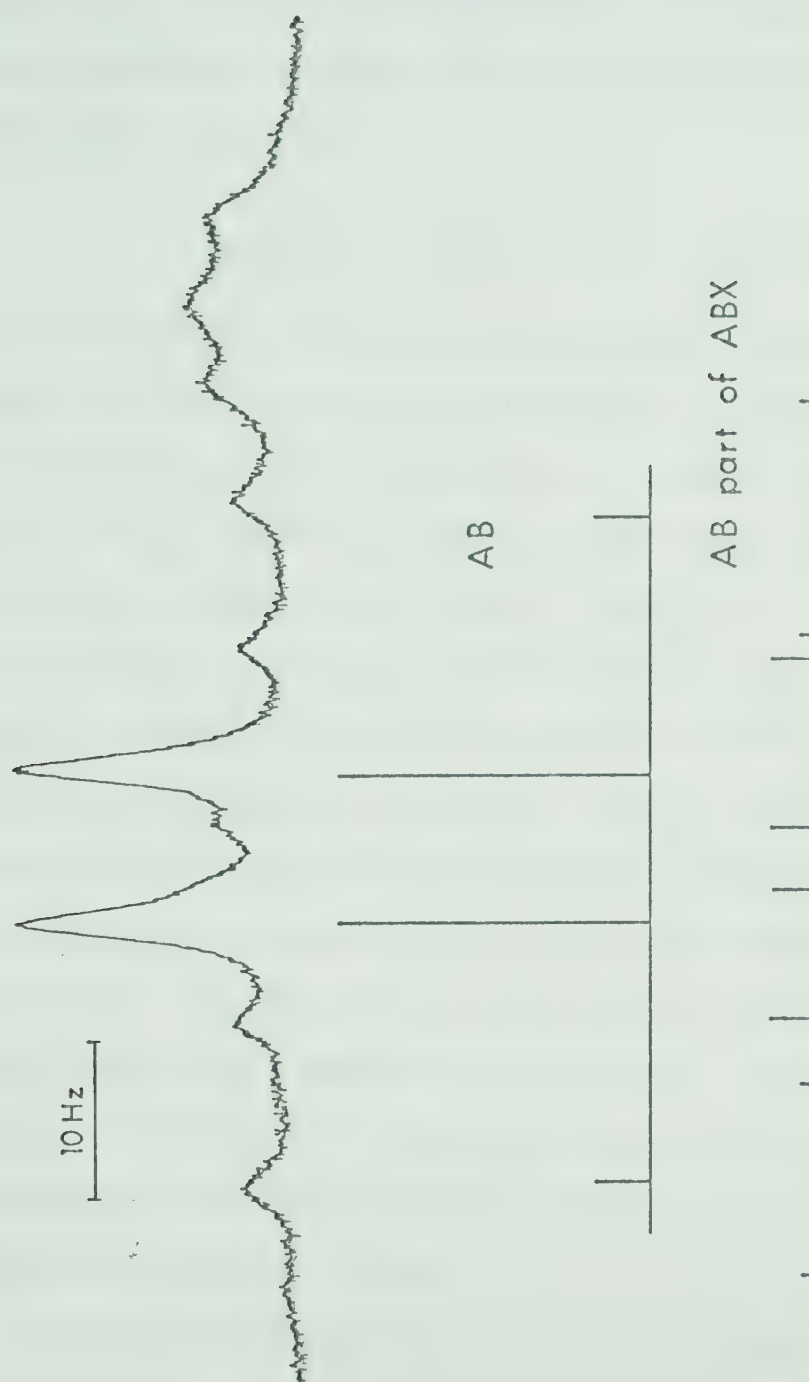


Figure 3: The 100 MHz pmr spectrum of the acetate methylenic protons of a D_2O solution of $\text{Cd}(\text{1,3-PDTA})^{2-}$.

3 to 26° yielded the value for J_{AB} listed in Table I. The chemical shift difference was found to decrease linearly as the temperature was increased, and a least squares analysis of the data yielded the following relation:

$$\Delta\delta_{AB}(\text{ppm}) = -5.00 \times 10^{-4} T + 0.205 \quad \text{I}$$

where T is the temperature in degrees centigrade. Analysis of the AB part of the ABX pattern using the value determined for J_{AB} gave a value of 3.2 Hz for $|J_{AX} - J_{BX}|$, where J_{AX} and J_{BX} are the coupling constants between the cadmium nuclei with spin numbers of 1/2 and H_A and H_B . The values for $|J_{AX}|$ and $|J_{BX}|$ shown in Table I were determined by varying them and calculating spectra until the best fit between experimental and calculated spectra was obtained (35), assuming the signs of the coupling constants to be the same. No significant variation of these coupling constants with temperature was found. The stick spectra presented in the bottom part of Figure 3 were calculated from the chemical shift and coupling constants obtained above.

The 60 MHz spectrum of the acetate methylenic protons of a solution of $\text{Pb}(1,3\text{-PDTA})^{2-}$ at 25° and pH 7.9 consists of a single resonance flanked symmet-

rically by two satellite peaks; the width of the central resonance is 1.2 Hz. The satellites arise from proton coupling to the ^{207}Pb isotope which has a nuclear spin quantum number of 1/2 and a natural abundance of 22.6%; the magnitude of the coupling constant J_{AX} is given in Table I. At both 100 and 220 MHz, the basic pattern of the spectrum of $\text{Pb}(1,3\text{-PDTA})^{2-}$ is the same as that at 60 MHz. The lack of an AB pattern could be due to more labile lead-nitrogen bonding resulting in averaging of the resonances (9) or to accidental equivalence of the methylenic proton chemical shifts (15).

The 220 MHz spectrum of the acetate methylenic protons of $\text{Cd}(1,4\text{-BDTA})^{2-}$ at 5° is shown at the bottom of Figure 4. The pH of this solution was 7.6 at 25°. The spectrum consists of the AB part of an ABX pattern superimposed on an AB pattern; analysis of the multiplet yielded the values listed in Table I.

The 60 MHz spectrum of the acetate protons of $\text{Zn}(1,4\text{-BDTA})^{2-}$ at 62° consists of a simple AB pattern; the results of an analysis are given in Table I. This work was done in collaboration with Dr. G. Blakney (30).

The acetate proton spectrum of $\text{Cd}(\text{EDDDA})^{2-}$ at 220 MHz and 5° is shown at the bottom left of Figure 5.

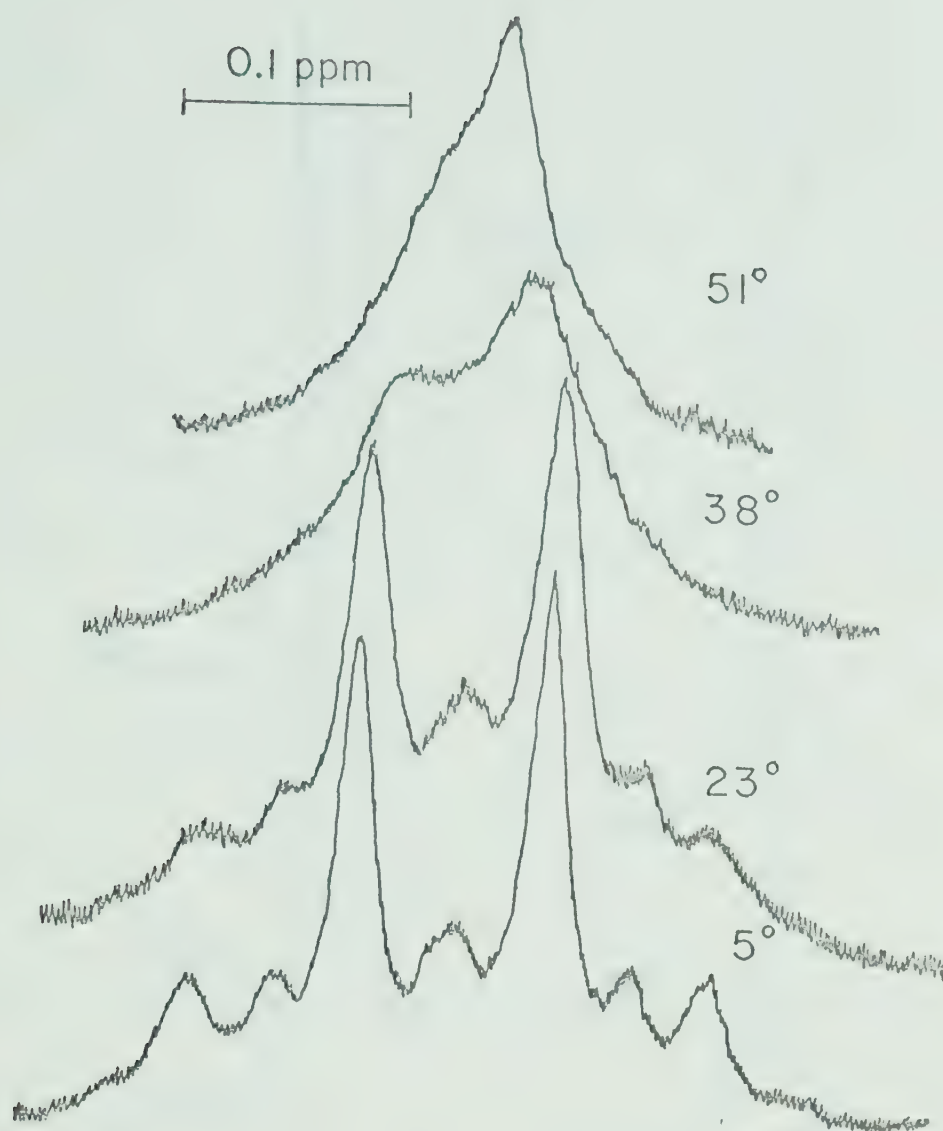


Figure 4: 220 MHz pmr spectra of the acetate methylenic protons of an aqueous solution of $\text{Cd}(1,4\text{-BDTA})^{2-}$ at the indicated temperatures.

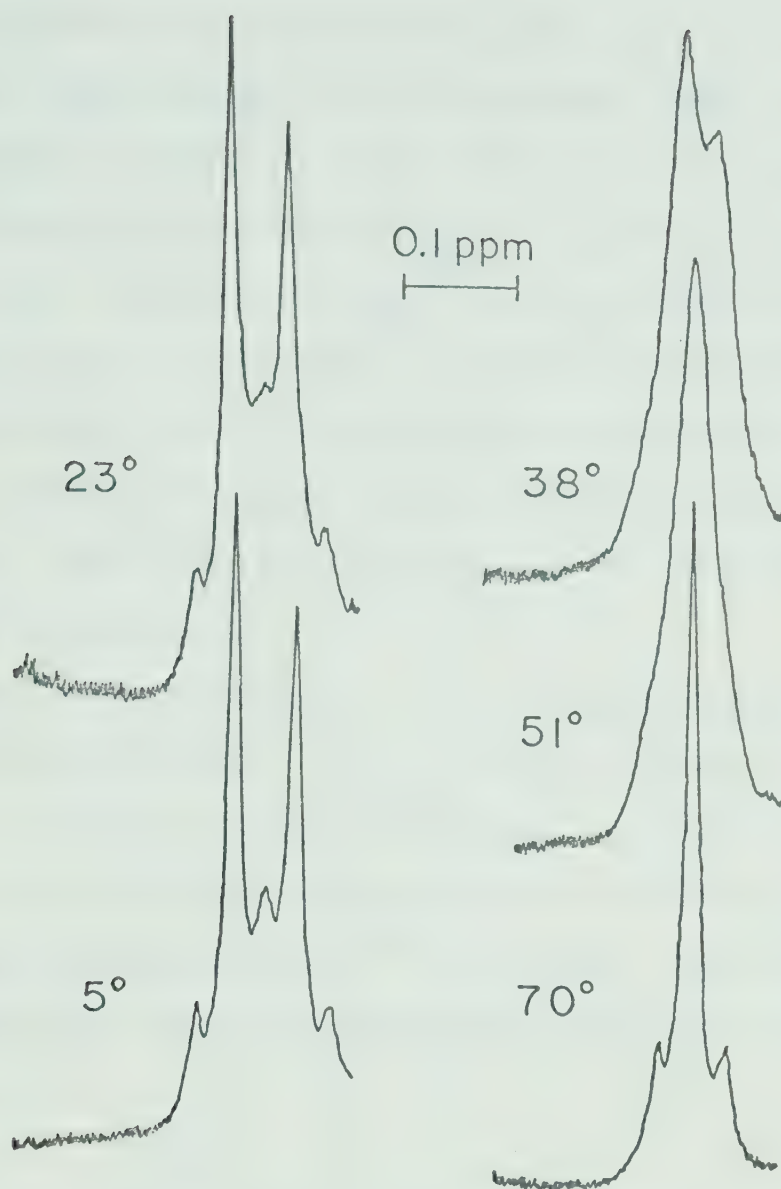


Figure 5: 220 MHz pmr spectra of the acetate methylenic protons of an aqueous solution of Cd(EDDDA)^{2-} at the indicated temperatures.

It is believed to consist of the AB part of an ABX spectrum superimposed on an AB pattern. The two low intensity peaks of the AB pattern are too weak to be observed and hence, $\Delta\delta_{AB}$ and J_{AB} could not be calculated. Values for $|J_{AX}|$ and $|J_{BX}|$ were estimated directly from the spectrum and are listed in Table I.

At 60 MHz and 25°, the acetate methylenic portion of the Zn(EDDDA)^{2-} spectrum consists of a simple AB pattern. The results of an analysis of this spectrum are shown in Table I.

The 220 MHz spectrum of the acetate methylenic protons of Pb(EDDDA)^{2-} at 5° consists of the AB part of an ABX spectrum superimposed on an AB spectrum. The AB part of an ABX spectrum arises from those complexes containing the ^{207}Pb isotope. Analysis of this multiplet pattern yielded the results shown in Table I.

AB Interchange Rates for the 1,3-PDTA and 1,4-BDTA Complexes

The lineshape of the multiplet pattern for the acetate methylenic protons of Cd(1,3-PDTA)^{2-} is temperature dependent, as shown by the 60 MHz spectra in Figure 6 for a solution of the complex which was pH 8.0 at 25°. The two low intensity peaks of the

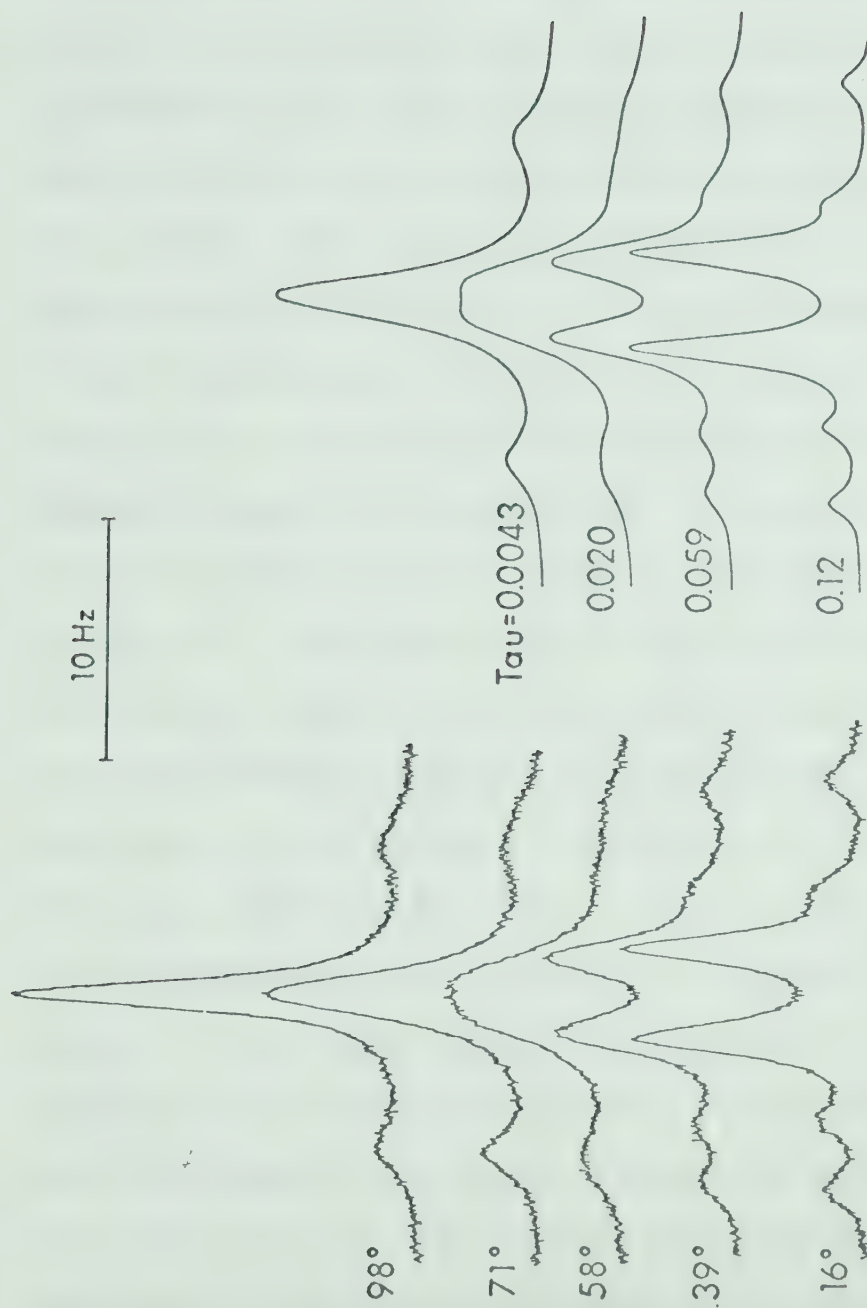


Figure 6: Representative experimental (left) and theoretical (right) 60 MHz spectra of the acetate methylenic protons of an aqueous solution of $\text{Cd}(\text{1,3-PDTA})^{2-}$.

AB pattern are barely visible at 16° and are not shown in the figure. As the temperature is increased, the AB pattern collapses to a single, averaged resonance while the AB part of an ABX pattern collapses to the A part of an A₂X pattern. The 98° spectrum clearly illustrates the limit of rapid interchange of the A and B protons of a given methylenic group on the pmr time scale. The coupling to the ¹¹¹Cd and ¹¹³Cd isotopes at 98° indicates that complete dissociation of the complex must be occurring slowly on the pmr time scale, since metal-proton coupling in multi-dentate ligand complexes is not collapsed as long as chelated ligand does not exchange rapidly with free ligand (9). The metal-proton coupling would be observed even if the ligand partially unwraps from the metal and then re-bonds because all nuclei remain in the same spin states and the coupling is not relaxed. The upper limit of the rate of first order dissociation of the complex at 98° is $2\pi|J_{AX}| \approx 87 \text{ sec}^{-1}$, where $|J_{AX}|$ is the average value of the magnitude of the cadmium-proton coupling constant in the limit of fast AB interchange. The slight broadening of the satellite peaks at 98° suggests that at this temperature the rate of complete dissociation is just becoming appreciable on the pmr time scale (43), that is,

the rate must be of the order of $2\pi|J_{AX}|$.

Average lifetimes before AB interchange were determined by lineshape analysis of spectra of which those in Figure 6 are representative. The density matrix method (78,79) was used to simulate spectra theoretically as a function of τ , the average lifetime before interchange. Other parameters used in the calculation were $\Delta\delta_{AB}$ (Hz), J_{AB} , J_{AX} , J_{BX} and T_2 , where T_2 is the effective spin-spin relaxation time. $\Delta\delta_{AB}$ at a given temperature was calculated with the aid of Equation I; similar chemical shift functions have been used previously in lineshape treatments (57). A constant T_2 calculated from an assumed natural linewidth of 1.0 Hz was used; the natural linewidth could not be measured directly because some exchange-broadening was observed even at the lowest temperatures attainable. Typical linewidths in similar complexes are about 1.0 Hz.

The computer program used to simulate the spectra (51) was modified so that it first calculated the lineshape of the AB spectrum and then the AB part of the ABX spectrum for a given set of parameters. It then normalized the intensities for the two sets of spectra so that the AB part of the ABX pattern represented 25.0% of the total intensity,

since this part of the pattern arises from the complexes of the isotopes of cadmium with spin numbers of $1/2$ which are present at a combined natural abundance of 25.0%. The normalized spectra were combined to give a spectrum which was compared to the experimental spectrum. For a given set of input parameters, τ was varied until the computed and experimental spectra matched. In the slow and rapid exchange regions the criterion for matching was the linewidth of the resonance peaks; in the intermediate exchange region it was the peak-to-valley ratio of the two central peaks. The terms slow, intermediate, and fast exchange will be explained in Chapter IV. The spectra shown in Figure 6 are typical of the fits obtained. Average lifetimes before AB interchange determined by this matching procedure over a range of temperatures are listed in Table II. The experimental error in the lifetime determinations was from ± 5 to $\pm 10\%$ due mainly to difficulties in matching computed and experimental spectra.

A pH of 8.0 was chosen for the Cd-1,3-PDTA lineshape study to minimize the contributions of reactions involving hydrogen or hydroxide ion to the overall rate of AB interchange. To determine the

Table II

Average Lifetimes of the Acetate Methylenic Protons
of $\text{Cd}(1,3\text{-PDTA})^{2-}$ and $\text{Cd}(1,4\text{-BDTA})^{2-}$
Before AB Interchange

Temp. ($^{\circ}\text{C}$)	τ (sec.)	
	$\text{Cd}(1,3\text{-PDTA})^{2-}_{\text{a,b}}$	$\text{Cd}(1,4\text{-BDTA})^{2-}_{\text{c,d}}$
5		0.10
16	0.12	
23	0.085	0.050
31	0.070	
38		0.012
39	0.059	
45	0.042	
51	0.029	0.0055
58	0.020	
64	0.011	
71	0.0043	

(a) pH 8.0 at 25° .

(b) Lifetimes determined by lineshape analysis of 60 MHz spectra.

(c) pH 7.6 at 25° .

(d) Lifetimes determined by lineshape analysis of 220 MHz spectra.

magnitude of any pH dependence, samples at pH's 7.2, 8.4 and 9.1 (at 25°) were studied over the same temperature range. The spectra obtained were identical, at the same temperatures, with those from which the results in Table II were obtained, indicating no pH dependence of the rate within this pH range.

To determine if the lineshape treatment is dependent on the spectrometer frequency, lifetimes were determined by the above procedure for a D₂O solution of Cd(1,3-PDTA)²⁻ at pD 7.5 over a range of temperatures from both 60 and 100 MHz spectra. D₂O was used as the solvent rather than H₂O because with H₂O as the solvent, the water resonance caused locking problems on the 100 MHz spectrometer. The results shown in Table III indicate that the lifetimes are independent of the measuring frequency within experimental error. The results in Tables II and III also show that, on the average, the rates of AB interchange for the D₂O solution are 0.6 times as fast as those for the H₂O solution. These results are discussed in a later section of this chapter.

The 60 MHz pmr spectrum of the acetate methylenic protons of Zn(1,3-PDTA)²⁻ in aqueous solution is

Table III

Comparison of Average Lifetimes of the Acetate
Methylenic Protons of $\text{Cd}(1,3\text{-PDTA})^{2-}$ ^a Before
AB Interchange Determined from 60 MHz
and 100 MHz Spectra

Temp. (°C)	τ (sec.)	
	60 MHz	100 MHz
23	0.12	
26		0.12
31	0.10	
39		0.094
45	0.065	
47		0.056
51	0.043	
56		0.034
58	0.028	
60		0.026

(a) D_2O solution of pD 7.5 at 25°.

shown as a function of temperature in Figure 2. As the temperature is increased, the AB pattern begins to collapse; however the extent of collapse and hence the rate of AB interchange is somewhat less than that for $\text{Cd}(1,3\text{-PDTA})^{2-}$. Average lifetimes before AB interchange were determined by matching computer-simulated and experimental spectra in the same way as for the cadmium complex as described above. The chemical shift difference and coupling constant used in the computer-simulation were found to be independent of temperature in the range over which they could be measured (25 to 62°). The lifetimes obtained are listed in Table IV, and some of the calculated spectra are shown in Figure 2.

The temperature dependence of the lineshape of the multiplet pattern for the acetate protons of $\text{Cd}(1,4\text{-BDTA})^{2-}$ at 220 MHz is shown in Figure 4. As observed for $\text{Cd}(1,3\text{-PDTA})^{2-}$, the AB pattern collapses to a single resonance as the temperature is increased and the AB part of the ABX pattern is just beginning to become the A part of an A_2X pattern by 70°. In the intermediate interchange region, the lineshape is slightly asymmetric with one side of the multiplet sharper than the other. Average lifetimes before AB interchange were determined by

Table IV

Average Lifetimes of the Acetate Methylenic Protons
of $\text{Zn}(1,3\text{-PDTA})^{2-}$ and $\text{Zn}(1,4\text{-BDTA})^{2-}$

Before AB Interchange

Temp. (°C)	τ (sec.) ^a	
	$\text{Zn}(1,3\text{-PDTA})^{2-}$ ^b	$\text{Zn}(1,4\text{-BDTA})^{2-}$ ^c
25	2.9	
39	1.2	
51	0.51	
56		0.50
62	0.25	0.30
73	0.17	0.20
80	0.12	0.095
87	0.084	0.063
93	0.060	0.047
100	0.040	0.035

(a) Determined by lineshape analysis of 60 MHz spectra.

(b) pH 8.7 at 25°.

(c) pH 7.8 at 25°.

the matching procedure used for the 1,3-PDTA complexes, but disregarding the asymmetry. The chemical shift and coupling constant values used in the calculation are given in Table I and a T_2 assuming a natural linewidth of 2.5 Hz obtained from the 220 MHz spectra was used. The lifetimes which were obtained are shown in Table II for comparison with those for $\text{Cd}(1,3\text{-PDTA})^{2-}$. The error introduced into the lifetime calculations for the 1,4-BDTA complex by the presence of the asymmetry in the intermediate exchange spectra is estimated to be $\pm 20\%$.

The temperature dependence of the lineshape for the acetate protons of $\text{Zn}(1,4\text{-BDTA})^{2-}$ at 60 MHz is shown by the spectra in Figure 7 (30). Average lifetimes before AB interchange determined by matching computer-simulated spectra with experimental spectra obtained above 48° are given in Table IV for comparison with the results for $\text{Zn}(1,3\text{-PDTA})^{2-}$.

Below 48° for $\text{Zn}(1,4\text{-BDTA})^{2-}$, the individual lines of the multiplet pattern broaden at different rates, resulting in an asymmetrical AB pattern as shown in Figure 7. Each half of the spectrum is broadened further at 100 and 220 MHz, indicating that the broadening results from a second kinetic process. One possibility is relatively slow exchange

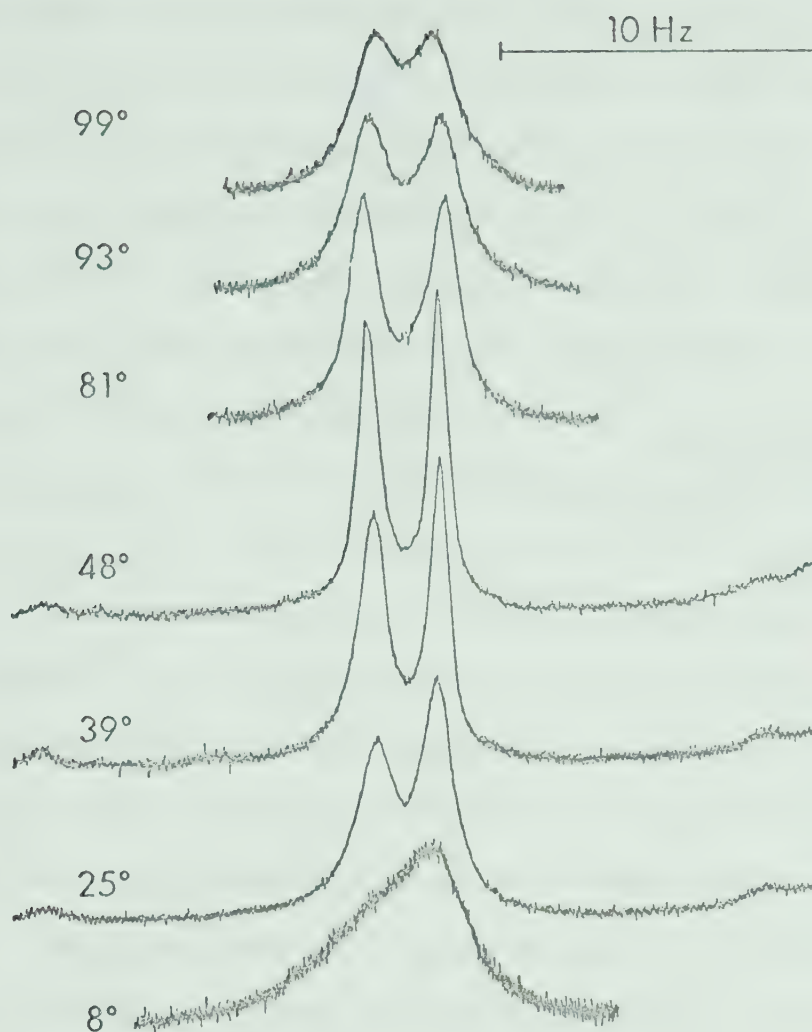


Figure 7: 60 MHz pmr spectra of the acetate methylenic protons of an aqueous solution of $\text{Zn}(1,4\text{-BDTA})^{2-}$ at the indicated temperatures.

of the acetate groups between the site in the plane formed by the metal and the two nitrogen atoms and the site out of the plane. Such a process would yield an asymmetrical pattern if J_{AB} , δ_A , and δ_B are different for the in-plane and out-of-plane acetate groups, as in the cobalt(III) and rhodium(III) complexes of EDTA (9,14,16,17), and if $\delta_{A(\text{in-plane})} - \delta_{A(\text{out-of-plane})}$ is different from $\delta_{B(\text{in-plane})} - \delta_{B(\text{out-of-plane})}$. It is possible that the asymmetry observed in the intermediate exchange spectra for $\text{Cd}(1,4\text{-BDTA})^{2-}$ also results from in-plane to out-of-plane exchange of acetate dentates. However, in this case, the chemical shift differences between the in-plane and out-of-plane sites must be very small, since in the slow exchange spectrum only a slightly greater intensity of one of the peaks can be observed.

Temperature Dependence of the AB Multiplet Patterns for the EDDDA Complexes

The multiplet pattern for the acetate methylenic protons of $\text{Cd}(\text{EDDDA})^{2-}$ at 220 MHz broadens asymmetrically as the temperature is increased as can be seen by the spectra in Figure 5. At 70° it consists of a single resonance flanked symmetrically by the A part of an A_2X pattern due to the proton coupling

to the ^{111}Cd and ^{113}Cd isotopes. The temperature dependence of this multiplet pattern could not be quantitatively studied because the chemical shift difference and coupling constants could not be obtained from the slow exchange spectra.

The AB pattern for $\text{Zn}(\text{EDDDA})^{2-}$ at 60 MHz broadens little at the highest temperatures studied, indicating only a slight degree of AB interchange. Lifetime determinations were not made because of the small temperature range (90 to 100°) over which broadening was observed.

The multiplet pattern for $\text{Pb}(\text{EDDDA})^{2-}$ at 220 MHz also broadens as the temperature is increased, indicating AB interchange. In the intermediate exchange region the broadened pattern is asymmetrical. Severe interference from the water resonance in this exchange region prevented a quantitative rate study from being undertaken.

Pmr Spectra of the EDTA Complexes

The 60 MHz pmr spectrum of the acetate methylenic protons of an aqueous solution of $\text{Cd}(\text{EDTA})^{2-}$ at a neutral pH consists of the AB part of an ABX pattern superimposed on an AB pattern (9), similar to that observed for $\text{Cd}(1,3\text{-PDTA})^{2-}$. In contrast to the

1,3-PDTA system, however, the lineshape of the multiplet pattern of the EDTA complex is temperature invariant up to 100°.

It has previously been observed that the acetate methylenic proton resonances of the zinc and lead complexes of EDTA (9,52) at 60 MHz consist of single peaks. Pmr measurements at 220 MHz (15), however, have revealed AB patterns for these two complexes.

B. DISCUSSION

Partial Dissociation Kinetics of the Complexes of 1,3-PDTA and 1,4-BDTA

The multiplets in the pmr spectra for the acetate methylenic protons of $\text{Cd}(1,3\text{-PDTA})^{2-}$, $\text{Zn}(1,3\text{-PDTA})^{2-}$ and $\text{Cd}(1,4\text{-BDTA})^{2-}$ at 25° and of $\text{Zn}(1,4\text{-BDTA})^{2-}$ at 62° consist of single AB patterns (or the AB part of an ABX pattern superimposed on a single AB pattern). The single AB patterns indicate that the four acetate groups of a given complex are equivalent on the pmr time scale. If it is assumed that coordination around the metal ion is octahedral and that all six dentates of the ligands are coordinated, two acetate groups are in the plane formed by the metal and two nitrogen atoms and two are out of the plane

in the instantaneous structures of the complexes. If a given structure is long-lived on the pmr time scale, the environments experienced by the acetate groups in the in-plane and out-of-plane sites must be equivalent to observe a single AB pattern. Pmr spectra of the nonlabile rhodium(III) (14) and cobalt(III) complexes of EDTA (9,16,17) suggest it is unlikely that the in-plane and out-of-plane environments will be equivalent and rather that the single AB patterns for the 1,3-PDTA and 1,4-BDTA complexes result from rapid exchange of acetate dentates between the two sites. Exchange could be by a sequence of reactions involving dissociation of labile metal-oxygen bonds (9) or by a twist mechanism of the type proposed by Bailar (18,53).

The AB patterns reveal that, for the given solution conditions, each nitrogen atom of the 1,3-PDTA and 1,4-BDTA complexes is permanently in one of its two possible inversion states on the pmr time scale. Increasing the temperature results in inversion of the nitrogen atom becoming more rapid, as evidenced by the collapse of the multiplet patterns for these complexes.

A series of stepwise reactions which could lead to interchange of nonequivalent acetate protons in

complexes of EDTA and its homologs via inversion of a nitrogen atom is shown schematically in Figure 8. The ligand is shown as being hexadentate in at least some of the complex, but the conclusions from the following discussion are not dependent on this assumption. It is assumed, however, that a metal-nitrogen bond can dissociate making possible nitrogen inversion only after dissociation of the metal bonds to the two acetate groups of the given nitrogen atom. If K_1 ($= k_1/k_{-1}$) and K_2 ($= k_2/k_{-2}$) are rapid pre-equilibria on the pmr time scale, the rate-determining step for AB interchange via the reaction sequence in Figure 8 is either nitrogen inversion or metal-nitrogen bond dissociation. Qualitatively, if $k_{-3} \gg k_i$, the metal-nitrogen bond dissociates and re-forms many times on the average before the noncoordinated nitrogen atom inverts, so that the rate-determining step is the nitrogen inversion. On the other hand, if $k_i \gg k_{-3}$, once the metal-nitrogen bond has broken the noncoordinated nitrogen atom inverts many times before the bond re-forms and the rate-determining step is metal-nitrogen bond dissociation. In the latter case, there is statistically a 50% chance that the nitrogen atom will be in an inverted state when it re-bonds to the metal,

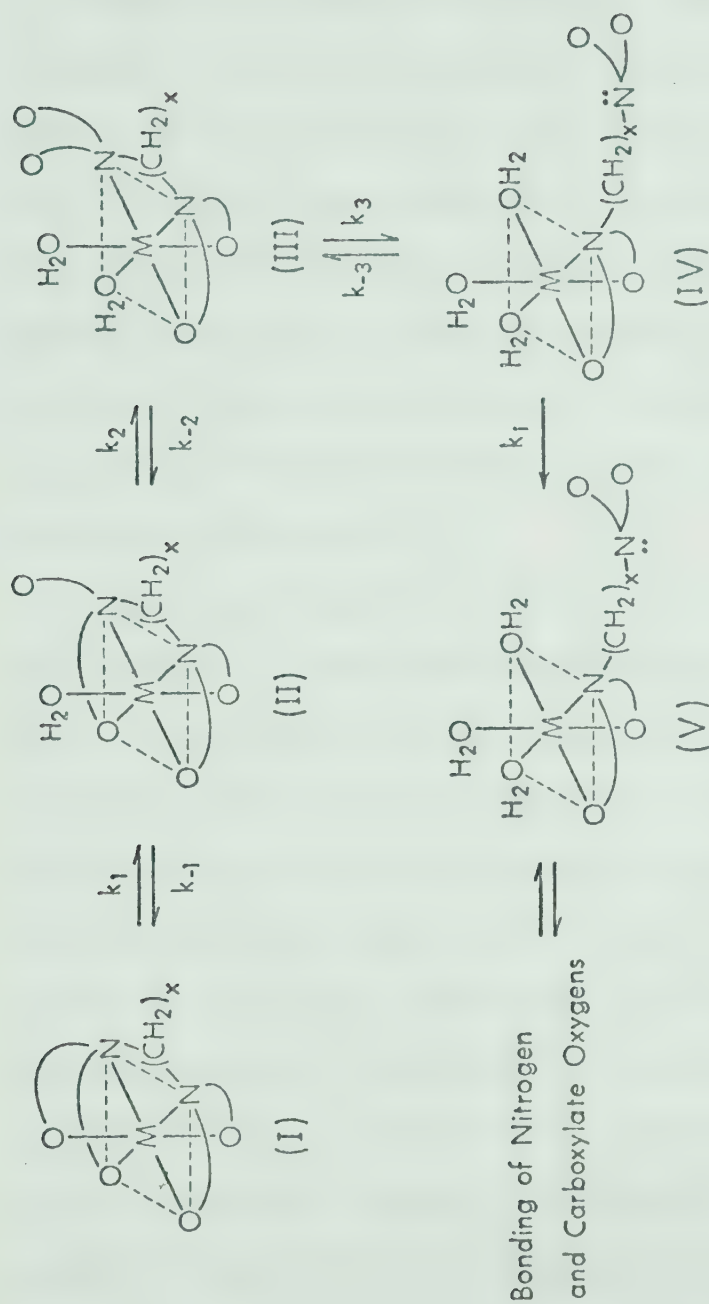


Figure 8: Possible stepwise reactions that can lead to the A to B inter-
change observed by the pmr method for the acetate methylenic
protons in complexes of EDTA and its homologs.

so that the observed rate of AB interchange will be half the rate of dissociation to species (IV) in Figure 8.

Inversion rates of nitrogen atoms in multidentate ligands of the type studied here are not known; however, they have been estimated to be 10^8 to 10^9 sec^{-1} for nitrogen atoms in tertiary amines of the type described earlier (26-28). In the absence of more appropriate inversion rate constants, k_i for nitrogen atoms in multidentate ligands of the EDTA type will be assumed to be of this magnitude in the following discussion.

The upper limit for the rate of formation of the metal-nitrogen bond described by the rate constant k_{-3} , is the rate of dissociation of the water molecule occupying the coordination site if the reaction occurs by the Eigen dissociative mechanism (31-33,70). In terms of this mechanism, a water molecule will first be released from a site cis to the site of coordination to the other nitrogen atom, and the noncoordinated nitrogen atom will then bond to the metal ion at the vacated coordination site. The rates of water release from totally aquated cadmium and zinc are 4×10^8 and 5×10^7 sec^{-1} respectively (54). The rates of water release from these metal ions

will be considered as the upper limits for k_{-3} in the following discussion.

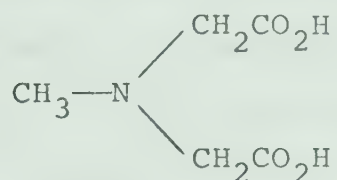
For k_{-3} to equal the rate of water release, the rate at which the noncoordinated nitrogen atom in species (IV) of Figure 8 coordinates to an unoccupied site has to be significantly larger than the rate at which a water molecule reoccupies the site. This requires that the nitrogen atom be properly oriented for bonding at the time the water molecule dissociates. Previous investigations of a number of fast complexation reactions of multidentate ligands would suggest that the rate at which the nitrogen atom will coordinate to the unoccupied site will be less when the chelate ring formed is six-membered than when it is five-membered. For example, Kustin and coworkers observed that the formation rate constants of the β -alanine complex of cobalt(II) is almost one order of magnitude less than that for the α -alanine complex (47). The difference was attributed to the difficulty in forming the six-membered chelate ring. Similar differences were observed for the nickel and cobalt(II) complexes of α - and β -aminobutyric acids (48). These results suggest that, for $\text{Cd}(1,3\text{-PDTA})^{2-}$ and $\text{Zn}(1,3\text{-PDTA})^{2-}$, k_{-3} may be somewhat less than the rates of water release from species (IV) in Figure 8 due to the

formation of a six-membered chelate ring. If so, k_i would be somewhat greater than k_{-3} for these complexes. On this basis, it is proposed that the AB patterns observed for these complexes are indicative of relatively inert metal-nitrogen bonding on the pmr time scale, and that the inverses of the lifetimes before AB interchange, which are listed in Tables II and IV, are half the first order rate constants for partial dissociation of the complexes to species (IV) at the indicated temperatures. If this proposal is correct, the lifetimes before AB interchange indicate that the relative order of lability of the metal-nitrogen bonds in the two metal complexes of 1,3-PDTA is cadmium > zinc.

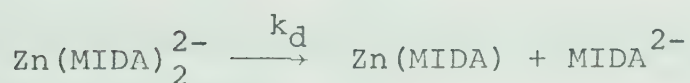
The rate at which the metal-nitrogen bond in the 1,4-BDTA complexes dissociates should be the same or slightly faster than in the 1,3-PDTA complexes since it may be easier to open the larger seven-membered chelate ring (47,48), while the rate at which the bond re-forms is predicted to be less since a seven-membered ring is formed (1,58). Therefore, if k_i is somewhat greater than k_{-3} for the 1,3-PDTA complexes, the rates of interchange in the 1,4-BDTA complexes of cadmium and zinc should be the same or slightly faster than in the 1,3-PDTA

complexes. The results in Tables II and IV indicate this to be the case. Furthermore, the lifetimes before AB interchange indicate that the order of lability of the metal-nitrogen bonds for the complexes of 1,4-BDTA is cadmium > zinc.

To determine if the rate constants calculated from the lifetimes in Tables II and IV are reasonable for the reaction represented in Figure 8, comparison can be made with the rate constant k_d , for dissociation of one N-methyliminodiacetic acid (MIDA) ligand from the complex Zn(MIDA)_2^{2-} ,



MIDA



which has previously been determined by pmr line-broadening measurements (30). The value for k_d is $40 \pm 5 \text{ sec}^{-1}$ at 25° . Taking the inverse of the lifetimes before AB interchange to be half the first order rate constants for partial dissociation to species (IV) in Figure 8, the partial dissociation rate constant

for $\text{Zn}(1,3\text{-PDTA})^{2-}$ is $0.69 \pm 0.14 \text{ sec}^{-1}$ at 25° .

The difference between k_d for $\text{Zn}(\text{MIDA})_2^{2-}$ and this value is of the magnitude expected if the energy barrier associated with the necessary twisting of the aliphatic chain in $\text{Zn}(1,3\text{-PDTA})^{2-}$ is accounted for (1).

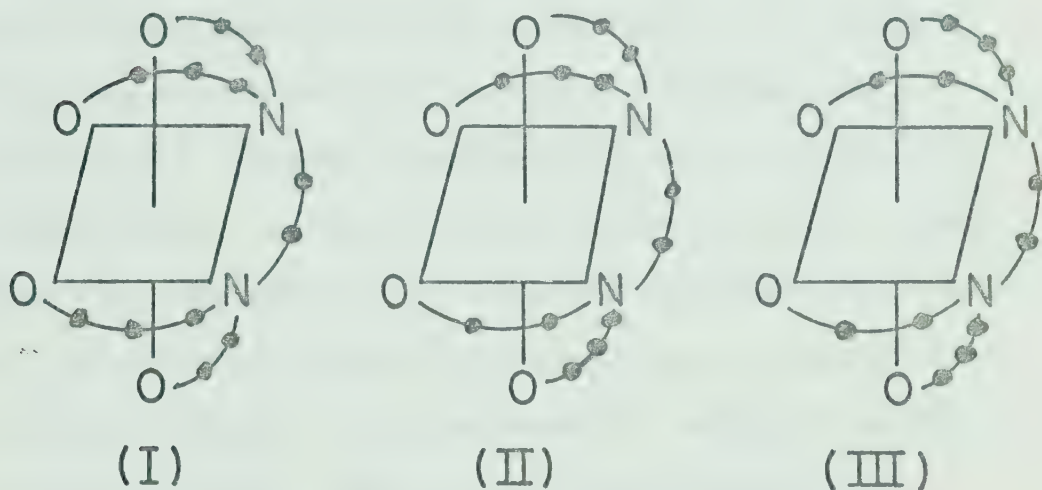
The results in Tables I and II which indicate that the rate of AB interchange in $\text{Cd}(1,3\text{-PDTA})^{2-}$ is different in H_2O and D_2O , can be accounted for if the fraction of the complex that exists in the various partially coordinated forms, shown in Figure 8, is different in these two solvents. This would be the case if the rate at which H_2O and D_2O dissociate from the metal complex is different. For example, K_1 ($= k_1/k_{-1}$) would be different in H_2O and D_2O if the rate of dissociation of H_2O from species (II) is different from the rate dissociation of D_2O .

Temperature Dependence of the AB Multiplet Patterns of the EDDDA Complexes

The multiplet patterns observed for the acetate methylenic protons of the cadmium, zinc and lead complexes of EDDDA indicate an inertness on the pmr time scale of the metal-nitrogen bonds. The collapse of these patterns with increasing temperature indicates that partial dissociation of these complexes is

occurring on the pmr time scale. The different degrees of collapse of the multiplet patterns for these complexes suggest that the relative order of lability of the metal-nitrogen bond is cadmium > lead > zinc.

Assuming that coordination in the EDDDA complexes is octahedral and that all six dentates are coordinated to the metal ion, three instantaneous structures are possible depending on whether the acetate or propionate groups are in-plane or out-of-plane (59).



The single AB pattern observed in the pmr spectrum for Zn(EDDDA)^{2-} suggests rapid exchange of the carboxylate dentates, but the values for J_{AB} and $\Delta\delta_{AB}$ indicate that one of the above structures is pre-dominant. The magnitude of the geminal coupling constant J_{AB} is approximately the same for all the

complexes listed in Table I except that for Zn(EDDDA)^{2-} . Sudmeier and coworkers (17) have reported the magnitude of the geminal coupling constants of the methylenic protons of the in-plane and out-of-plane acetate groups in the inert cobalt(III) complexes of EDTA type ligands to be 16 ± 0.5 Hz and 18 ± 0.5 Hz respectively. Since geminal coupling is sensitive to the electronegativity of substituents, the magnitudes of in-plane and out-of-plane coupling constants of aminocarboxylic acid ligands coordinated to divalent metal ions may be different. Assuming the relative magnitudes to be in the same direction as those for the cobalt complexes, the results in Table I suggest that Zn(EDDDA)^{2-} exists predominantly as structure (III) shown above. Support for this structure also comes from the observation of Legg and coworkers (60) that $\Delta\delta_{AB}$ for out-of-plane acetate groups of cobalt(III)-aminocarboxylic acid complexes is larger than for in-plane groups, and the results of Byers and Douglas (59) which show the structure of one isomer of Co(EDDDA)^- to be similar to the one proposed here for Zn(EDDDA)^{2-} .

If the preceding conclusions are correct, the geminal coupling constant reported for the AB pattern of Pb(EDDDA)^{2-} as the temperature is increased might then be explained

by a temperature dependence of the populations of the above three structures. The value for J_{AB} could not be determined from the multiplet pattern for $\text{Cd}(\text{EDDDA})^{2-}$, but the asymmetric broadening of this pattern might also be explained by a temperature dependence of the populations of the given structures.

The lack of broadening in the multiplet for $\text{Cd}(\text{EDTA})^{2-}$ up to 100° indicates that the rate of AB interchange is significantly less than the rate in $\text{Cd}(1,3\text{-PDTA})^{2-}$. This difference could result from more inert cadmium-nitrogen bonding in $\text{Cd}(\text{EDTA})^{2-}$, as predicted by the observation that it is easier for a six-membered chelate ring to open than for a five-membered ring (1,58), or it may indicate that $k_{-3} \gg k_i$. Bond re-formation, the reaction step described by the rate constant k_{-3} , is predicted to be faster for $\text{Cd}(\text{EDTA})^{2-}$ than for the 1,3-PDPA complex since a five-membered chelate ring is being formed (47,48). Considering the EDDDA results, the rate of partial dissociation to yield species (IV) in Figure 8 is predicted to be larger for $\text{Cd}(\text{EDDDA})^{2-}$ than for the EDTA complex on the basis that intermediates in the stepwise sequence will be present at higher concentrations while the rate of cadmium-nitrogen bond re-formation is assumed to

be the same. Thus, if the AB pattern of $\text{Cd}(\text{EDTA})^{2-}$ is due to the cadmium-nitrogen bond re-forming before inversion occurs, the AB pattern of $\text{Cd}(\text{EDDDA})^{2-}$ should be temperature invariant. Rather the multiplet for the acetate methylenic protons of the EDDDA complex is completely collapsed to a single resonance flanked by the A part of an A_2X pattern at 70° , indicating rapid AB interchange on the pmr time scale. These considerations provide support for the proposal of Day and Reilley (9) that the multiplet pattern for $\text{Cd}(\text{EDTA})^{2-}$ results from inert cadmium-nitrogen bonding.

CHAPTER III
LIGAND EXCHANGE KINETICS OF METAL COMPLEXES
OF 1,3-PDTA AND EDDDA

In this chapter, the results of a pmr line-broadening study of the ligand exchange kinetics of the 1,3-PDTA and EDDDA complexes of cadmium, zinc and lead are presented. These systems were investigated with the objective of elucidating the mechanisms of ligand exchange reactions of cadmium, zinc and lead complexes of aminocarboxylic acid ligands with emphasis on the formation reactions of the mono-protonated forms of the ligands. These two particular ligands were chosen in order to observe the effects of slight structural changes on the rates of reactions of aminocarboxylic acids of the EDTA type.

A. RESULTS

pH Dependence of the Chemical Shifts

The pmr spectrum of 1,3-PDTA consists of a sharp singlet for the acetate methylenic protons, a broad triplet-like pattern for the protons of the two nitrogen-bonded methylenic groups of the propylene part of the ligand and a broad quintet-like pattern for the central methylenic protons over the pH range 2 to 13. The lack of any broadening of the exchange-

averaged acetate methylenic resonance indicates that exchange of the acidic carboxylate and nitrogen protons is fast on the pmr time scale. The resonances due to the propylene protons, which form an A_4B_2 spin system, were not used in the ligand exchange studies because of their complexity.

The chemical shifts of the 1,3-PDTA resonances are pH dependent as illustrated by curve A for the acetate methylenic protons in Figure 9. By analogy with EDTA, the two nitrogen atoms of the tetraanion of 1,3-PDTA are protonated first, followed by protonation of the carboxylate groups (61-63). From the chemical shift vs. pH data, values were determined for the third and fourth ionization constants of 1,3-PDTA, defined by Equations II and III, by methods described previously (44,67) and are given in

$$K_3 = \frac{a_H [HL^{3-}]}{[H_2L^{2-}]} \quad \text{II}$$

$$K_4 = \frac{a_H [L^{4-}]}{[HL^{3-}]} \quad \text{III}$$

Table V. These constants are mixed mode constants involving hydrogen ion activity and 1,3-PDTA concentrations.

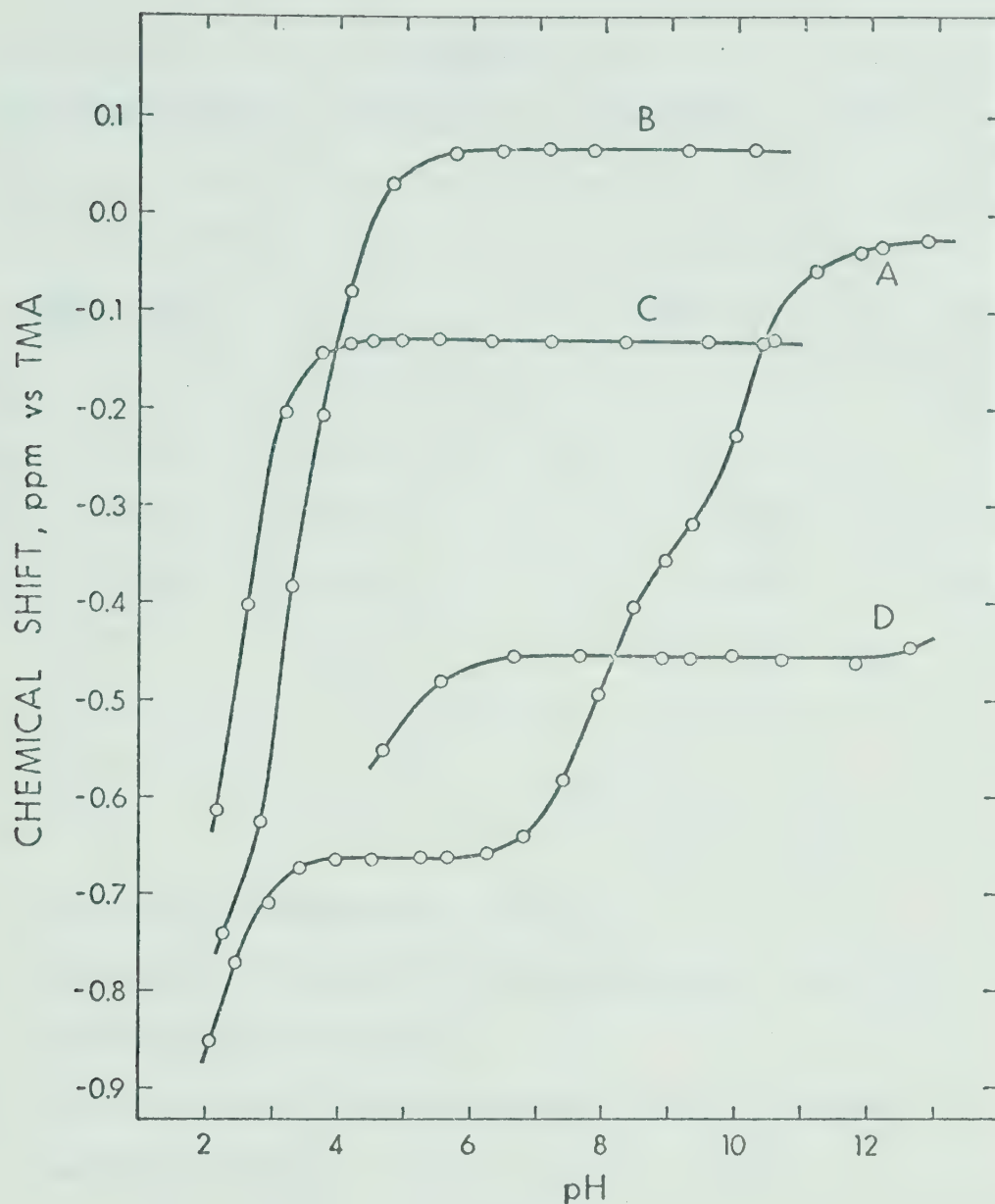


Figure 9: pH dependence of the chemical shift of the acetate methylenic protons of 1,3-PDTA. Curve A, 0.20 M 1,3-PDTA; curve B, 0.20 M Cd(1,3-PDTA)²⁻; curve C, 0.20 M Zn(1,3-PDTA)²⁻; curve D, 0.20 M Pb(1,3-PDTA)²⁻.

Table V

Acid Ionization Constants of 1,3-PDTA and EDDDA

	1,3-PDTA		EDDDA	
	This work ^a	lit. ^b	This work ^a	lit. ^c
pK ₁		1.88		3.00
pK ₂		2.57		3.79
pK ₃	7.93	8.02	6.00	5.98
pK ₄	10.25	10.46	9.88	9.83

(a) 25°C, ionic strength \approx 0.6 M.

(b) References 64 and 65, ionic strength = 0.1 M,
mixed mode constants.

(c) Reference 66, ionic strength = 0.1 M, mixed
mode constants.

Over the pH range 3 to 13, the pmr spectrum of EDDDA consists of a sharp singlet for the acetate methylenic protons, a sharp singlet for the ethylenic protons between the two nitrogen atoms and a complex multiplet pattern for the carbon-bonded protons of the two propionate groups. The spectrum at pH 10 has been described previously (59). On the basis of chemical shift data for other structurally-related aminocarboxylic acids (62,63,68), the down-field singlet was assigned to the acetate methylenic protons. The chemical shifts of the EDDDA resonances are pH dependent as illustrated by curve A for the acetate methylenic protons in Figure 10. The third and fourth ionization constants were determined from these data; the results are given in Table V.

The spectra of the acetate methylenic protons of the cadmium, zinc and lead complexes of 1,3-PDTA and EDDDA are reported in Chapter II. In most cases they consist of complex multiplet patterns due to inert metal-nitrogen bonding. To a first approximation, the resonances of the remaining carbon-bonded protons of these two complexed ligands appear the same as those of the uncomplexed ligands, but have different chemical shifts.

The chemical shifts of the acetate methylenic

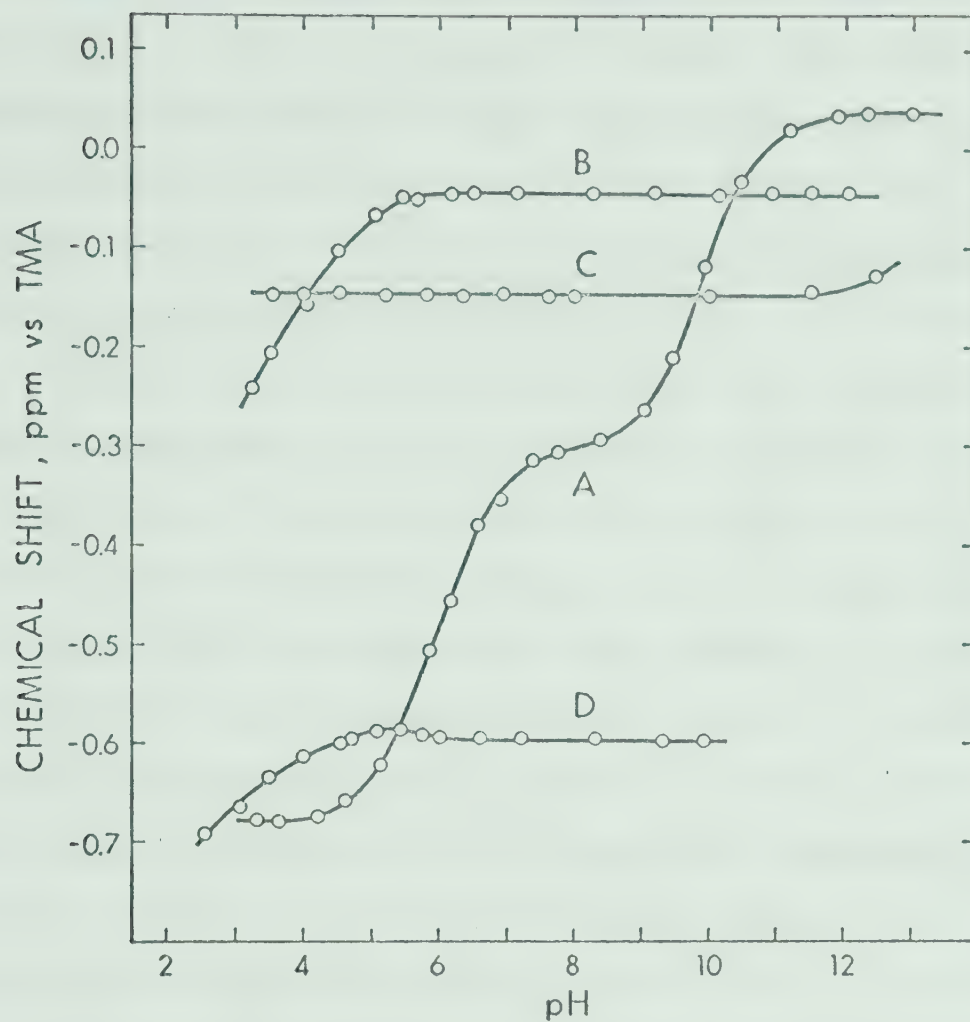


Figure 10: pH dependence of the chemical shift of the acetate methylenic protons of EDDDA. Curve A, 0.20 M EDDDA; curve B, 0.20 M Cd(EDDDA)²⁻; curve C, 0.20 M Zn(EDDDA)²⁻; curve D, 0.20 M Pb(EDDDA)²⁻.

protons of the cadmium, zinc and lead complexes of 1,3-PDTA and of EDDDA are pH dependent as shown by curves B, C and D in Figures 9 and 10. These data were obtained from solutions made up from equimolar quantities of both metal nitrate and ligand. For those complexes in which an AB pattern was observed, the chemical shift values used in these curves were the chemical shifts at the centres of the patterns. For all the metal complexes studied, the chemical shifts remain constant above a certain pH, corresponding to the chemical shifts of the 1:1 complexes. Below this pH, the resonances move towards those of the free ligand and are exchange-broadened. Calculations of the species present in solution for the 1,3-PDTA systems using the literature ionization constants in Table V and the literature formation constants (64-66) indicate that dissociation of the 1:1 complexes and formation of protonated complexes is occurring at those pH's when the resonances are shifting and are broadened. For example, calculations indicate that in a solution with a cadmium to 1,3-PDTA ratio of one, dissociation of the 1:1 complex and formation of a protonated complex begin to take place at pH less than 5.5. It is also below this pH that broadening and shifting of the resonance begins to take place

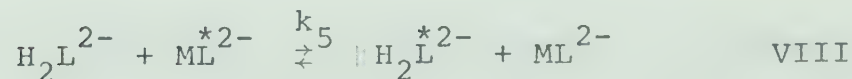
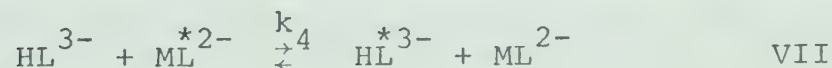
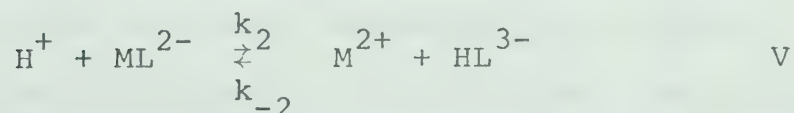
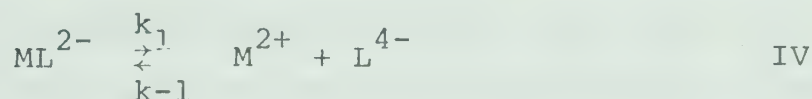
as can be seen from Figure 9. For the EDDDA systems, no formation constants are available for the protonated complexes, but such species are indicated by the exchange-broadening and the chemical shift data shown in Figure 10.

An attempt was made to calculate formation constants for the nonprotonated and the protonated complexes from the chemical shift data presented in Figures 9 and 10 using the method described previously (44). These formation constants would have been useful in subsequent calculations since they would have been obtained under ionic strength conditions similar to those used in all experiments reported in this work. This attempt, however, yielded inconsistent results, possibly because of the uncertainties in the chemical shift values of the observed resonances and those of the protonated complexes. The observed resonances are broad and hence it was difficult to measure their chemical shift positions. The chemical shift values of the protonated complexes could not be measured directly, but had to be approximated in the attempted calculation of formation constants. Therefore, in the subsequent rate constant determinations it was necessary to use literature values of the formation constants (64,65). However, the

error involved using these literature values is within the experimental error of the lifetime measurements.

Ligand Exchange Kinetics of the 1,3-PDTA Complexes

Exchange-broadening was observed in the pmr spectra of each of the 1,3-PDTA complexes under conditions where some noncomplexed ligand was present. From the broadening for a given set of experimental conditions, the mean lifetime τ between events which lead to exchange of the ligand from the free form to the complexed form or vice versa may be determined. The following reactions are considered to be pathways by which exchange can occur:



The AB multiplet patterns observed for the acetate

methylenic protons of $\text{Cd}(1,3\text{-PDTA})^{2-}$ and $\text{Zn}(1,3\text{-PDTA})^{3-}$ at intermediate pH values in the absence of non-complexed ligand, which were discussed in detail in Chapter II, indicate that for these conditions the mean lifetimes before AB interchange are greater than 0.1 sec. This value was obtained by computer-simulating spectra by the method described in Chapter II. Since AB interchange may occur even when the complex is partially bonded, the above lifetime is a lower limit for the mean lifetime of the complex before it completely dissociates via the reaction represented by Equation IV and indicates that the rate of this reaction is too slow to be measured by the pmr line-broadening method. Similarly the metal-proton coupling observed for the cadmium and lead complexes in the absence of noncomplexed ligand indicates that for these complexes the reaction represented by Equation IV contributes a negligible amount to the exchange-broadening (43). Neglecting this reaction, the rate equation for exchange of ligand from the free form to the complexed form is

$$\begin{aligned} \frac{-d[L_f]}{dt} = & k_{-2}[M^{2+}][HL^{3-}] + k_3[L^{4-}][ML^{2-}] + k_4[HL^{3-}][ML^{2-}] \\ & + k_5[H_2L^{2-}][ML^{2-}] \end{aligned} \quad \text{IX}$$

where $[L_f]$ represents the sum of the concentrations of the free ligand in the various protonated forms. The reciprocal of the mean lifetime of the free form, $1/\tau_{L_f}$, is related to the exchange rate, $-d[L_f]/dt$, by

$$\frac{1}{\tau_{L_f}} = - \frac{d[L_f]}{dt} \frac{1}{[L_f]} \quad \text{X}$$

which yields

$$\frac{1}{\tau_{L_f}} = k_{-2}\alpha_3[M^{2+}] + k_3\alpha_4[ML^{2-}] + k_4\alpha_3[ML^{2-}] + k_5\alpha_2[ML^{2-}] \quad \text{XI}$$

where $\alpha_2 = [H_2L^{2-}]/[L_f]$, $\alpha_3 = [HL^{3-}]/[L_f]$ and $\alpha_4 = [L^{4-}]/[L_f]$. Expressing the concentrations in terms of fractional concentrations and the term for the contribution from the reaction represented by Equation V in terms of $[ML^{2-}]$ by the relation $k_{-2}[M^{2+}] = k_2[H^+][ML^{2-}]/\alpha_3[L_f]$ yields

$$P_{L_f}/(\tau_{L_f} P_{ML}) = k_2[H^+] + (k_3\alpha_4 + k_4\alpha_3 + k_5\alpha_2)[L_f] \quad \text{XII}$$

where P_{L_f} and P_{ML} are the fractional concentrations of ligand in the free and complexed forms ($P_{L_f} + P_{ML} = 1$). The individual rate constants were evaluated from the dependence of τ_{L_f} on $[H^+]$ and $[L_f]$.

A typical example of the spectra obtained as a function of pH for a solution 0.10 M in both Cd(1,3-PDTA)²⁻ and free 1,3-PDTA is given in Figure 11. At pH 6.42 separate acetate methylenic proton resonances are observed for both the free and the complexed forms of 1,3-PDTA; only the two strong central peaks of the AB pattern for the complexed form can be seen. An increase in the pH results in broadening of the resonances indicating faster exchange. Since the linewidth of the free ligand resonance for most of the systems in this study could easily be measured over a wide range of solution conditions, τ_{L_f} was calculated using Equation XVIII, the slow exchange expression, which will be discussed in more detail in Chapter IV. The errors involved in determining the values of $1/\tau_{L_f}$ arise mainly from the linewidth measurements and are estimated to be between $\pm 5\%$ and $\pm 15\%$.

Lifetime data are given in Table VI for the Cd-1,3-PDTA system for experiments in which the pH was held constant at six different values and the concentration of free ligand was varied at each value. A typical plot using the data at pH 6.51 is shown in Figure 12. According to Equation XII, the slope of a plot of $P_{L_f}/(\tau_{L_f} P_{ML})$ vs. $[L_f]$ at constant

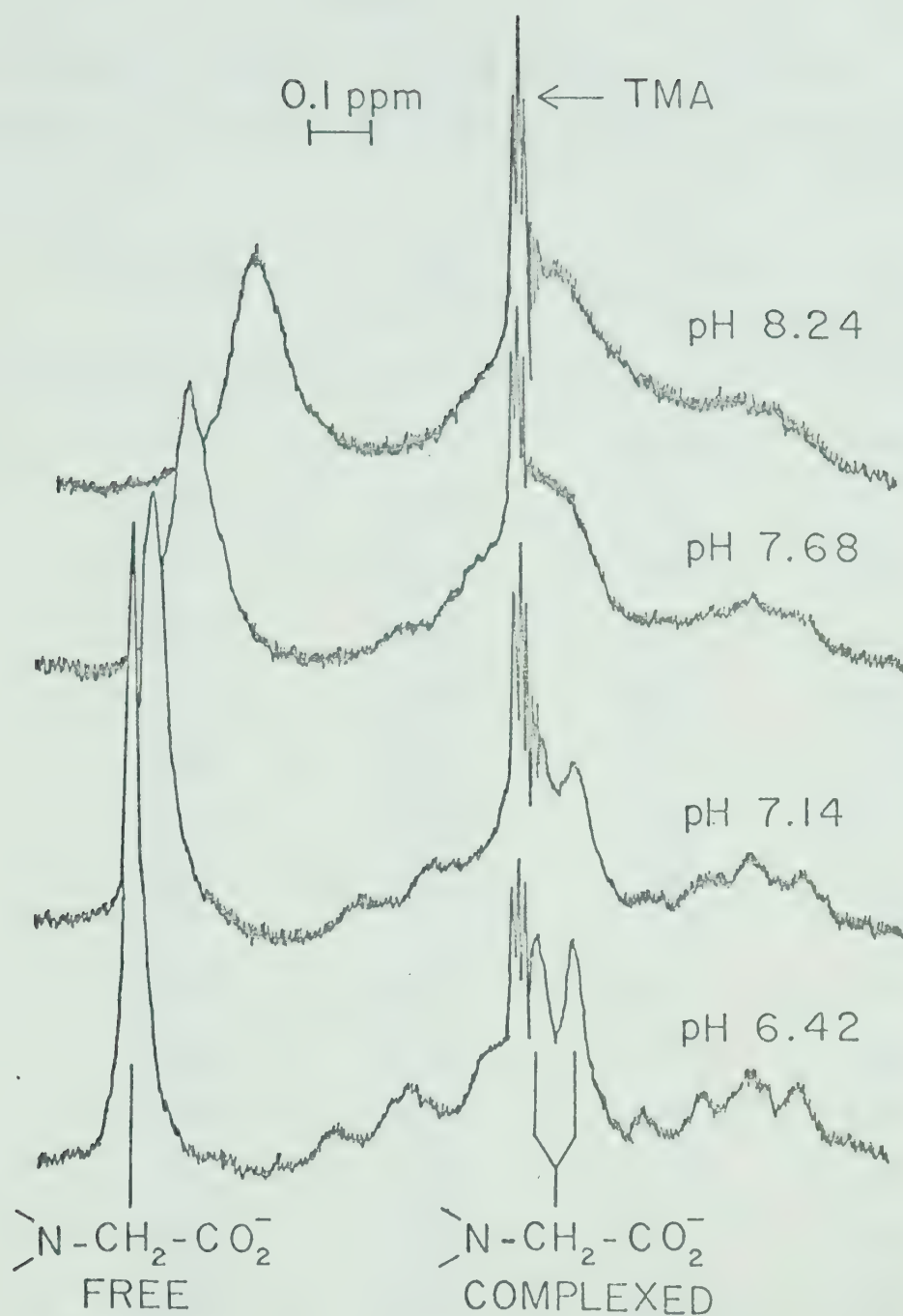


Figure 11: 60 MHz pmr spectra showing the acetate methylenic resonances for an aqueous solution containing both free 1,3-PDTA and Cd(1,3-PDTA)^{2-} at the indicated pH values. The solution was 0.1 M in both free 1,3-PDTA and Cd(1,3-PDTA)^{2-} .

Table VI

Kinetic Data for the Cd-1,3-PDTA System at Constant
pH Values as a Function of Free Ligand Concentration^{a,b}

pH	[L _f] (M)	P _{L_f} /P _{ML}	W _{1/2} ' (Hz)	1/τ _{L_f} (sec ⁻¹)
5.52	0.180	11.5	1.05	0.816
	0.162	5.28	1.26	1.48
	0.143	3.15	1.54	2.36
	0.125	2.10	1.87	3.39
	0.107	1.46	2.16	4.30
	0.090	1.04	2.49	5.34
	0.073	0.726	2.83	6.41
	0.057	0.497	3.37	8.10
5.72	0.180	11.5	0.99	0.691
	0.161	5.25	1.16	1.22
	0.143	3.16	1.39	1.95
	0.125	2.08	1.59	2.57
	0.107	1.45	1.74	3.05
	0.090	1.03	2.13	4.27
	0.073	0.724	2.38	5.06
	0.055	0.476	2.76	6.25

(Table VI, continued)

pH	$[L_f]$ (M)	P_{L_f}/P_{ML}	$W'_{1/2}$ (Hz)	$1/\tau_{L_f}$ (sec ⁻¹)
6.00	0.163	5.67	1.08	0.879
	0.145	3.39	1.18	1.19
	0.127	2.19	1.32	1.63
	0.109	1.53	1.51	2.23
	0.092	1.08	1.70	2.83
	0.075	0.763	1.87	3.36
	0.058	0.515	2.23	4.49
6.51	0.162	5.35	1.12	1.10
	0.143	3.13	1.33	1.76
	0.125	2.08	1.48	2.23
	0.107	1.45	1.74	3.05
	0.091	1.05	1.96	3.74
	0.074	0.742	2.15	4.33
	0.058	0.510	2.35	4.96
7.09	0.181	11.76	1.17	0.88
	0.162	5.32	1.50	1.92
	0.145	3.29	1.80	2.86
	0.127	2.18	2.00	3.49
	0.109	1.51	2.31	4.46
	0.092	1.08	2.55	5.21
	0.075	0.758	2.90	6.31
	0.059	0.527	3.16	7.33

(Table VI, continued)

pH	$[L_f]$ (M)	P_{L_f}/P_{ML}	$W'_{1/2}$ (Hz)	$1/\tau_{L_f}$ (sec ⁻¹)
8.03	0.182	12.43	1.78	2.79
	0.162	5.41	2.68	5.62
	0.144	3.21	3.48	8.13
	0.125	2.12	4.15	10.2
	0.108	1.48	4.73	12.1
	0.091	1.05	5.46	14.4
	0.074	0.740	6.00	16.1
	0.057	0.510	6.90	18.9

(a) 25°.

(b) $W_{1/2}$ of free ligand resonance for no ligand exchange is 0.73 Hz.

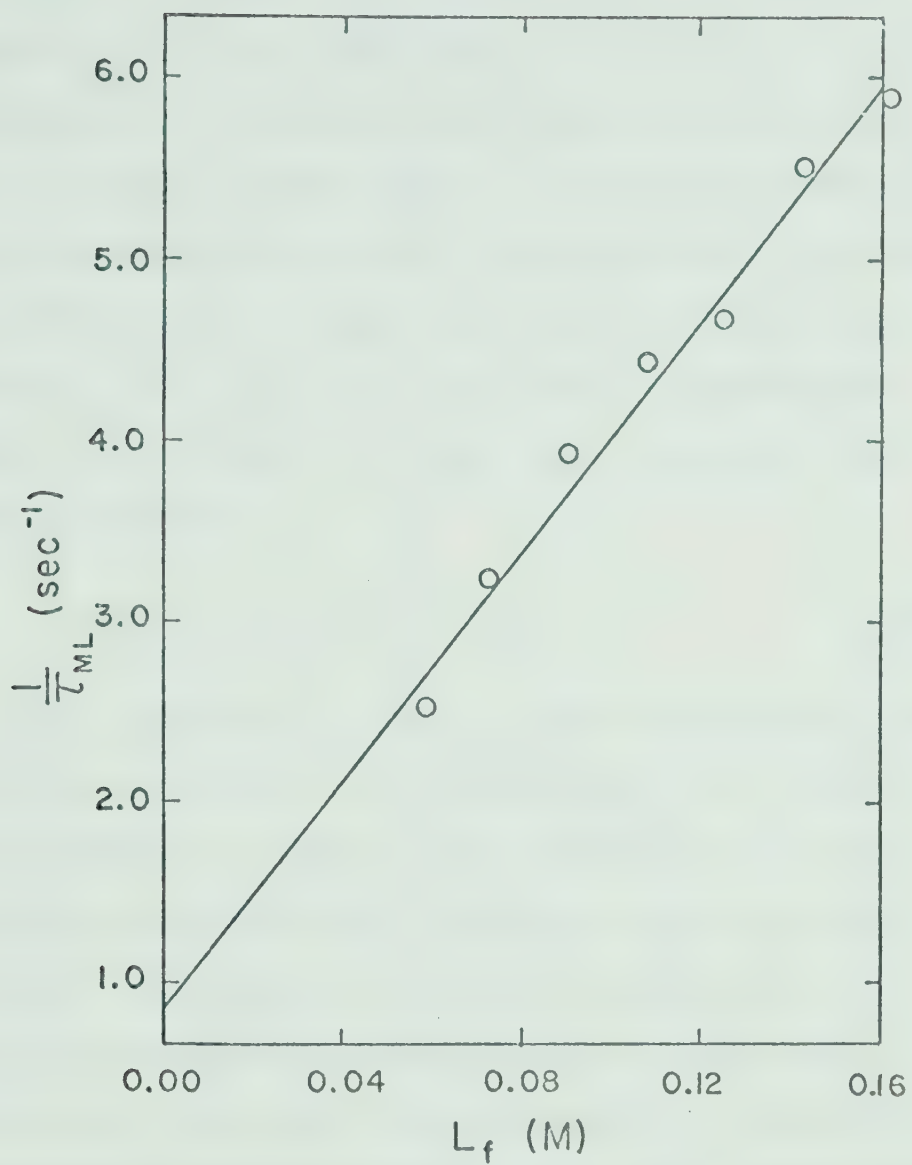


Figure 12: Pmr rate data for the Cd-1,3-PDTA system at pH 6.51 as a function of the free 1,3-PDTA concentration.

pH is equal to $k_3\alpha_4 + k_4\alpha_3 + k_5\alpha_2$ and the intercept is equal to $k_2[H^+]$. At the pH values listed in Table VI, α_3 ranges from factors of 10^5 to 3×10^2 greater than α_4 while k_3 has been found to be only 10 to 20 times larger than k_4 in similar reactions of EDTA complexes (39,40), suggesting that the term $k_3\alpha_4$ contributes a negligible amount to the slopes of the $P_{L_f}/(\tau_{L_f} P_{ML})$ vs. $[L_f]$ plots. Assuming the slope \underline{m} to be equal to $k_4\alpha_3 + k_5\alpha_2$, Equation XIII can be derived.

$$\underline{m}/\alpha_2 = k_4(\alpha_3/\alpha_2) + k_5 \quad \text{XIII}$$

Rate constants k_4 and k_5 were evaluated from the slope and intercept of a plot of \underline{m}/α_2 vs. α_3/α_2 ; the values for α_2 and α_3 were calculated from the literature dissociation constants listed in Table V. A linear least squares analysis was used for this and all subsequent determinations of slopes and intercepts. The rate constants and their standard deviations are given in Table VII. The uncertainty in the intercepts of the plots of $P_{L_f}/(\tau_{L_f} P_{ML})$ vs. $[L_f]$ for which the data are given in Table VI, was too large to allow evaluation of k_2 .

Lifetime data are given in Table VIII as a function of pH for a solution 0.10 M in both

Table VII

Experimentally Determined Ligand Exchange Rate Constants for
1,3-PDTA and EDDDA Complexes ^a

	$k_2 (M^{-1} \text{sec}^{-1})$	k_{-2}	k_3	k_4	k_5
$\text{Cd}(1,3\text{-PDTA})^{2-}$	$9.1(\pm 0.3) \times 10^5$	$4.1(\pm 0.1) \times 10^9$		$3.0(\pm 0.1) \times 10^{2b}$	$3.6(\pm 1.0) \times 10^b$
$\text{Pb}(1,3\text{-PDTA})^{2-}$	$2.0(\pm 0.1) \times 10^7$	$6.8(\pm 0.3) \times 10^{10}$	$2.0(\pm 0.9) \times 10^4$	$2.5(\pm 0.1) \times 10^{2c}$	$3.2(\pm 0.3) \times 10^c$
$\text{Zn}(1,3\text{-PDTA})^{2-}$	$3.9(\pm 0.1) \times 10^4$	$4.0(\pm 0.1) \times 10^9$		$1.5(\pm 0.2) \times 10^3$	$1.7(\pm 0.4) \times 10^2$
$\text{Cd}(\text{EDDDA})^{2-}$	$4.8(\pm 0.2) \times 10^6$	$4.0(\pm 0.2) \times 10^8$	$1.5(\pm 0.3) \times 10^3$	6.5 ± 0.2	$2.5(\pm 0.1) \times 10$
$\text{Pb}(\text{EDDDA})^{2-}$	$1.2(\pm 0.1) \times 10^7$	$2.5(\pm 0.2) \times 10^{10}$	$2.0(\pm 0.1) \times 10^4$		
$\text{Zn}(\text{EDDDA})^{2-}$	$2.0(\pm 0.1) \times 10^4$	$8.3(\pm 0.4) \times 10^8$			

(a) $\pm 25^\circ$.

(b) From experiments at constant pH and varying L_f .

(c) From experiments at constant L_f and varying pH.

Table VIII
Kinetic Data as a Function of pH for the
Cd-1,3-PDTA System^{a,b,c}

pH	$W'_{1/2}$ (Hz)	$1/\tau_{L_f}$ (sec ⁻¹)
4.80	6.23	17.3
4.99	4.78	12.7
5.23	3.53	8.80
5.49	2.84	6.64
5.76	2.20	4.62
6.00	2.04	4.12
6.24	1.95	3.84
6.42	1.85	3.51
6.51	1.95	3.84
6.84	2.35	5.09
7.14	2.73	6.28
7.68	4.58	12.1
8.24	6.25	17.3

(a) 0.10 M Cd(1,3-PDTA)²⁻ and 0.10 M free 1,3-PDTA.

(b) $W_{1/2}$ of free ligand resonance for no ligand exchange is 0.73 Hz.

(c) 25°.

$\text{Cd}(1,3\text{-PDTA})^{2-}$ and free 1,3-PDTA. As can be seen from these data and from the spectra in Figure 11, the rate of ligand exchange decreases as the pH is increased from 4.8, goes through a minimum at pH 6.4 and then increases as the pH is increased further. Above pH 8.5, the exchange rate is so fast that the lineshapes are of the intermediate to fast types. Since exchange occurs between a single line, an AB pattern, and the AB part of an ABX pattern, the theory is quite complicated and no attempt was made to evaluate lifetimes from data at pH's greater than 8.5.

Rate constant k_2 was obtained from the data in Table VIII at pH less than 6.4. At these pH's, α_4 is negligible relative to α_2 and α_3 , and the contribution to the total exchange by the reaction represented by Equation VI may be neglected. Since P_{L_f} equals P_{ML} , rearrangement of Equation XII leads to

$$\frac{1}{\tau_{L_f}} - (k_4\alpha_3 + k_5\alpha_2)[L_f] = k_2[H^+] \quad \text{XIV}$$

The value given in Table VII for k_2 was obtained from the slope of a plot of $1/\tau_{L_f} - (k_4\alpha_3 + k_5\alpha_2)[L_f]$ vs. $[H^+]$ using the data in Table VIII and the values

determined above for k_4 and k_5 . This plot is shown in Figure 13. Rate constant k_{-2} was obtained from k_2 using the relation $k_{-2} = k_2 K_4 K_f$ where K_f is the formation constant of $\text{Cd}(1,3\text{-PDTA})^{2-}$ (64-66).

Rate constants k_4 and k_5 were also determined from the data in Table VIII in the pH range 6.4 to 8.2. In this pH range, calculations using the value of k_2 show the amount of ligand exchange via the reaction represented by Equation V to be negligible. The reaction represented by Equation VI has also been neglected for reasons given above, leading to

$$\frac{1}{\tau_{L_f} [L_f]^{\alpha_2}} = k_4 \frac{\alpha_3}{\alpha_2} + k_5 \quad \text{XV}$$

by rearrangement of Equation XII. The values obtained for k_4 and k_5 from the slope and intercept of a plot of $1/(\tau_{L_f} [L_f]^{\alpha_2})$ vs. α_3/α_2 are given in Table VII.

Above pH 8.5, the rate of ligand exchange increases, as evidenced by the intermediate to fast exchange spectra, presumably due to increased contributions from the reactions represented by Equations VI and VII.

Lifetime data are given in Table IX as a function of pH for a solution 0.10 M in both $\text{Zn}(1,3\text{-PDTA})^{2-}$ and free 1,3-PDTA. Slow exchange spectra were obtained throughout the whole pH range studied and Equation

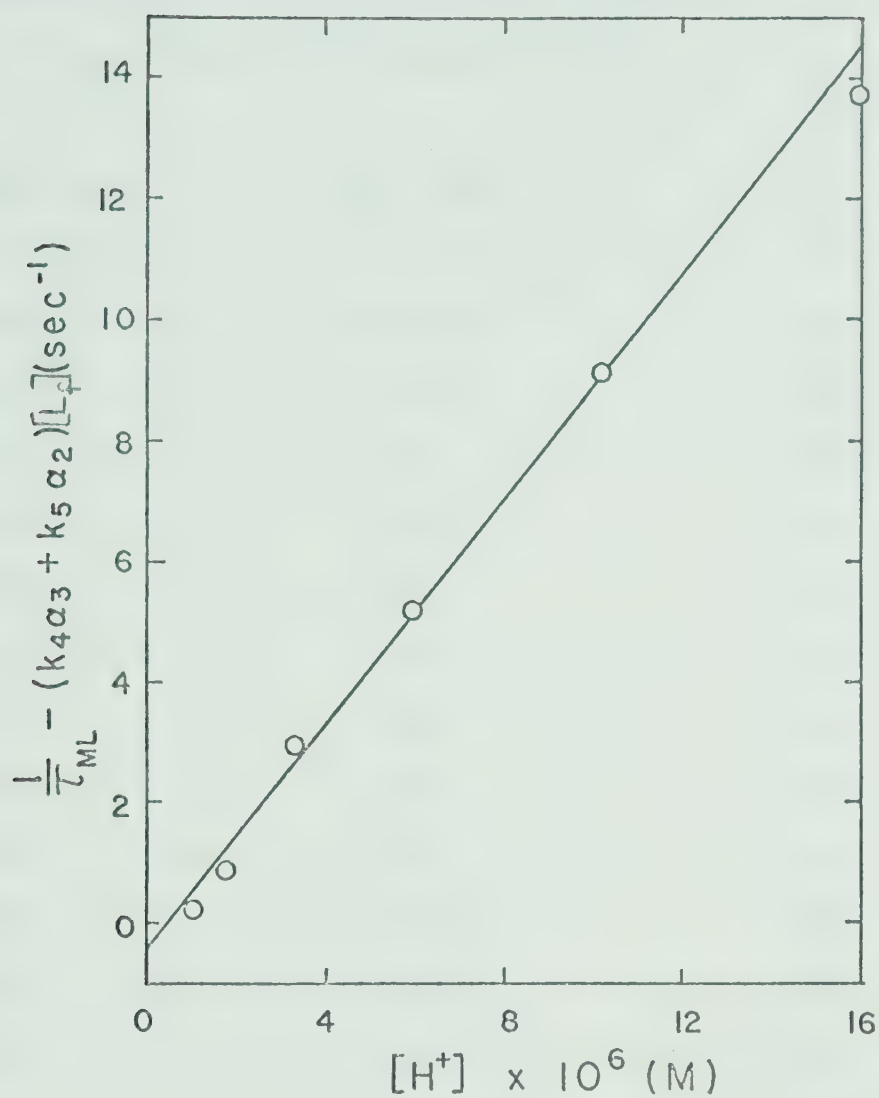


Figure 13: Pmr rate data for the Cd-1,3-PDTA system as a function of $[H^+]$.

Table IX
Kinetic Data as a Function of pH for the
Zn-1,3-PDTA System ^{a,b,c}

pH	$W'_{1/2}$ (Hz)	$1/\tau_{L_f}$ (sec ⁻¹)
3.64	4.35	11.34
4.03	2.72	6.22
4.65	1.90	3.64
4.97	1.75	3.17
5.60	1.55	2.54
6.03	1.53	2.48
6.34	1.55	2.54
6.68	1.49	2.36
7.02	1.44	2.20
7.53	1.35	1.92
7.95	1.25	1.60
8.38	1.12	1.19
9.01	0.98	0.75

(a) 0.10 M Zn(1,3-PDTA)²⁻ and 0.10 M free 1,3-PDTA.

(b) $W_{1/2}$ of free ligand resonance for no ligand exchange is 0.73 Hz.

(c) 25°.

XVIII was used to calculate the lifetime τ_{L_f} from the acetate methylenic proton resonance of the free 1,3-PDTA. As in the Cd-1,3-PDTA system, the rate constants k_4 and k_5 were obtained from the slope and intercept of a plot of $1/(\tau_{L_f} [L_f]^{\alpha_2})$ vs. α_3/α_2 using the kinetic data at pH's greater than 7. The value for k_2 was obtained from the slope of a plot of $1/\tau_{L_f} - (k_4\alpha_3 + k_5\alpha_2)[L_f]$ vs. $[H^+]$ using the lifetime data at pH less than 6 and the values of k_4 and k_5 determined above. All rate constants so obtained are listed in Table VII.

Intermediate to fast exchange spectra for the acetate methylenic protons are exhibited by the Pb-1,3-PDTA system; examples of such spectra are shown on the left hand side of Figure 14 for a 0.10 M solution of $Pb(1,3-PDTA)^{2-}$ at pH 7.00 which contained the indicated concentrations of free 1,3-PDTA. Because of the complexity of this exchange case, kinetic data were obtained from the experimental spectra by comparison with computer-simulated spectra. The simulation was accomplished with a four-site exchange program (43) formulated using modified Bloch equations. The four sites are free 1,3-PDTA and 1,3-PDTA complexed to lead in three different nuclear spin states, $+1/2$ and $-1/2$ for ^{207}Pb and

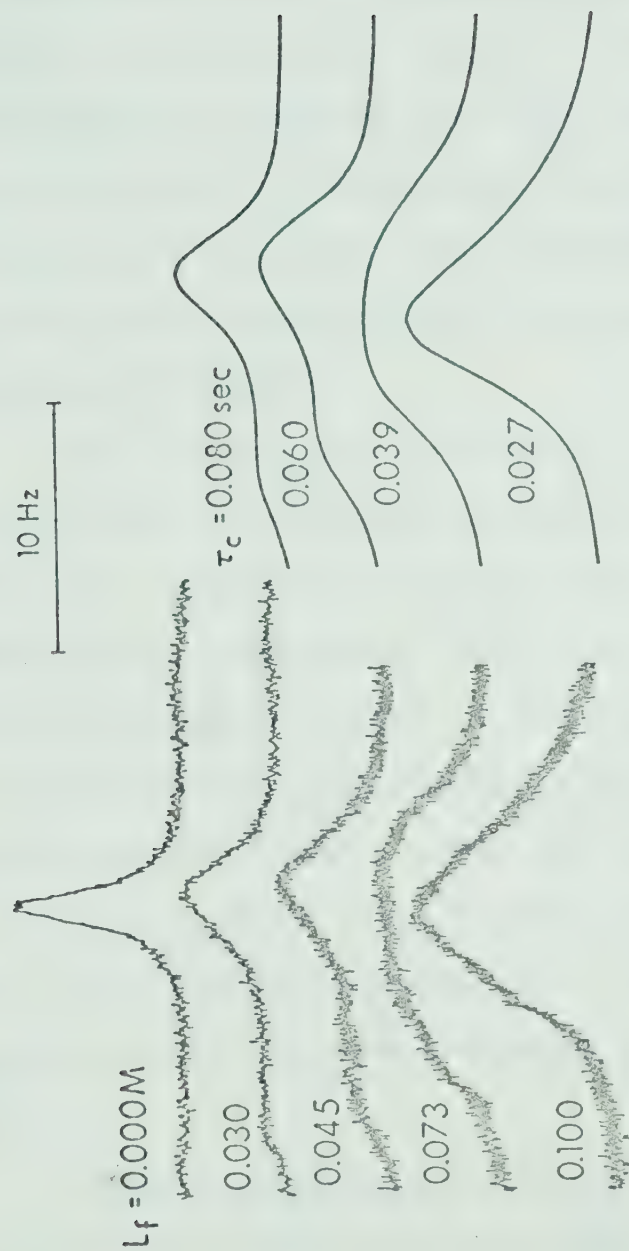


Figure 14: Representative experimental (left) and theoretical (right) 60 MHz pmr spectra of the acetate methylenic protons of an aqueous solution of $\text{Pb}(1,3\text{-PDTPA})^{2-}$ containing the indicated concentrations of free 1,3-PDTPA at pH 7.00.

zero for all the other lead isotopes. The procedure was to simulate a series of spectra as a function of the mean lifetime of the Pb-1,3-PDTA complex before ligand exchange τ_{ML} , using the following input parameters: populations, chemical shifts and natural linewidths at each of the four sites. The individual lifetimes for given solution conditions were then obtained by comparing the linewidths of the resonance peaks and by superimposing the experimental and calculated spectra.

The lifetime data presented in Table X were obtained from experiments in which the pH was held constant and the free ligand concentration was varied. The matched experimental and computer-simulated spectra shown in Figure 14 are typical of the fits obtained in such experiments. Applying Equation XII to the above lifetime data, the slopes of the plots of $P_{L_f} / (\tau_{L_f} P_{ML})$ vs. $[L_f]$ yielded the values for k_3 , k_4 and k_5 listed in Table VII. The intercepts of such plots gave an approximate value of $2.2 \times 10^7 \text{ M}^{-1} \text{ sec}^{-1}$ for k_2 .

A more precise value for k_2 was obtained using the data given in Table XI which gives the pH dependence of $1/\tau_{L_f}$ for a solution 0.10 M in both $\text{Pb}(1,3\text{-PDTA})^{2-}$ and free 1,3-PDTA. Equation XIV was applicable in

Table X
Kinetic Data for the Pb-1,3-PDTA System at
Constant pH Values as a Function of Free
Ligand Concentration ^a

pH	[L _f] (M)	P _{L_f} /P _{ML}	1/τ _{L_f} (sec ⁻¹) ^b
6.00	0.015	0.153	163
	0.030	0.307	93.2
	0.044	0.468	69.2
	0.058	0.634	52.5
	0.073	0.808	45.9
	0.087	0.980	39.6
	0.100	1.15	36.5
	0.114	1.34	33.1
7.00	0.015	0.155	32.3
	0.030	0.314	39.8
	0.045	0.479	34.9
	0.059	0.639	35.7
	0.073	0.808	31.7
	0.087	0.984	31.7
	0.100	1.16	29.2
	0.113	1.33	27.9
9.03	0.015	0.157	79.6
	0.030	0.314	290
	0.045	0.474	201
	0.059	0.645	174
	0.074	0.814	189
	0.089	1.00	185
	0.103	1.18	212

(a) 25°.

(b) Determined by matching experimental and computer-simulated spectra.

Table XI
Kinetic Data as a Function of pH for the
Pb-1,3-PDTA System ^{a,b}

pH	$1/\tau_{L_f} \text{ (sec}^{-1}\text{)}$ ^c
4.64	465
4.87	303
5.31	108
5.83	50.0
6.71	31.9

(a) 0.10 M Pb(1,3-PDTA)²⁻ and 0.10 M free 1,3-PDTA.

(b) 25°.

(c) Determined by matching experimental and computer-simulated spectra.

this case, so that the slope of a plot of $1/\tau_{L_f} - (k_4\alpha_3 + k_5\alpha_2)[L_f]$ vs. $[H^+]$ yielded the value for k_2 shown in Table VII. Rate constant k_{-2} was obtained from the relation $k_{-2} = k_2K_4K_f$.

Ligand Exchange Kinetics of the EDDDA Complexes

The reactions represented by Equations IV to VIII were considered to be the predominant pathways by which EDDDA exchanges between the free and complexed forms for the solution conditions used in this work. As in the 1,3-PDTA systems, the AB multiplet patterns observed for the acetate methylenic protons of the EDDDA complexes at intermediate pH values in the absence of noncomplexed ligand indicate that the mean lifetime of the complexes before first order dissociation by the reaction represented by Equation IV is greater than 0.1 sec. Thus, this reaction can be neglected in the kinetic analysis of the data. Free ligand lifetimes were determined from the linewidths of the exchanged-broadened acetate resonance of the free ligand using Equation XVIII.

Lifetime data for the Cd-EDDDA system for experiments in which the pH was held constant and the free ligand concentration was varied are given in Table XII. Using Equation XII, the slopes obtained from

Table XII
Kinetic Data for the Cd-EDDDA System at
Constant pH Values as a Function of
Free Ligand Concentration ^{a,b}

pH	[L _f] (M)	P _{L_f} /P _{ML}	W' _{1/2} (Hz)	1/τ _{L_f} (sec ⁻¹)
8.20	0.160	5.02	1.28	0.82
	0.140	2.92	1.40	1.19
	0.121	1.93	1.57	1.73
	0.102	1.29	1.75	2.30
	0.084	0.898	1.87	2.67
	0.066	0.613	2.04	3.20
8.50	0.160	4.95	1.57	1.82
	0.141	2.94	1.85	2.70
	0.122	1.95	2.16	3.68
	0.103	1.31	2.31	4.15
	0.084	0.894	2.63	5.15
	0.066	0.608	3.18	6.88

(a) 25°.

(b) W_{1/2} of free ligand resonance for no ligand exchange
is 1.03 Hz.

plots of $P_{L_f}/(\tau_{L_f} P_{ML})$ vs. $[L_f]$ yielded the value for k_3 listed in Table VII and values of zero within experimental error for k_4 and k_5 , indicating that the latter rate constants are too small to be measured by the pmr method. From the lifetime data as a function of pH for a solution 0.10 M in both $Cd(EDDDA)^{2-}$ and free EDDDA shown in Table XIII, the value for k_2 was determined. Over the pH range studied, Equation XII could be reduced to

$$\frac{1}{\tau_{L_f}} = k_2 [H^+] \quad \text{XVI}$$

The terms in k_4 and k_5 were neglected because it was shown above that their exchange contributions are too small to be detected by pmr line-broadening methods. Knowing the value of k_3 , calculations indicated that the term containing this rate constant could also be neglected. For the given solution conditions

$P_{L_f} = P_{ML}$, and the slope of the plot of $1/\tau_{L_f}$ vs. $[H^+]$ yielded the value for k_2 shown in Table VII.

Lifetime data for the Pb-EDDDA system at constant pH varying the free ligand concentration are presented in Table XIV. Using Equation XII the slopes obtained from plots of $P_{L_f}/(\tau_{L_f} P_{ML})$ vs. $[L_f]$ yielded the value of k_3 listed in Table VII and values of zero within

Table XIII

Kinetic Data as a Function of pH for the
Cd-EDDDA System ^{a,b,c}

pH	$W'_{1/2}$ (Hz)	$1/\tau_{L_f}$ (sec ⁻¹)
5.60	5.28	13.3
5.74	4.09	9.61
5.90	3.44	7.57
5.99	3.13	6.59
6.15	2.63	5.02
6.37	2.04	3.17
6.67	1.59	1.76
7.03	1.32	0.91

(a) 25°C.

(b) 0.10 M Cd(EDDDA)²⁻ and 0.10 M free EDDDA.

(c) $W_{1/2}$ of free ligand resonance for no ligand exchange is 1.03 Hz.

Table XIV
Kinetic Data for the Pb-EDDDA System
at Constant pH Values as a Function of
Free Ligand Concentration ^{a,b}

pH	[L _f] (M)	P _{L_f} /P _{ML}	W _{1/2} ' (Hz)	1/τ _{L_f} (sec ⁻¹)
7.20	0.178	9.87	1.26	0.818
	0.156	4.37	1.56	1.76
	0.135	2.49	1.84	2.64
	0.113	1.59	2.16	3.64
	0.0924	1.04	2.43	4.50
	0.0727	0.70	2.85	5.81
	0.0530	0.44	3.18	6.85
7.50	0.178	9.88	1.50	1.60
	0.159	4.81	1.91	2.91
	0.141	2.94	2.26	3.99
	0.123	1.98	2.64	5.19
	0.105	1.38	3.02	6.39
	0.0875	0.981	3.33	7.35
	0.0702	0.685	3.66	8.40
	0.0534	0.460	4.55	11.2

(a) 25°C

(b) W_{1/2} of free ligand resonance for no ligand exchange is 1.03 Hz.

experimental error for k_4 and k_5 . Data as a function of pH for this system are given in Table XV. In the determination of k_2 from these data, Equation XII was reduced to

$$\frac{1}{\tau_{L_f}} - k_3 \alpha_4 [L_f] = k_2 [H^+] \quad \text{XVII}$$

In this case the term containing k_3 was too large to be neglected over the pH range shown in Table XV. Therefore, a plot of $1/\tau_{L_f} - k_3 \alpha_4 [L_f]$ vs. $[H^+]$ yielded the value of k_2 given in Table VII.

For the Zn-EDDDA system it was found that the rates of the reactions represented by Equations VI to VIII are too slow to be measured by pmr line-broadening methods. The value for k_2 , however, was determined from the slope of a plot of $1/\tau_{L_f}$ vs. $[H^+]$ using the lifetime data in Table XVI.

B. DISCUSSION

Mechanism of Formation of the $M(1,3\text{-PDTA})^{2-}$ and $M(\text{EDDDA})^{2-}$ Complexes

In the present investigation, the rate constants for the complexation of cadmium and zinc by mono-protonated 1,3-PDPA (k_2 in Table VII) were found to be essentially the same as those with mono-

Table XV
Kinetic Data as a Function of pH
for the Pb-EDDDA System ^{a,b,c}

pH	$W'_{1/2}$ (Hz)	$1/\tau_{L_f}$ (sec ⁻¹)
6.30	3.08	6.15
6.50	2.50	4.34
6.77	2.27	3.62
6.97	2.25	3.77

(a) 25°C.

(b) 0.10 M Pb(EDDDA)²⁻ and 0.10 M free EDDDA.

(c) $W_{1/2}$ of free ligand resonance for no ligand exchange is 1.03 Hz.

Table XVI
Kinetic Data as a Function of pH
for the Zn-EDDDA System ^{a,b,c}

pH	$W_{1/2}'$ (Hz)	$1/\tau_{L_f}$ (sec ⁻¹)
3.48	2.99	6.28
3.67	2.46	4.62
3.87	1.88	2.80
4.06	1.59	1.89
4.26	1.31	1.01
4.46	1.16	0.54

(a) 25°C.

(b) 0.10 M Zn(EDDDA)²⁻ and 0.10 M free EDDDA.

(c) $W_{1/2}$ of free ligand resonance for no ligand exchange is 1.03 Hz.

protonated EDTA (15,24,34). This finding contrasts with that of Pearson and de Wit (69) who determined that the rate of the reaction of zinc with monoprotonated EDTA was less than that with monoprotonated 1,3-PDTA using stopped-flow kinetic measurements. Their results can only be considered approximate, however, since the observed rates were just at the detection limits for their stopped-flow apparatus. The rate constants for complexation of cadmium, zinc and lead by monoprotonated EDDDA are from 2.5 to 10 times smaller than the corresponding ones with monoprotonated 1,3-PDTA.

In the dissociative mechanism (1,70) of complex formation, the reaction takes place in a stepwise fashion, with metal ion and ligand first diffusing together to form an outer-sphere complex. A water molecule then dissociates from the aquated metal ion and a donor group of the multidentate ligand coordinates at the vacated site. When a second water molecule dissociates at a position *cis* to the metal-ligand bond the second metal-ligand bond forms. The reaction continues with a separate step for each of the bonds. Depending on the structure of the ligand, the rate of formation of a specific metal-ligand bond will govern the complexation rate. For the majority of complexes whose formation kinetics have been studied,

formation of the first bond is rate-determining, its rate being governed by the rate of water dissociation from the aquated metal ion in the outer-sphere complex (70).

A possible sequence for the stepwise reaction of aquated metal ions with monoprotonated hexadentate ligands of the EDTA type is shown in Figure 1. Reaction proceeds by dissociation of water molecules followed by metal-ligand bond formation to yield an intermediate in which the three dentates of one end of the ligand are metal-coordinated while coordination at the other end is blocked by the proton on the nitrogen. For further coordination to occur, the second metal-nitrogen bond has to form before the intermediate dissociates to reactants. Presumably the second metal-nitrogen bond can form only after the proton has been transferred to a carboxylate oxygen or to a solvent molecule.

The similarity of the rate constants for the reaction of monoprotonated EDTA and 1,3-PDTA with aquated cadmium and zinc (k_2) suggests that, once the nitrogen-protonated intermediate has formed with these ligands, coordination of the remaining dentates is not rate-determining. If it were rate-determining, it is likely the overall complexation rate constants

for monoprotonated 1,3-PDTA would be less than those for monoprotonated EDTA due to closure of the six-membered ring which is necessary in the former complexes. Kustin and coworkers (47,48) have found that when ring closure is the rate-determining step, the rates of certain complex formation reactions are slower when six-membered rings are involved than when five-membered rings must be closed. The present results are consistent with the rate-determining step being formation of one of the first three metal-ligand bonds, its rate being governed by the rate of water loss from the metal ion.

The smaller rate constants for reaction with monoprotonated EDDDA (k_2) suggest that the rate-determining step is different in these reactions. It is possible that, when the first ligand dentate to bond is a propionate carboxylate oxygen, the rate of formation of the metal-nitrogen bond to close the six-membered chelate ring is less than when the first ligand dentate to bond is an acetate carboxylate oxygen. If this were the only factor responsible for the smaller rate constants, the rates of complexation with monoprotonated EDDDA should be at least half those with monoprotonated 1,3-PDTA.

A larger decrease, the magnitude of which would

be metal ion dependent, might result if the rates of dissociation of the nitrogen-protonated intermediates in the EDDDA reactions are sufficiently large that a significant amount of intermediate dissociates to reactants prior to proton transfer from the nitrogen atom. Kinetic data are not available for model tridentate complexes from which the rates of dissociation of the nitrogen-protonated, tridentate intermediates of 1,3-PDTA and EDDDA can be obtained. However, assuming the rate constants for formation of the nitrogen-protonated intermediates to be equal to the rate constants for the reaction with monoprotonated 1,3-PDTA (k_{-2}) and the formation constants for the intermediates to be approximately those of complexes of model tridentate ligands, order of magnitude rates of intermediate dissociation can be predicted. The dissociation rate constant is given by k_{-2}/K_f , where K_f is the formation constant. Using the formation constants of the iminodiacetic acid (IDA) complexes (71) as approximate values for tridentate coordination to monoprotonated 1,3-PDTA and assuming the analogous formation constants with monoprotonated EDDDA to lie between those for IDA and iminodipropionic acid, the predicted value for the dissociation rate constant of the cadmium inter-

mediate with 1,3-PDTA is $1.8 \times 10^4 \text{ sec}^{-1}$ while that with EDDDA is between 1.8×10^4 and $1.1 \times 10^6 \text{ sec}^{-1}$. The predicted value for the dissociation rate constant of the zinc intermediate with 1,3-PDTA is $3.7 \times 10^2 \text{ sec}^{-1}$ while that with EDDDA is between 3.7×10^2 and $4.5 \times 10^4 \text{ sec}^{-1}$. The formation constant of the lead complex of iminodipropionic acid is not available.

The reaction by which the proton leaves the nitrogen to permit formation of the second metal-nitrogen bond could involve either direct transfer to solvent water or migration to a neighbouring carboxylate group. The kinetics of these two reactions for the nitrogen-protonated isomer of neutral glycine have been studied by Sheinblatt and Gutowsky (72), who report a pseudo first order rate constant of 5 sec^{-1} for the transfer of the nitrogen-bonded proton to water and a rate constant of 175 sec^{-1} for migration of the proton to the carboxylate group. The rate constants for proton transfer in the nitrogen-protonated intermediates of 1,3-PDTA and EDDDA would probably be somewhat larger than either of those for glycine because of charge-charge interaction between the metal ion and the proton and the additional carboxylate group to which proton transfer can occur.

The preceding considerations suggest that the rates of dissociation of the metal ions from the EDDDA intermediates are larger than from the corresponding 1,3-PDTA intermediates, and that they may be comparable to the rate of proton transfer from the nitrogen atom. If so, there is a greater chance that EDDDA intermediates will dissociate before proton transfer and formation of the second metal-nitrogen bond can take place, and consequently k_{-2} would be less for the EDDDA complexes. The preceding considerations also suggest that the rate of reaction with cadmium should be decreased more than with zinc, as observed experimentally. If these conclusions are correct, a further decrease would be predicted for the formation reactions of the monoprotonated form of ethylenediaminetetrapropionic acid. Pearson and de Wit (69) found this to be the case for the zinc complex.

Second Order Ligand Displacement Reactions

The reactions represented by Equations VI to VIII are second order ligand displacement reactions. The mechanism (7,24,73) for similar EDTA type ligand exchange reactions has been demonstrated to involve the bound ligand being successively displaced by

the incoming ligand with intermediates present in which both ligands are simultaneously bound in varying degrees to the metal ion. The mechanism for the ligand displacement reactions studied in this chapter is probably similar. Comparison of the rate constants k_3 , k_4 and k_5 in Table VII for the cadmium and lead complexes of 1,3-PDTA shows a decrease in the values with increasing degree of protonation of the incoming ligand, indicating that proton transfer might be a rate-determining step in these reactions. Similar results have been found for other systems (7,39,40,44,73).

CHAPTER IV

EXPERIMENTAL

A. CHEMICALS

1,3-PDTA was synthesized by the method of Weyh and Hamm (74). The following analytical data were obtained for the ligand: Calculated for $C_{11}H_{18}N_2O_8$: C, 43.1; H, 4.9; N, 9.1. Found, C, 42.9; H, 5.1; N, 9.1. The 1,4-BDTA was prepared by Dr. George Blakney by a procedure analogous to that used for 1,3-PDTA. EDDDA (Lamont Laboratories) was used without further purification. No impurities could be detected in the pmr spectra of solutions of each of these ligands. Reagent grade metal nitrate salts were used as received. Tetramethylammonium (TMA) hydroxide (Eastman Organic Chemicals), tertiary-butanol (t-butanol) and 1,4-dioxane (Fisher Scientific) were used as received.

B. SOLUTIONS

A stock solution of TMA nitrate, used as a reference for some of the chemical shift measurements, was prepared by titration of a 25% aqueous solution of TMA hydroxide with nitric acid to a neutral pH.

The solutions used in the pmr measurements were prepared in either triply distilled water or in D_2O from the appropriate amounts of metal salt and ligand at concentrations varying between 0.10 and 0.20 M. For making chemical shift measurements TMA or t-butanol was added at concentrations of 0.01 M and 0.03 M respectively to serve as a reference. To avoid dilution, the pH or pD was adjusted with concentrated HNO_3 , KOH or KOD and samples of about 0.5 ml were withdrawn at appropriate pH or pD values. When kinetic measurements were being made at constant pH as a function of free ligand (or metal nitrate) concentration, the requisite amount of ligand (or metal nitrate) was added, the pH adjusted and a sample withdrawn. More ligand was added to the solution and the same procedure followed for all samples at this pH. The concentrations were corrected for the decreasing solution volume. Since high concentrations are necessary in the pmr experiment, no attempt was made to control the ionic strength.

C. pH MEASUREMENTS

All pH measurements were made at 25°C with an

Orion Model 801 pH meter equipped with either a standard glass electrode and a fibre-junction saturated calomel reference electrode or a micro-combination electrode. Saturated potassium acid tartrate and 0.01 M sodium tetraborate solutions, pH 3.56 and 9.18 at 25°, were used to standardize the meter. For D₂O solutions, the meter readings were converted to pD values using the expression of Glascoe and Long (75)

$$\text{pD} = \text{pH meter reading} + 0.40.$$

D. PMR MEASUREMENTS

The proton spectra were obtained at 60 MHz on a Varian A-60D, at 100 MHz on a Varian HA-100 and at 220 MHz on a Varian HR-220 spectrometer. These instruments were equipped with Varian variable temperature controllers. The temperature of the probe was determined using the standard methanol and ethylene glycol solutions and the plot of chemical shift vs. temperature prepared by Varian.

At 60 MHz, spectra were recorded at sweep rates of 0.1 Hz/sec for both the chemical shift and line-shape measurements. The chemical shifts are reported in ppm relative to the central resonance of the TMA

triplet which is 3.17 ppm downfield from the methyl resonance of sodium 3-(trimethylsilyl)-1-propane sulfonic acid. For linewidth measurements, each spectrum was recorded at least four times and the linewidths at half height of the resonances in the individual spectra were averaged.

The HA-100 spectrometer was operated in the frequency sweep mode with the methyl resonance of internal t-butanol providing the lock signal. Interference from the water resonance necessitated the use of D_2O as the solvent. Each spectrum was recorded at least four times at sweep rates of 0.1 Hz/sec for the linewidth measurements. Frequencies were measured from the differences between the manual and sweep oscillator frequencies.

At 220 MHz the chemical shift differences and linewidths were measured directly from the spectra.

E. KINETIC APPLICATIONS OF NUCLEAR MAGNETIC RESONANCE

The basic theories used in the study of chemical exchange by nuclear magnetic resonance (nmr) have been treated extensively in several monographs and review articles (50,76-79). Two of these theories, the modified Bloch approach and density matrix theory,

have been utilized in the present work to extract kinetic data from the pmr spectra. Only a brief qualitative description of these two approaches will be given.

Bloch (80) obtained a set of equations to describe the variation of the components of the total nuclear magnetic moment per unit volume for a collection of nuclei with non-zero spins in the presence of a varying magnetic field. The simplest chemical exchange system which may be studied by nmr is one for which the nuclei may interchange between two different chemical environments, A and B with different Larmour frequencies. For this case, there will be two independent magnetic moments for environments A and B which can be described by the Bloch equations. Addition of terms to these equations to account for the transfer of magnetization between the two sites leads to the modified Bloch equations (81). From these equations a general expression may be derived describing the intensity of the nmr absorption at a given frequency when there is exchange between the sites (82,83). This general equation may be simplified under certain limiting conditions.

One such condition is that of slow exchange for which the spectrum consists of two separate resonances

at frequencies δ_A and δ_B (in Hz). For this situation the lifetimes τ_A and τ_B of the nuclei in each of the sites before exchange to the other site are large compared to the inverse of the separation of the resonances; that is, $\tau_A, \tau_B > (\delta_A - \delta_B)^{-1}$. These lifetimes may be determined from the extent of broadening of each of the resonances by an equation of the form (76),

$$\frac{1}{\tau_A} = \pi (W'_{1/2,A} - W_{1/2,A}) \quad \text{XVIII}$$

where $W'_{1/2,A}$ is the linewidth at half height of the exchange-broadened resonance of nuclei at site A and $W_{1/2,A}$ is the linewidth of the same resonance in the absence of exchange. An analogous equation may be written for the lifetime τ_B . The natural linewidth $W_{1/2,A}$ is related to the effective spin-spin relaxation time $T_{2,A}$ by the relation $1/T_{2,A} = \pi W_{1/2,A}$. The effective spin-spin relaxation time takes into account the actual spin-spin relaxation time and broadening due to magnetic field inhomogeneities.

For the condition of intermediate exchange, the lifetimes are of the order of the inverse of the separation of the resonances and the spectrum consists of the transition from two resonances to one. When the

lifetimes are small compared to the inverse of the separation of the resonances, rapid exchange occurs and the spectrum consists of one resonance at an intermediate frequency between δ_A and δ_B .

Most of the ligand exchange systems studied in Chapter III are ones for which Equation XVIII is applicable. The two sites are free ligand and complexed ligand.

The modified Bloch equation approach may be extended to the many-site exchange problem by the addition of appropriate exchange terms and the derivation of an expression describing the intensity of the nmr absorption as a function of the frequency. The lifetimes in the individual sites may then be obtained by computing theoretical spectra and matching them to the experimental spectra. Such an approach was used for the Pb-1,3-PDTA exchange system which was analyzed as a four-site exchange problem.

The exchange problem becomes much more complex when there is spin-spin coupling between the nuclei at the different sites. For such systems the modified Bloch approach is no longer valid; however, a quantum mechanical method based on the use of density matrices is applicable. In this theoretical treatment (78,79), exchange and relaxation matrix

terms are added to the basic density matrix equation using as the basis set the spin product functions for the spin system in question. A final lineshape expression for the nmr absorption spectrum can then be derived. For an AB spin system, the lifetimes τ_A or τ_B may be obtained by computing theoretical spectra using the above lineshape expression and matching them to the experimental spectra. Such an approach was used in Chapter II for determining the lifetimes before AB interchange.

BIBLIOGRAPHY

1. R. G. Wilkins, Accounts Chem. Res., 3, 408 (1970).
2. A. K. Ahmed and R. G. Wilkins, J. Chem. Soc., 3700 (1959).
3. D. W. Margerum, D. B. Rorabacher and J. F. G. Clarke, Jr., Inorg. Chem., 2, 667 (1963).
4. D. W. Margerum, Rec. Chem. Progress, 24, 237 (1963).
5. D. W. Margerum and T. J. Bydalek, Inorg. Chem., 1, 852 (1962).
6. D. W. Margerum, D. L. Janes and H. M. Rosen, J. Amer. Chem. Soc., 87, 4463 (1965).
7. D. B. Rorabacher and D. W. Margerum, Inorg. Chem., 3, 382 (1964).
8. D. W. Margerum and H. M. Rosen, ibid., 7, 299 (1968).
9. R. J. Day and C. N. Reilley, Anal. Chem., 36, 1073 (1964).
10. S. Chan, R. J. Kula and D. T. Sawyer, J. Amer. Chem. Soc., 86, 377 (1964).
11. Y. O. Aochi and D. T. Sawyer, Inorg. Chem., 5, 2085 (1966).
12. T. J. Bydalek and D. W. Margerum, J. Amer. Chem. Soc., 83, 4326 (1961).
13. L. V. Haynes and D. T. Sawyer, Inorg. Chem., 6, 2146 (1967).
14. B. B. Smith and D. T. Sawyer, ibid., 7, 2020 (1968).
15. G. H. Reed and R. J. Kula, ibid., 10, 2050 (1971).
16. G. L. Blackmer and J. L. Sudmeier, ibid., 10, 2019 (1971).
17. J. L. Sudmeier, A. J. Senzel, and G. L. Blackmer, ibid., 10, 90 (1971).

18. R. J. Day and C. N. Reilley, Anal. Chem., 37, 1326 (1965).
19. T. J. Bydalek and D. W. Margerum, Inorg. Chem., 2, 678 (1963).
20. R. J. Kula, Anal. Chem., 39, 1171 (1967).
21. J. I. Legg and D. W. Cooke, Inorg. Chem., 4, 1576 (1965).
22. D. W. Cooke, ibid., 5, 1141 (1966).
23. P. Letkeman and J. B. Westmore, Can. J. Chem., 49, 2073 (1971).
24. J. L. Sudmeier and C. N. Reilley, Inorg. Chem., 5, 1047 (1966).
25. M. Saunders and F. Yamada, J. Amer. Chem. Soc., 85, 1882 (1963).
26. C. H. Bushweller and J. W. O'Neal, ibid., 92, 2159 (1970).
27. W. R. Morgan and D. E. Leyden, ibid., 92, 4527 (1970).
28. D. E. Leyden and W. R. Morgan, J. Phys. Chem., 75, 3190 (1971).
29. D. L. Rabenstein and B. J. Fuhr, Inorg. Chem., 11, 2430 (1972).
30. D. L. Rabenstein, G. Blakney and B. J. Fuhr, submitted for publication.
31. M. Eigen, Z. Elektrochem., 64, 115 (1960).
32. M. Eigen in "Advances in the Chemistry of Coordination Compounds", S. Kirschner, Ed., MacMillan, New York, N.Y., 1961, p.371.
33. M. Eigen and K. Tamm, Z. Electrochem., 66, 93, 107 (1962).
34. N. Tanaka, R. Tamanushi and M. Kodama, Z. Physik. Chem. (Frankfurt), 14, 141 (1958).

35. J. W. Emsley, J. Feeney and L. H. Sutcliffe, "High Resolution Nuclear Magnetic Resonance", Vol. 1, Pergamon Press, Oxford, 1965, pp. 357-363.
36. N. Tanaka, H. Osawa and M. Kamada, Bull. Chem. Soc. Japan, 36, 67 (1963).
37. N. Tanaka, H. Osawa and M. Kamada, ibid., 36, 530 (1963).
38. D. W. Margerum and B. A. Zabin, J. Phys. Chem., 66, 2214 (1962).
39. R. J. Kula and D. L. Rabenstein, J. Amer. Chem. Soc., 89, 552 (1967).
40. R. J. Kula and G. H. Reed, Anal. Chem., 38, 697 (1966).
41. T. J. Bydalek and M. L. Blömster, Inorg. Chem., 3, 667 (1964).
42. N. Tanaka, K. Ebata, T. Takahari and T. Kumagai, Bull. Chem. Soc. Japan, 35, 1836 (1962).
43. D. L. Rabenstein, J. Amer. Chem. Soc., 93, 2869 (1971).
44. D. L. Rabenstein and R. J. Kula, ibid., 91, 2492 (1969).
45. J. C. Cassatt and R. G. Wilkins, ibid., 90, 6045 (1968).
46. D. B. Rorabacher, Ph.D. Dissertation, Purdue University, Lafayette, Ind., 1963.
47. K. Kustin, R. F. Pasternack and E. M. Weinstock, J. Amer. Chem. Soc., 88, 4610 (1966).
48. A. Kowalak, K. Kustin, R. F. Pasternack and S. Petrucci, ibid., 89, 3126 (1967).
49. B. J. Fuhr and D. L. Rabenstein, Inorg. Chem., 12, 1868 (1973).
50. Reference 35, pp. 481-488.

51. B. W. Goodwin, Master's Thesis, University of Manitoba, Winnipeg, Manitoba, 1969.
52. R. J. Kula, Anal. Chem., 37, 989 (1965).
53. J. C. Bailar, J. Inorg. Nucl. Chem., 8, 165 (1958).
54. M. Eigen, Pure Appl. Chem., 6, 97 (1963).
55. J. P. Jones, E. J. Billo and D. W. Margerum, J. Amer. Chem. Soc., 92, 1875 (1970).
56. M. W. Grant, H. W. Dodgen and J. P. Hunt, ibid., 93, 6828 (1971).
57. M. Rabinovitz and A. Pines, ibid., 91, 1585 (1969).
58. H. Hoffmann, Ber. Bunsenges. Phys. Chem., 73, 432 (1969).
59. W. Byers and B. E. Douglas, Inorg. Chem., 11, 1470 (1972).
60. P. F. Coleman, J. I. Legg and J. Steele, ibid., 9, 937 (1970).
61. G. Schwarzenbach and H. Ackermann, Helv. Chim. Acta, 31, 1029 (1948).
62. R. J. Kula, D. T. Sawyer, S. I. Chan and C. M. Finley, J. Amer. Chem. Soc., 85, 2930 (1963).
63. D. Chapman, D. R. Lloyd and R. Prince, J. Chem. Soc., 3645 (1963).
64. F. L'Eplattenier and G. Anderegg, Helv. Chim. Acta, 47, 1792 (1964).
65. G. Anderegg, ibid., 47, 1801 (1964).
66. S. Chaberek and A. E. Martell, J. Amer. Chem. Soc., 74, 6228 (1952).
67. D. L. Rabenstein, Can. J. Chem., 50, 1036 (1972).
68. J. L. Sudmeier and C. N. Reilley, Anal. Chem., 36, 1698 (1964).

69. R. G. Pearson and D. G. de Wit, J. Coord. Chem., 2, 175 (1973).
70. M. Eigen and R. G. Wilkins, "Mechanisms of Inorganic Reactions", in Advances in Chemistry Series, No. 49, R. K. Murmann, R. T. M. Fraser and J. Bauman, eds., American Chemical Society, Washington, D.C., 1965, pp. 55-65.
71. L. G. Sillen and A. E. Martell, "Stability Constants of Metal Ion Complexes", The Chemical Society, London, 1964.
72. M. Sheinblatt and H. S. Gutowsky, J. Amer. Chem. Soc., 86, 4814 (1964).
73. J. D. Carr, R. A. Libby and D. W. Margerum, Inorg. Chem., 6, 1083 (1967).
74. J. A. Weyh and R. E. Hamm, ibid., 7, 2431 (1968).
75. P. K. Glascoe and F. A. Long, J. Phys. Chem., 64, 188 (1960).
76. J. A. Pople, W. G. Schneider and H. J. Bernstein, "High Resolution Nuclear Magnetic Resonance," McGraw-Hill Book Co. Inc., New York, N.Y., 1959, pp. 218-225.
77. C. S. Johnson, Jr., in "Advances in Magnetic Resonance", Vol. 1, J. S. Waugh, Ed., Academic Press Inc., New York, N.Y., 1965, pp. 33-102.
78. R. M. Lynden-Bell, in "Progress in Nuclear Magnetic Resonance Spectroscopy", Vol. 2, J. W. Emsley, J. Feeney and L. H. Sutcliffe, Eds., Pergamon Press Ltd., Oxford, 1967, pp. 163-204.
79. G. Binsch, in "Topics in Stereochemistry", Vol. 3, E. L. Eliel and N. L. Allinger, Eds., John Wiley and Sons Inc., New York, N.Y., 1968.
80. F. Bloch, Phys. Rev., 70, 460 (1946).
81. H. S. Gutowsky, D. W. McCall and C. P. Slichter, J. Chem. Phys., 21, 279 (1953).
82. H. S. Gutowsky and C. H. Holm, ibid., 25, 1228 (1956).
83. H. M. McConnell, ibid., 28, 430 (1958).

PART II

THE BINDING OF METAL IONS BY GLUTATHIONE

refer to solid state structure; they may be useful for

CHAPTER V

INTRODUCTION

The binding of metal ions by molecules such as peptides and proteins is of fundamental interest in view of the importance of metal ions in biological systems (1-4). For example, the catalytic function of many enzymes is dependent upon the presence of metal ions which may be coordinated to certain functional groups of the enzyme or substrate. In an enzyme many groups are available as potential coordination sites, but only certain ones are actually metal-coordinated in an enzymatic reaction.

Metal-peptide complexes are potential models for metal-enzyme interactions since peptides can be synthesized which contain the functional groups involved at the active sites of enzymes. Moreover, peptides are relatively small molecules making them more amenable to study by a variety of techniques. Freeman has summarized X-ray crystallographic data for many metal-peptide complexes (5). Even though these data refer to solid state structures they may be useful for at least suggesting possible metal binding sites and conformations of the complexes in solution. A great deal of research has also been devoted to the solution

chemistry of metal-peptide complexes. Several of these studies will be reviewed briefly below.

Representative of the early work in this area are the studies in which the formation constants of the cadmium, zinc, and lead complexes of a series of polyglycine peptides were determined (6-8) using potentiometric measurements. By comparing the formation constant data, it was proposed that the binding sites in these complexes consist of the terminal amino group and the adjacent peptide linkage, but it was not possible to establish any carboxyl coordination. The copper and nickel complexes of the polyglycine peptides have also been extensively investigated (9-12,18) using pH titration, infrared and spectrophotometric methods in order to determine formation constants. Ionization of the peptide protons and subsequent metal binding to the negative nitrogen atoms was proposed by some of the workers for these complexes. pH titration and spectrophotometric studies have also been carried out on the copper complex of β -alanyl-L-histidine (carnosine) (9,13,14). From this work it was suggested that ionization of the peptide proton takes place with subsequent copper binding to the negatively charged peptide nitrogen, but there was lack of agreement as to the binding sites and the structure of

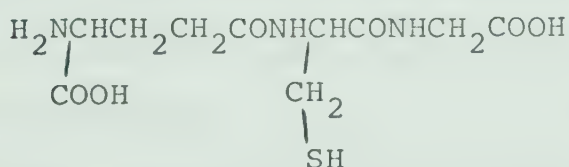
the complex.

The techniques used in the above examples have the disadvantage that they measure macroscopic properties and hence, do not provide definitive information at the molecular level. Pmr spectroscopy has proven useful for elucidating the binding of metal ions by simple peptides at the molecular level. For example the functional groups of polyglycine peptides involved in coordination to diamagnetic cadmium, zinc, lead and nickel (15-17) have been established from changes in the chemical shifts of carbon-bonded protons close to the binding site. The groups of polyglycine peptides involved in binding to paramagnetic copper and nickel (16,17) and of carnosine with copper (38) have been identified from the dependence of the line-widths of the pmr resonances on their proximity to the binding site. This application of pmr is limited, however, to those peptides whose spectra are relatively simple because of the need for distinct, well resolved resonances for monitoring interactions at the potential binding sites. Spectra which consist of overlapping peaks and complex multiplet patterns are of limited use in metal binding studies.

Carbon-13 magnetic resonance (cmr) spectroscopy is potentially more useful than pmr for the study of

metal-peptide interactions. First of all, proton-decoupled cmr spectra are comprised of single resonances for each of the nonequivalent carbon atoms of peptides. Secondly, the range of chemical shifts in cmr is at least an order of magnitude greater than in pmr, so that often a resonance can be resolved for each of the carbon atoms. In addition, carbon atoms are bonded directly to the possible binding sites in peptides making cmr potentially more sensitive as a probe for studying binding at the molecular level.

In Chapter VI, the results of a cmr investigation of the binding of cadmium, zinc, lead and mercury by the tripeptide γ -L-glutamyl-L-cysteinyl-glycine (glutathione) are presented and discussed (23). This peptide was chosen to evaluate the



GLUTATHIONE

potential of cmr for the elucidation of metal binding by peptides because there is a lack of agreement as to which of the six possible coordination sites are involved in binding to these metal ions (19-22).

CHAPTER VI
THE BINDING OF ZINC, CADMIUM, LEAD AND MERCURY
BY GLUTATHIONE

The tripeptide glutathione, which is widely distributed in nature, contains the following six potential sites for metal ion coordination: the sulfhydryl group, the amino group, the two carboxyl groups and the two peptide linkages. Formation constants for the zinc, cadmium and lead complexes of glutathione have been determined previously using the pH titration method (19-22), but the results are different in each case because of the lack of agreement as to which of the sites are involved in metal ion coordination. The validity of microscopic formation constants determined from pH titration data is questionable when the binding sites are not known because the method is based on the competition between the metal ion and the proton for the site. Furthermore, microscopic ionization constants must be used in the calculations and only in one instance (21) was this done.

Li and coworkers (19,20) obtained formation constants for the zinc, cadmium and lead complexes of glutathione by assuming that all ionizable protons are removed from the peptide when it binds

to these metal ions. They suggested that in these complexes the metal ion is bound to the ionized sulfhydryl and amino groups. Martin and Edsall (21) on the other hand, considered that divalent metal ions could be bound to glutathione either through the amino and carboxyl groups of the glutamyl residue or to the sulfhydryl group of the cysteinyl residue with possible chelate formation through a peptide bond. By assuming that sulfur binding could be excluded in S-methylglutathione and that bonding to the glutamyl residue would be equivalent in glutathione and its S-methyl derivative, they assigned stability constant values to the sulfhydryl bound and to the glutamyl bound complexes of zinc. At $\text{pH} < 8$ these workers postulated that zinc binding could take place at a peptide bond, but that ionization of a peptide proton was unlikely. Perrin and Watt (22) considered a number of different zinc and cadmium complexes of glutathione of the type ML^- , ML_2^{4-} , MHL , $\text{ML}(\text{HL})^{3-}$, and calculated formation constants for each of these species. These workers proposed structures involving simultaneous coordination of sulfhydryl and glutamyl groups to the same metal ion, and suggested that ionization of the peptide protons can occur on complex formation.

Because of the differing results of the previous studies of the metal complexes of glutathione, this particular peptide was chosen to evaluate the potential of cmr for the elucidation of metal binding by peptides. The results of a cmr investigation of the binding of zinc, cadmium, lead and mercury by glutathione are reported in this chapter. Binding to mercury has been studied previously by the polarographic method (24), and binding to CH_3Hg^+ has been studied by pmr (25). In addition, the acid-base chemistry of the four acidic groups of glutathione, which is necessary for quantitative studies of metal binding, has already been characterized at the molecular level (25,26).

A. RESULTS

Glutathione

Cmr spectra of glutathione were obtained over a pD range 1 to 13 for a 0.30 M solution of the tripeptide in D_2O using 1,4-dioxane as an internal reference. The spectrum obtained at pD 7.37 is the one designated (a) in Figure 15. The carbon atoms are identified by Glu, Cys or Gly to specify the amino acid residue glutamyl, cysteinyl or glycyl in which the carbon is located and C_α , C_β , C_γ , CONH or

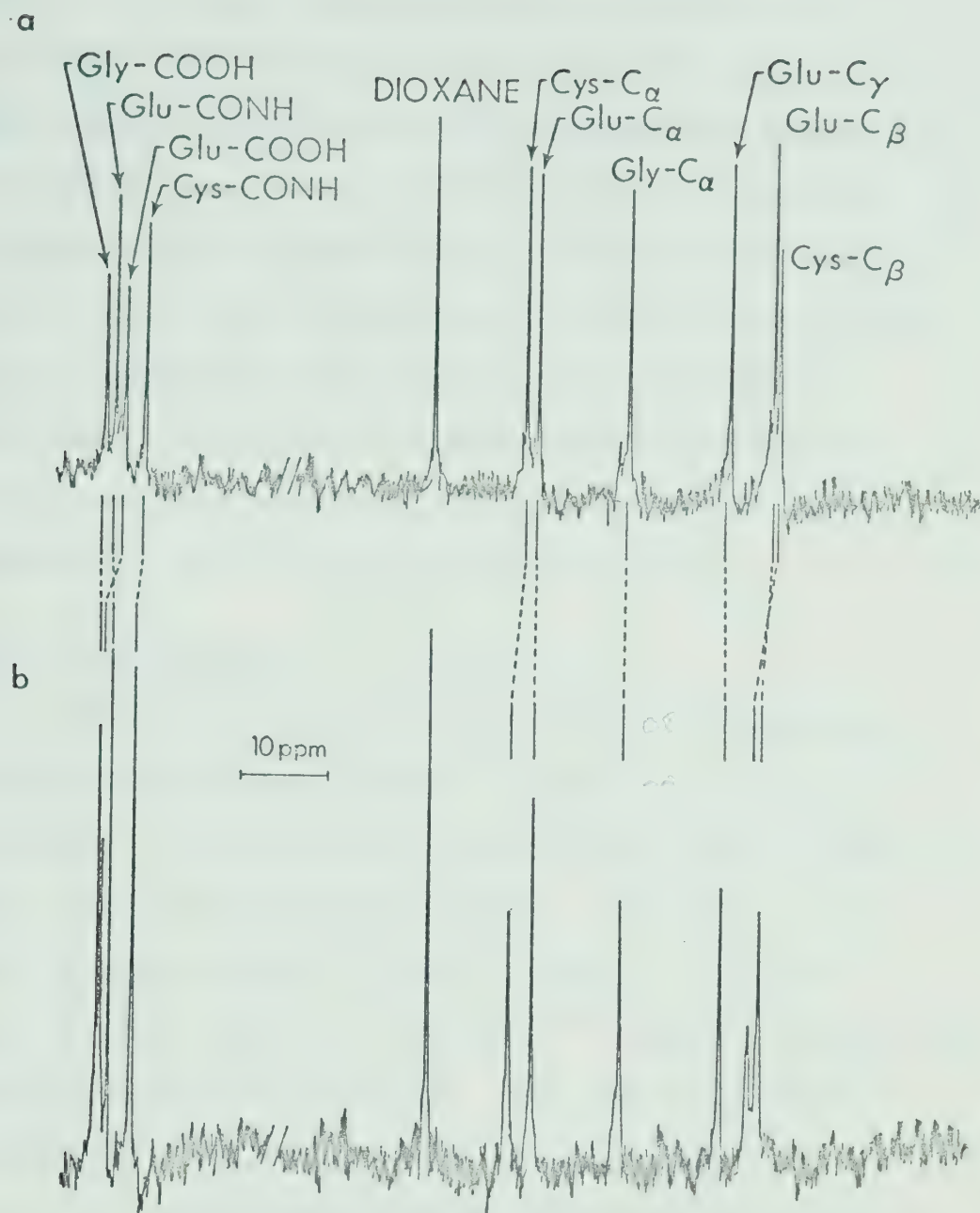


Figure 15: ^{13}C magnetic resonance spectra of glutathione.

(a) D_2O solution containing 0.30 M glutathione at pD 7.37.

(b) D_2O solution containing 0.30 M glutathione and 0.15 M $\text{Zn}(\text{NO}_3)_2$ at pD 7.84.

COOH to indicate the particular carbon of that residue. The assignments of the carbon resonances were made by comparison with the chemical shifts of the constituent amino acids (27,28), and from the chemical shift dependence of each of the resonances on the pD. These assignments are in agreement with those reported by Jung and coworkers who have previously given the cmr spectrum of glutathione (29), and have presented chemical shift vs. pH curves for each of the carbon atoms (30).

Zinc-glutathione

Addition of zinc to a solution of glutathione causes the chemical shifts of selected resonances to change, as illustrated by spectrum (b) in Figure 15. This spectrum was obtained from a solution 0.30 M in glutathione and 0.15 M in $\text{Zn}(\text{NO}_3)_2$ in D_2O at pD 7.84 and indicates that the ^{13}C chemical shifts are sensitive to metal binding. The resonances were assigned by following their pD dependence from low pD values where little metal binding takes place. The chemical shifts of the three cysteinyl carbon resonances are shown as a function of pD for a zinc to glutathione ratio of 1:2 by the solid curves in Figure 16, while the chemical shifts of selected carbon atoms of the glutamyl and glycyl residues

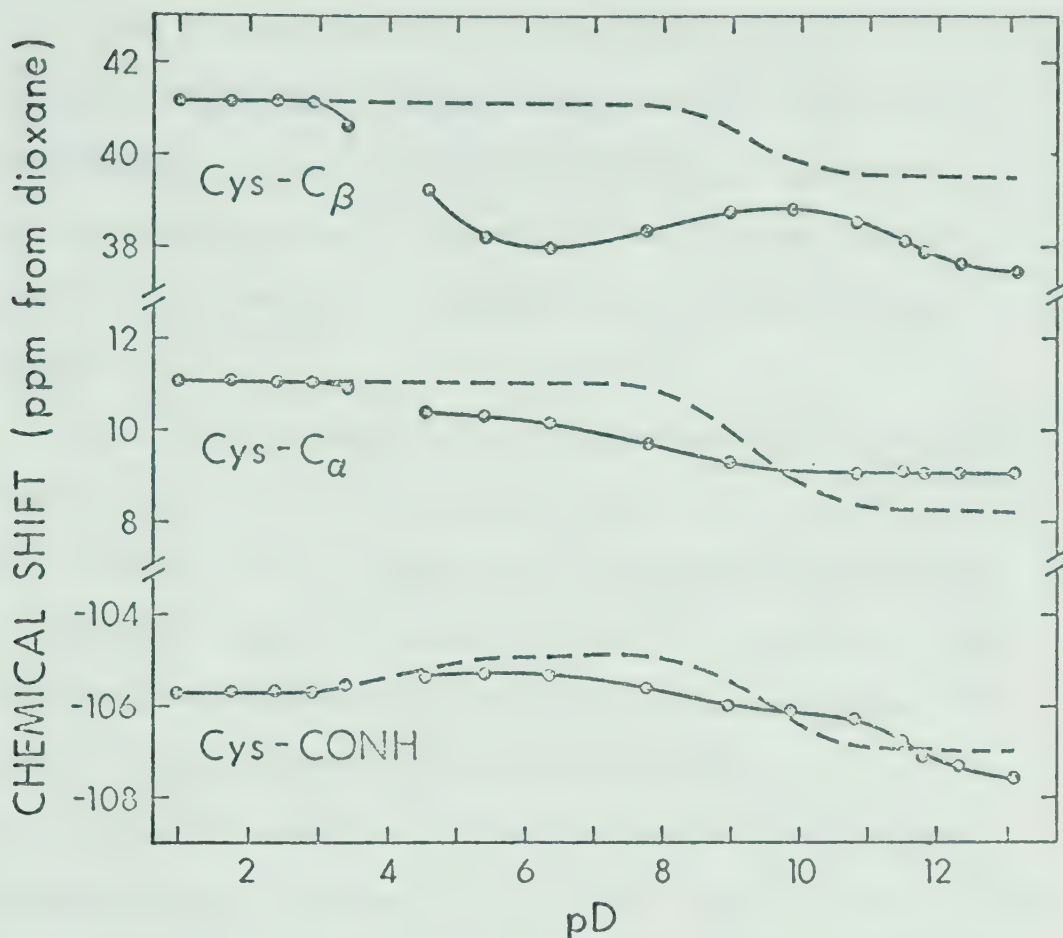


Figure 16: pD dependence of the chemical shifts of the cysteinyl carbons for a D_2O solution containing 0.30 M glutathione and 0.15 M $Zn(NO_3)_2$. The dashed curves represent the chemical shift behavior of the same carbon atoms for a solution of glutathione containing no complexing metal ion.

are shown for the same solution conditions in Figure 17. The discontinuity in these solid curves indicates the pD region over which precipitation occurred. The dashed curves in Figures 16 and 17 represent the chemical shift vs. pD behaviour of the indicated carbon resonances in the absence of coordinating metal ion.

The lack of any large dependence of the chemical shifts plotted in Figures 16 and 17 on the presence of zinc at $pD < 3$ indicates no strong coordination in this pD range. A small amount of binding to both carboxylic acid groups, which previous studies (25) have shown to be partially ionized at $pD > 0$, is indicated by the small chemical shift differences observed for the Gly- C_{α} , Gly-COOH, Glu- C_{α} and Glu-COOH carbons. A chemical shift difference for a given carbon atom refers to the difference between the solid and dotted curves in Figures 16 and 17 and in subsequent figures, and is assumed to be indicative of some degree of metal binding to a specific site near the given carbon atom. Some carboxylic acid group coordination is consistent with the known binding of zinc by the carboxylic acid groups of acetylglycine and the C-terminal end of polyglycine peptides (15,31).

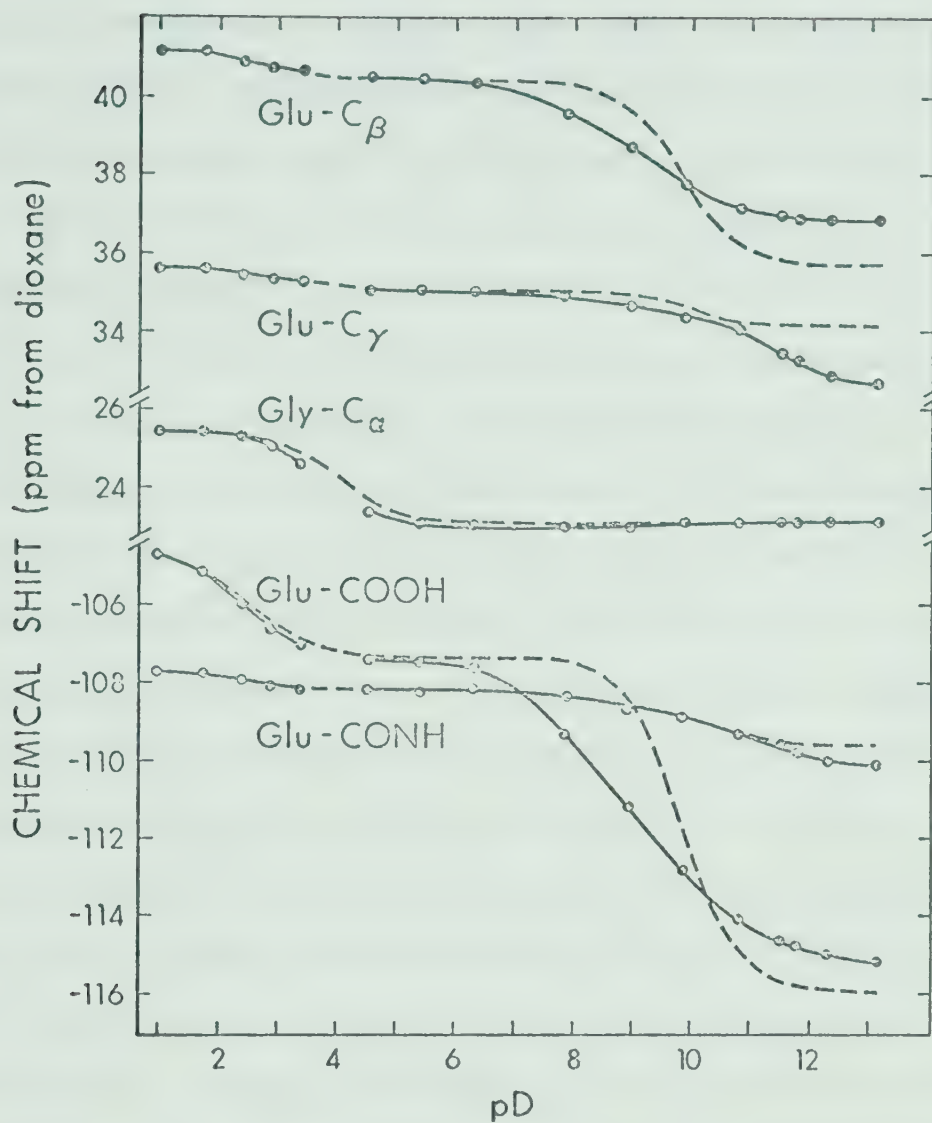


Figure 17: pD dependence of the chemical shifts of selected glutamyl and glycylic carbons for a D_2O solution containing 0.30 M glutathione and 0.15 M $Zn(NO_3)_2$.

Between pD 3.0 and 13.2, the large chemical shift differences exhibited by all three cysteinyl carbon resonances indicate that zinc is bound to some extent to the sulfhydryl group and possibly to the peptide linkage between the cysteinyl and glycyl residues. The lack of any chemical shift difference for the Glu-CONH carbon at pD < 10.5 indicates no binding to the peptide linkage between the glutamyl and cysteinyl residues. The Glu-COOH resonance indicates a small amount of binding to the glutamyl residue up to pD 6, presumably involving only the carboxyl group. An increase in the binding to the glutamyl residue at pD > 6, indicated by the chemical shift differences for the Glu-COOH, $-C_{\alpha}$, $-C_{\beta}$ and $-C_{\gamma}$ carbon resonances, probably involves simultaneous zinc coordination to the amino and carboxyl groups by analogy with the coordination of zinc by glycine. The small chemical shift differences observed for the Gly- C_{α} and Gly-COOH resonances over the pD range 3 to 9 are consistent with a small amount of binding to the glycyl carboxylic acid group.

The rather large downfield shifts exhibited by the Cys-CONH, Cys- C_{β} , Glu-CONH and Glu- C_{γ} carbon resonances at pD > 10.5 indicate a change in the nature of the binding to the peptide linkages. If

binding does take place at the peptide linkages at $pD < 10.5$, it is presumably to the carbonyl oxygen of the neutral peptide linkage, since it is known to be the more basic site (5,32-34). The downfield shift behaviour suggests that, in the presence of zinc, ionization of one or both of the peptide protons might occur at $pD > 10.5$ with subsequent binding of zinc to a negatively charged nitrogen atom. Separate resonances for the free amino acids of which glutathione is comprised were not observed, indicating that hydrolysis of the peptide bonds had not occurred under the given solution conditions.

The specificity of the zinc binding in the pD range 3 to 6 was investigated further by monitoring the chemical shifts as a function of the zinc to glutathione ratio for an H_2O solution at a constant pH of 5.51; the results of this study are presented in Figure 18. It can be seen that the chemical shift of the Cys- C_β carbon varies continuously as the ratio is increased from 0.0 to 0.5 and then levels out at a constant value of 38.2 ppm; the total chemical shift variation is 2.7 ppm. This indicates that at a ratio of 0.5 and a pH of 5.51, the main species in solution is a complex consisting of one zinc and two glutathione molecules. The chemical shift

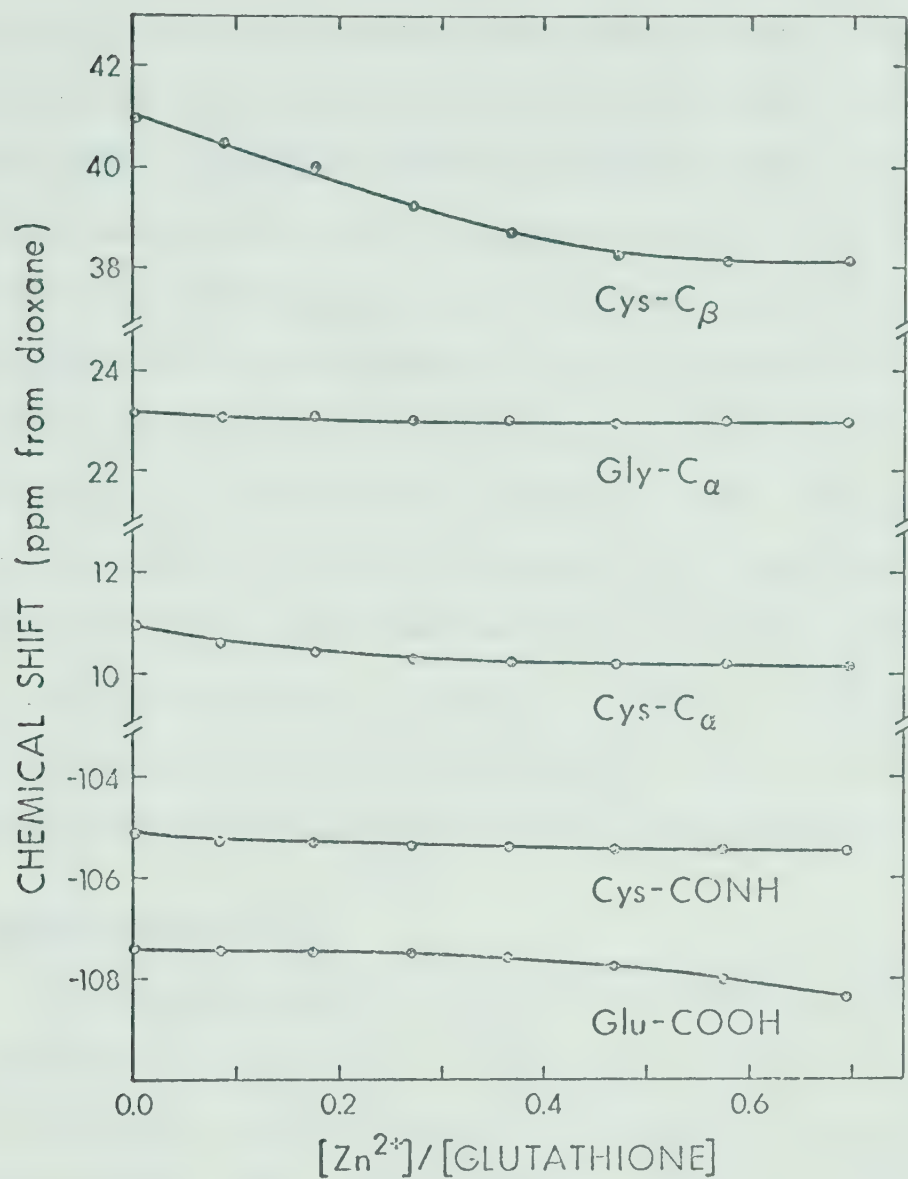


Figure 18: The chemical shifts of selected carbons as a function of the zinc to glutathione ratio for an aqueous solution at pH 5.51.

change of only 0.3 ppm for the Glu-COOH carbon up to a ratio of 0.5 suggests that only a small amount of binding takes place at the glutamyl end. For comparison, ionization of the glutamyl ammonium proton results in a change of 8.4 ppm for this carbon resonance. On changing the ratio from 0.5 to 0.7, however, when the sulfhydryl group is presumably completely complexed, the additional chemical shift change of 0.6 ppm for the Glu-COOH carbon indicates that the glutamyl end is becoming more important as a binding site. The chemical shift variation of only 0.1 ppm for the Gly-C_α carbon in Figure 18 indicates very weak glycyl carboxyl binding at the given pH. Precipitation occurred at ratios greater than 0.7.

Cadmium-glutathione

The chemical shifts of the three cysteinyl carbons for a cadmium to glutathione ratio of 1:2 are shown as a function of pD in Figure 19 by the solid curves. The corresponding curves for selected carbon atoms of the glutamyl and glycyl residues are shown in Figure 20. The dotted curves in these figures represent the data points for a glutathione solution containing no complexing metal ion. At pD < 2, evidence for a small amount of cadmium binding to the two carboxyl groups is given by the

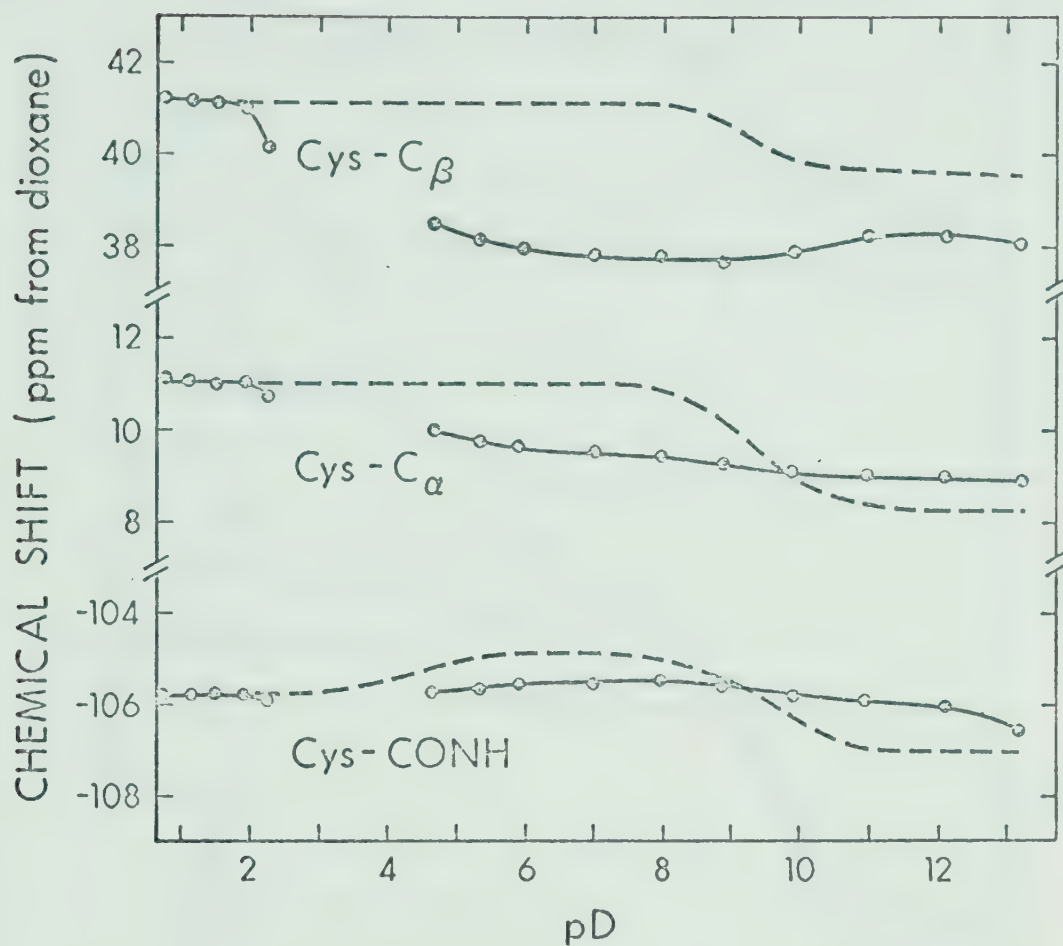


Figure 19: pD dependence of the chemical shifts of the cysteinyl carbons for a D₂O solution containing 0.30 M glutathione and 0.15 M Cd(NO₃)₂.

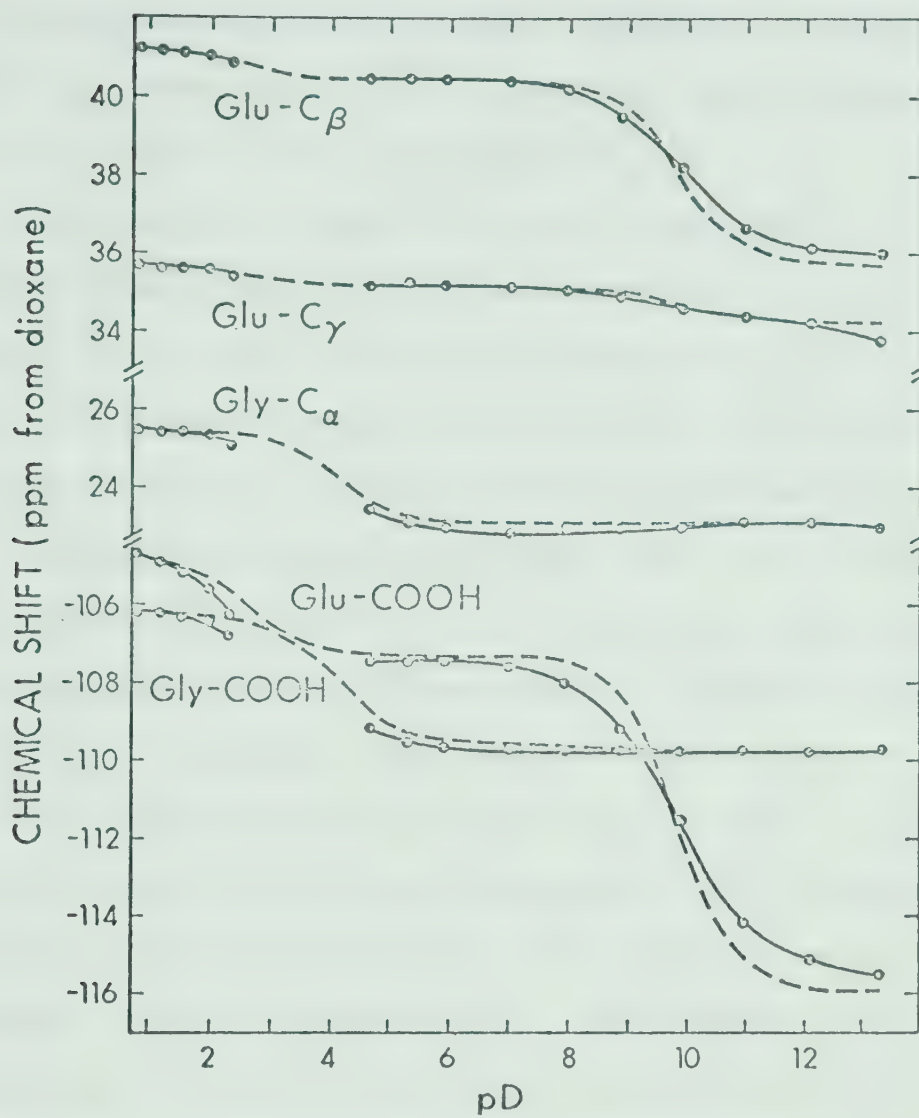


Figure 20: pD dependence of the chemical shifts of selected glutamyl and glycyl carbons for a D_2O solution containing 0.30 M glutathione and 0.15 M $Cd(NO_3)_2$.

small chemical shift differences observed for the Gly- C_{α} , Gly-COOH, Glu- C_{α} and Glu-COOH carbons. As in the zinc system, this type of binding is consistent with the known binding of cadmium by the carboxylic acid groups in certain peptides (31).

Between pD 2.0 and 13.2, the large chemical shift differences observed for the three cysteinyl carbon resonances indicate that cadmium is bound to the sulfhydryl group and possibly to the peptide linkage between the cysteinyl and glycyl residues. No detectable binding to the other peptide linkage is indicated by the fact that the chemical shift of the Glu-CONH carbon resonance is not changed by the presence of cadmium. The chemical shift curves for the Glu-COOH carbon suggest that a small amount of glutamyl binding takes place up to pD 7, probably involving the carboxyl group. An increase in glutamyl binding at pD > 7, indicated by the chemical shift behaviour of the Glu-COOH, $-C_{\alpha}$, $-C_{\beta}$ and $-C_{\gamma}$ carbon resonances, most likely involves simultaneous coordination of cadmium to both the glutamyl amino and carboxyl groups. Finally, the small chemical shift differences observed for the Gly- C_{α} and Gly-COOH carbons over the pD range 2 to 9 indicates weak glycyl carboxyl coordination.

The above results indicate that, in the pD range 2 to 7, cadmium binding occurs almost exclusively at the cysteinyl residue of glutathione. This specificity was further investigated by monitoring the chemical shifts as a function of the cadmium to glutathione ratio for an H_2O solution at a constant pH of 6.59. The chemical shifts of selected carbon resonances are plotted as a function of the ratio in Figure 21. The cysteinyl residue is the principal coordination site up to a ratio of 0.5, as evidenced by the chemical shift variations of the cysteinyl carbons. In particular, the chemical shift of the Cys- C_β carbon changes by 3.2 ppm and then levels out above a ratio of 0.5. The chemical shift of the Glu-COOH carbon changes by only 0.3 ppm up to this ratio, indicating very little glutamyl binding. However, an increase in this interaction takes place at ratios greater than 0.5, when presumably the sulfhydryl group is fully coordinated. Finally, the chemical shift change of only 0.2 ppm for the Gly- C_α resonance indicates weak binding to the glycyl carboxyl group under these conditions. Precipitation occurred at ratios greater than 0.7.

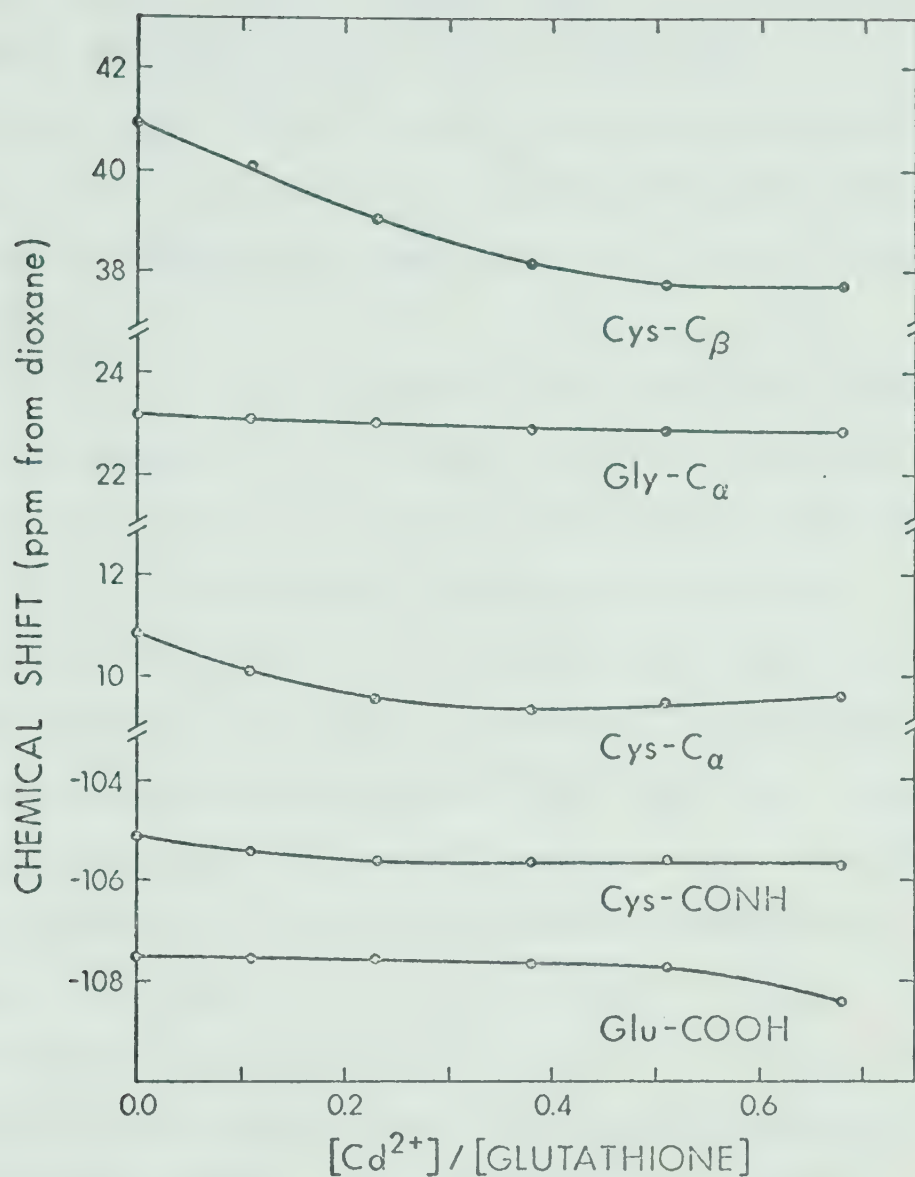


Figure 21: The chemical shifts of selected carbons as a function of the cadmium to glutathione ratio for an aqueous solution at pH 6.59.

Lead-glutathione

The chemical shift curves of the three cysteinyl, the Gly-C_α and the Glu-COOH carbons are shown as a function of pD in Figure 22 for a lead to glutathione ratio of 1:2. Precipitation from pD 2.3 to 5.4 and above pD 12 limited the range over which binding could be studied.

At pD < 2.3, weak coordination to the two carboxyl groups is indicated by the small chemical shift differences for the Gly-C_α and Glu-COOH carbons. Between pD 5.4 and 12, the chemical shift curves provide evidence for lead binding to only the cysteinyl and glycyl residues. The large differences between the solid and dotted curves for the three cysteinyl carbon resonances indicate lead coordination to the sulfhydryl group and possibly the peptide linkage between the cysteinyl and glycyl residues. Evidence for weak glycyl carboxyl binding between pD 5.4 and 9.0 is also provided by the chemical shift curves for the Gly-C_α and Gly-COOH carbons. The extent of this binding decreases at pD > 9 presumably due to carboxyl displacement by hydroxide ions with the formation of lead-hydroxy-glutathione mixed complexes. The lack of any change in the chemical shifts due to the presence of lead for all the glutamyl carbon resonances is evidence

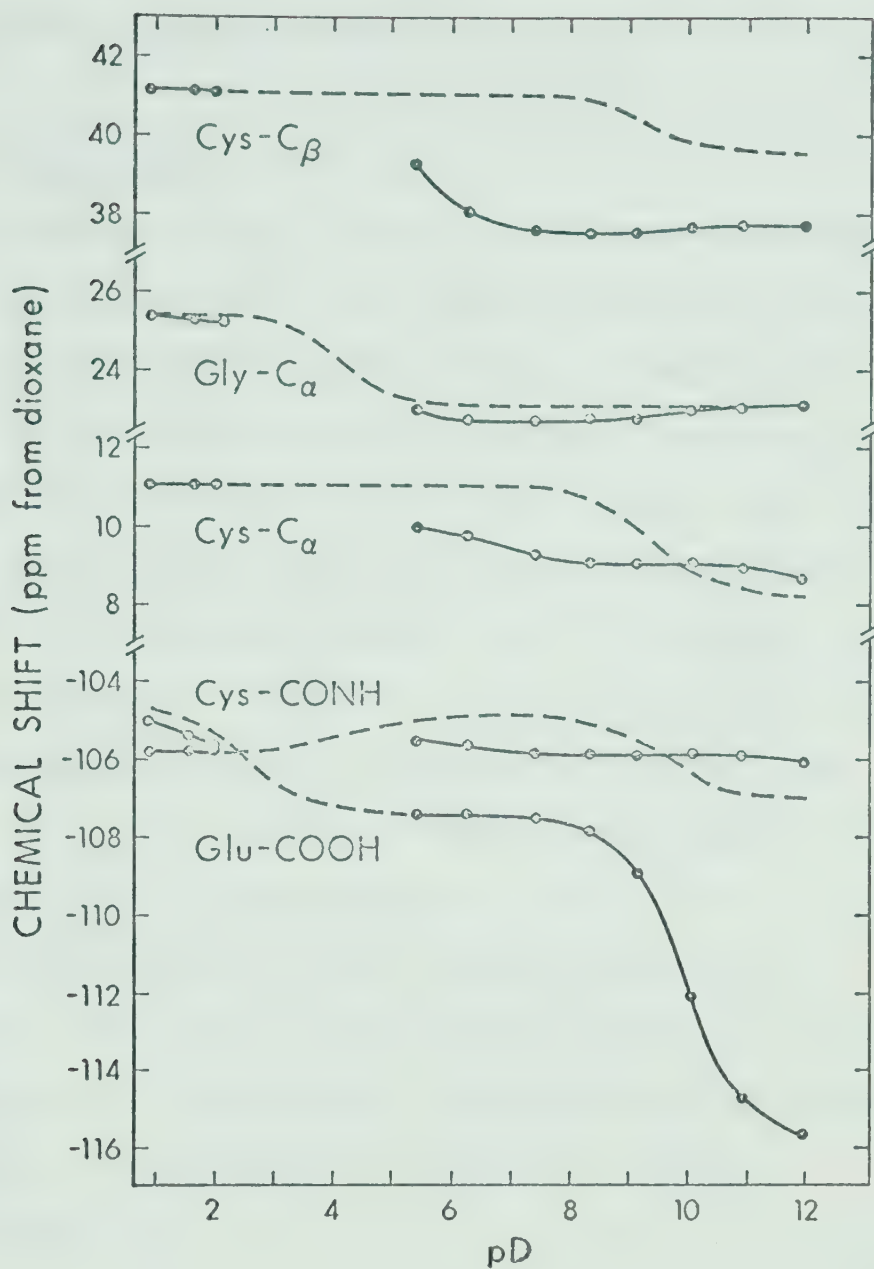


Figure 22: pD dependence of the chemical shifts of selected carbons for a D_2O solution containing 0.30 M glutathione and 0.15 M $Pb(NO_3)_2$.

that the glutamyl functional groups do not act as binding sites in the pD range 5.4 to 12.

Mercury-glutathione

The chemical shift curves for the three cysteinyl carbons as a function of pD, shown in Figure 23 for a mercury to glutathione ratio of 1:2, are seen to be nearly constant over the entire accessible pD range. The chemical shifts for all the other carbon atoms of glutathione are identical with those obtained from solutions containing no mercury ions. Therefore, the binding of mercury appears to take place exclusively to the sulfhydryl group at a mercury to glutathione ratio of 0.5. The results of further experiments, in which the ratio was varied from 0.0 to 0.5 for an H₂O solution at a constant pH of 5.01 are presented in Figure 24. These plots confirm the specificity of the sulfhydryl group for mercury. Precipitation prevented investigations at mercury to glutathione ratios greater than 0.5.

B. DISCUSSION

The cmr results show that all of the metal ions studied in this work bind to the sulfhydryl group of glutathione at metal to peptide ratios of 1:2 and at

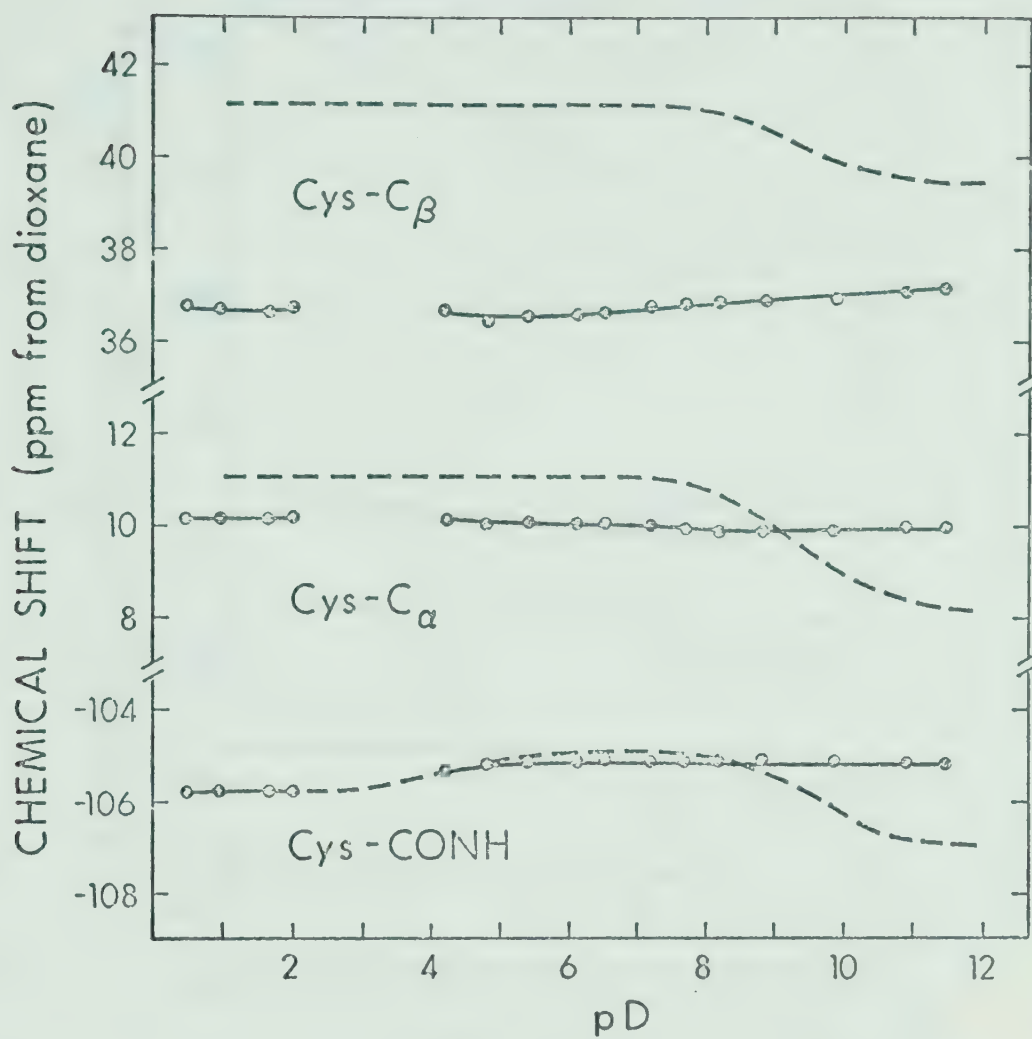


Figure 23: pD dependence of the chemical shifts of the cysteinyl carbons for a D_2O solution containing 0.30 M glutathione and 0.15 M $Hg(NO_3)_2$.

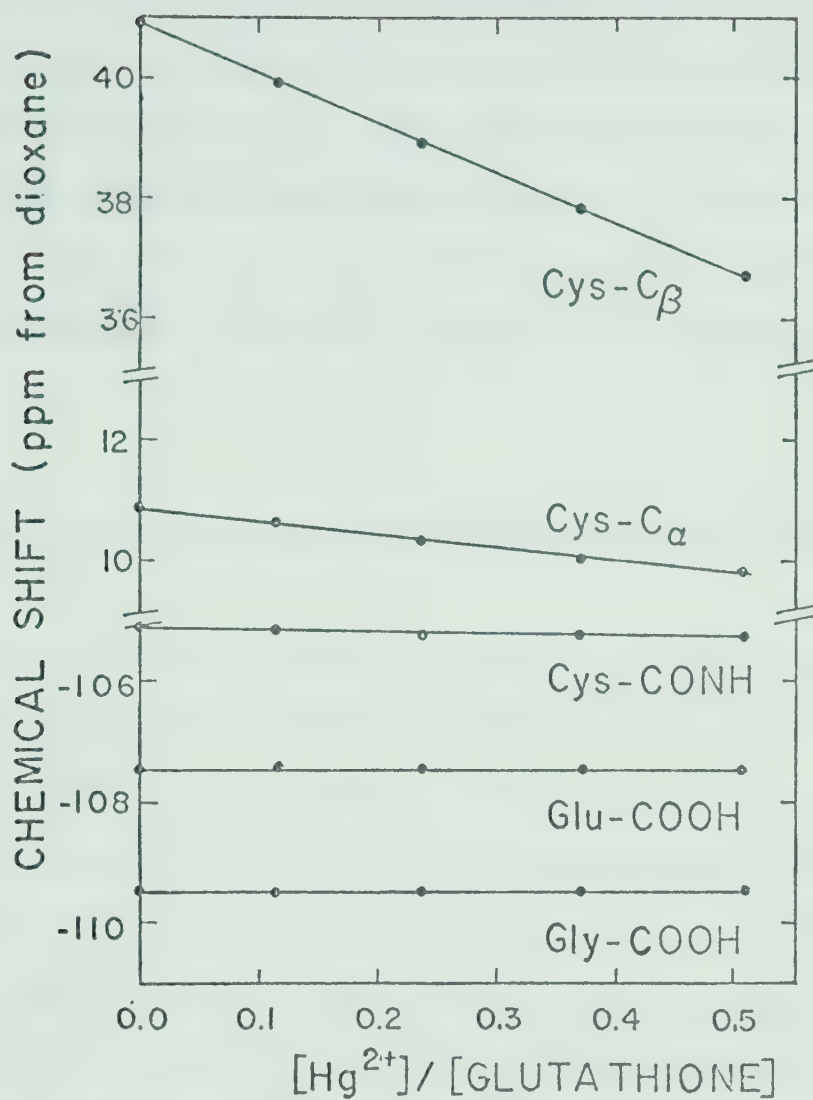


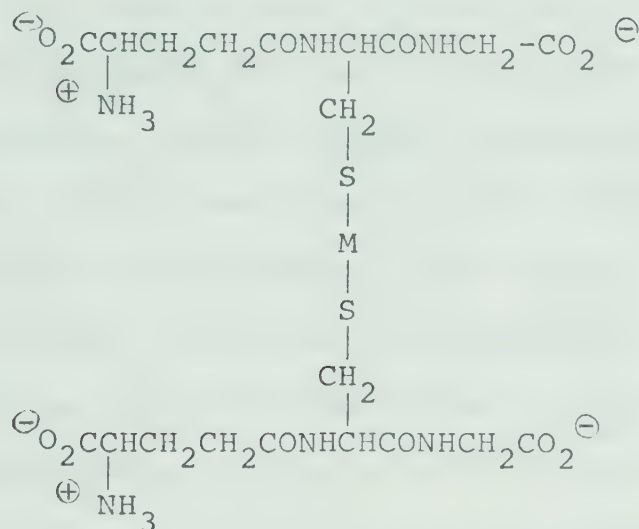
Figure 24: The chemical shifts of selected carbons as a function of the mercury to glutathione ratio for an aqueous solution at pH 5.01.

pD > 3. Also, all of the metal ions except mercury coordinate rather weakly to the glycyl and glutamyl carboxyl groups, while only zinc and cadmium bind to the glutamyl amino group. The extent of binding to the various sites is dependent upon the solution pD, except in the case of mercury which is bound strongly to the sulfhydryl group over the entire accessible pD range.

Zinc and Cadmium Binding to the Sulfhydryl and Glutamyl Groups

Because of the similarity in the binding of cadmium and zinc, the results for these systems will be discussed together. The strongest binding of these two metal ions occurs to the sulfhydryl group, as evidenced by the fact that the metal ions bind to this group at a much lower pD than to the glutamyl amino group, even though the pK_A of the sulfhydryl group is only 0.2 units less than that of the amino group (25). The chemical shifts of the Cys- C_β carbon indicate that, for a metal to glutathione ratio of 0.5, all the sulfhydryl groups are complexed at pD 6 in the zinc system and at pD 7 in the cadmium system. The results of experiments in which the metal to glutathione ratio was varied at pH 5.51 for the zinc system and at pH 6.59

for the cadmium system also indicate that binding occurs almost exclusively to the sulfhydryl group at these pH values up to a ratio of 0.5. Thus, a 1:2 complex such as that shown below is the major species in solution for these conditions.



This 1:2 complex is analogous to the complex $\text{M}(\text{HL})_2^{2-}$, where M^{2+} is Cd^{2+} or Zn^{2+} and HL^{2-} represents monoprotonated glutathione, proposed by Perrin and Watt (22). These workers were unable to assign the binding sites due to the uncertainty in the pK_A values of the amino and sulfhydryl groups. The amino group is still protonated as evidenced by the chemical shift curves for the Glu-COOH, $-\text{C}_\alpha$ and $-\text{C}_\beta$ carbons. Li and coworkers (19,20) interpreted pH titration data for the binding of cadmium and zinc by glutathione in terms of complexes in which the two carboxyl, the amino

and the sulfhydryl groups are all ionized. The present chemical shift data show this not to be the case, but rather that several different complexes may form and in some, those functional groups which are not coordinated are protonated.

It is possible that, in the zinc and cadmium complexes discussed above, binding might also occur to the peptide linkage between the cysteinyl and glycyl residues. Of the two sites in this linkage, protonated nitrogen and carbonyl oxygen, the oxygen is the more basic (5,32-34) and hence a more probable binding site. Such binding occurring simultaneously with sulfhydryl group coordination would result in a six-membered chelate ring. The cysteinyl carbon chemical shift data for the zinc system at pD 7 are consistent with carbonyl oxygen binding.

As shown by the chemical shift vs. pD curves, observable metal binding to the glutamyl amino group takes place at pD > 6 for the zinc system and at pD > 7 for the cadmium system. The extent of this binding is pD dependent, as illustrated by the results in Table XVII which were calculated from the chemical shift data for the Glu-COOH and Glu-C_β carbon resonances using the equation,

$$f = \frac{\delta_{\text{OBS}} - \delta_f}{\delta_c - \delta_f}$$

Table XVII

Fraction of Glutamyl Groups of Glutathione
Complexed by Zn^{2+} and Cd^{2+} as a Function of pD ^a

pD	Zn^{2+}		Cd^{2+}	
	Glu-COOH ^b	Glu-C _{β} ^c	Glu-COOH	Glu-C _{β}
6.0	0.03	0.00	0.03	0.00
7.0	0.10	0.12	0.05	0.00
8.0	0.34	0.29	0.14	0.06
8.5	0.49	0.41	0.21	0.14
9.0	0.58	0.53	0.35	0.36
10.5	0.63	0.55	0.37	0.32
11.0	0.58	0.56	0.27	0.21

(a) Data obtained from solutions of metal to glutathione ratio of 1:2.

(b) Glu-COOH carbon chemical shift data.

(c) Glu-C _{β} carbon chemical shift data.

where f is the fraction of glutamyl groups complexed, δ_{OBS} is the observed chemical shift of a glutamyl carbon in the presence of complexing metal ion, δ_f is the chemical shift in the absence of metal ion and δ_c is the chemical shift of glutamyl complexed glutathione. The value of δ_c used in these calculations was obtained from the point where the solid and dashed curves cross in Figures 17 and 20 (31). The δ_{OBS} values were obtained from the chemical shift vs. pD curves for solutions of a metal to glutathione ratio of 1:2, and those for δ_f from the corresponding curves for a solution of glutathione. The fractions shown in Table XVII reveal that cadmium is bound less strongly to the glutamyl end of glutathione than is zinc.

A change in the nature of the zinc binding to the cysteinyl residue in the pD range 6 to 10.5 is indicated by the chemical shift data for the cysteinyl carbon resonances shown in Figure 16. Simultaneous coordination to the sulfhydryl group and the peptide carbonyl oxygen, as suggested above, would be expected to have a different effect on all three cysteinyl carbons than coordination to the sulfhydryl group alone. Therefore, it is suggested that at $\text{pD} < 6$, simultaneous sulfhydryl-peptide oxygen binding takes place, and at $\text{pD} > 6$ the amount of binding to the peptide oxygen decreases. Presumably

the decreased peptide binding is due to glutamyl group competition for the coordination sites on the zinc. The smaller affinity of cadmium for the glutamyl group probably causes a smaller decrease in peptide binding and hence, the effect on the cysteinyl carbon chemical shifts is less than in the zinc system.

At $pD > 6$ for the zinc-glutathione system and $pD > 7$ for the cadmium system, the principal binding sites are the glutamyl residue and the cysteinyl residue. Glutamyl binding most likely involves simultaneous metal coordination to the amino and carboxyl groups by analogy with the coordination of these two metal ions by glycine. As indicated above, cysteinyl binding could involve simultaneous coordination to the sulfhydryl group and the oxygen of the peptide linkage between the cysteinyl and glycyl residues. In any case, it is unlikely that both the cysteinyl and glutamyl residues of a glutathione molecule are simultaneously coordinated to the same metal ion; this would involve an unstable 10-membered ring (35), since the present chemical shift data have shown that the peptide linkage between the glutamyl and cysteinyl residues is not bonded to cadmium nor to zinc at $pD < 10.5$. The structure proposed by Perrin and Watt (22) for the ML^- complexes, where M^{2+} is Cd^{2+} or Zn^{2+} and L^{3-} represents fully ionized glutathione,

involves simultaneous coordination to the glutamyl amino and carboxyl groups, the glutamyl peptide linkage and the sulfhydryl group. This clearly is not in agreement with the ^{13}C chemical shift data. In the structure proposed for the ML_2^{4-} complexes by these workers, the second glutathione molecule was assumed to be bonded to the metal only through the glutamyl carboxyl and amino groups. More likely structures for these complexes are ones in which the cysteinyl or glutamyl group of one glutathione molecule and the cysteinyl or glutamyl group of another are bound to the same metal ion, as considered by Martin and Edsall (21) in the analysis of pH titration data. Another likely structure might be one in which the cysteinyl and glutamyl groups of a glutathione molecule are bound to different metal ions, resulting in polynuclear complexes which have been proposed previously for polyglycine peptide complexes (15,16). Molecular models indicate that polynuclear complexes in which a metal is bonded to the sulfhydryl groups of two glutathione ligands and the glutamyl amino and carboxyl dentates of two other sulfhydryl-complexed glutathione molecules are possible.

Ionization of the Peptide Protons

It is known that, in certain metal-peptide complexes, the metal ion promotes the ionization of peptide protons with subsequent binding to the negatively charged nitrogen atom (9,10,16,18,33,36,37). The large downfield shifts observed for the Glu-CONH, Glu-C_γ, Cys-CONH, and Cys-C_β carbon resonances for the zinc system at pD > 10.5 suggest that zinc might promote ionization of the peptide protons of glutathione. After such ionization the most basic site is the nitrogen atom (5,34) where zinc binding could take place. Simultaneous zinc coordination to the sulfhydryl group and glutamyl peptide nitrogen would result in a five-membered ring and to the cysteinyl peptide nitrogen would result in a six-membered ring. Ionization of a peptide proton and binding of the negatively charged nitrogen atom to a zinc ion presumably have different effects on the chemical shifts of the neighbouring carbon atoms. The fact that the chemical shift of the Cys-C_α carbon, which is near both peptide nitrogens, experiences no change at pD > 10.5 might be due to the combined effects of ionization and binding cancelling each other out. The chemical shift data for the cadmium, lead and mercury systems provide no evidence for peptide proton ionization.

Perrin and Watt (22), from pH titration data, suggested that ionization of the peptide protons of glutathione can occur upon complex formation with both zinc and cadmium and that the metal-peptide bond interaction is slightly greater in the zinc system. However, the pK_A of 9.86 which they interpreted as corresponding to ionization of a peptide proton from a coordinated peptide group in the ZnL_2^{4-} complex, is approximately two orders of magnitude too low to be consistent with the present chemical shift data. Martin and Edsall (21) found that their pH titration data for zinc-glutathione did not necessitate the postulation of the ionization of peptide protons; however their experiments were carried out at $pH < 8$. These same workers have suggested that zinc ion does promote peptide ionization in the zinc-glycylhistidine complex (13).

Mercury and Lead Binding to the Sulfhydryl Group

The binding of mercury and lead to glutathione is somewhat different from that of zinc and cadmium; neither mercury nor lead binds to the glutamyl end at $pD > 3$ for metal to peptide ratios of 0.5. Mercury binds exclusively to the sulfhydryl group at ratios up to 0.5 over the pD range 0.5 to 12, resulting in 1:2

complexes with the protonation state of the carboxyl and amino groups dependent on the solution pD. No binding to any of the other potential coordination sites is indicated by the chemical shift data. This is in agreement with the results of Stricks and Kolthoff (24) who found that in the complex HgL_2 , where L represents glutathione in any of its protonation states, mercury is firmly bound to glutathione as a mercaptide. Since mercury and CH_3Hg^+ (25,39) bind to the sulfhydryl group with such a high degree of specificity and since such binding results in large chemical shift changes in the Cys- C_α and $-\text{C}_\beta$ resonances, it may be possible to identify these two resonances in the cmr spectra of proteins by observing changes in the spectrum as the protein is titrated with mercury or CH_3Hg^+ at constant pH.

The binding of lead to the sulfhydryl group of glutathione is not as strong as that of mercury, as evidenced by the decrease in the extent of binding at $\text{pD} < 7$ and by the fact that no binding to the sulfhydryl group is observed at $\text{pD} < 2.3$ for the lead-glutathione system. The chemical shift data for the Cys-CONH carbon indicate that lead might be simultaneously bound to the sulfhydryl group and to the oxygen of the peptide linkage between the cysteinyl and

glycyl residues. The chemical shift data also indicate that the glutamyl amino group is not a binding site for a lead to glutathione ratio of 0.5 over the accessible pD range.

Chemical Shift Differences

Addition of metal ions to a solution of glutathione causes the chemical shifts of selected carbons close to the binding site to change. Results of quantitative measurements of the magnitudes of the differences between the chemical shifts of selected carbon atoms, when a given functional group is complexed and when the group is not complexed, are given in Table XVIII. The magnitudes of these chemical shift differences are denoted by Δ .

In the determination of the Δ values for the cysteinyl carbon resonances, the chemical shifts when the sulfhydryl group is complexed were obtained from the chemical shift vs. pD curves for the metal complex solutions at pD 7. The chemical shifts when the sulfhydryl group is not complexed were obtained from the chemical shift vs. pD curves for glutathione solutions at pD 7, where the sulfhydryl group is protonated. The order of decreasing Δ values for the Cys-C $_{\beta}$ carbon is $\text{Hg}^{2+} > \text{Pb}^{2+} > \text{Cd}^{2+} > \text{Zn}^{2+}$, in agree-

Table XVIII

^{13}C Chemical Shift Changes for Selected Carbon
Resonances of Glutathione upon Complexation

CARBON	Δ (ppm)			
	Zn^{2+}	Cd^{2+}	Pb^{2+}	Hg^{2+}
Cys- C_β	3.1	3.3	3.5	4.4
Cys- C_α	1.0	1.5	1.6	1.0
Cys-CONH	0.5	0.5	0.8	0.2
Glu-COOH	6.0	3.9	a	a
Glu- C_β	2.6	1.8	a	a
Gly- C_α	0.1	0.2	0.3	b

(a) No coordination of Hg^{2+} or Pb^{2+} to the glutamyl amino group was detected.

(b) No coordination of Hg^{2+} to the glycyl carboxyl group was detected.

ment with the order of decreasing affinity of the sulfhydryl group of bovine serum albumin for these metal ions (40). The data in Table XVIII also illustrate that the Δ values decrease as the number of bonds separating the carbon atom from the sulfhydryl group increases. The much greater decrease for the Cys-C $_{\alpha}$ and Cys-CONH carbons in the mercury system is consistent with no binding of this metal ion to the oxygen of the peptide linkage between the cysteinyl and glycyl residues.

The Δ values for the Glu-COOH and Glu-C $_{\beta}$ carbon resonances are presented in Table XVIII for the cadmium and zinc systems; no glutamyl amino coordination by mercury or lead was detected by the chemical shift data. The chemical shifts for the glutamyl complexed species were obtained from the points where the solid and dashed curves intersect in Figures 17 and 20 (31), whereas the corresponding values for noncomplexed glutamyl species were obtained from the chemical shift vs. pD curves for glutathione at pD 7 where the amino group is protonated and the glutamyl carboxyl group is ionized. It can be seen from Table XVIII that the values are larger for zinc than for cadmium, in agreement with the relative order of stabilities of the corresponding glutamic acid complexes of these metal

ions (41). It is also evident that binding at the glutamyl end of glutathione affects the chemical shift of the Glu-COOH carbon more than that of the Glu-C_β carbon, which in turn experiences a larger effect than the Glu-C_α carbon. The order of these chemical shift effects is similar to that observed on protonation of the amino group in amino acids and peptides (27).

The Δ values for the Gly-C_α carbon listed in Table XVIII were obtained from the differences between the solid and dashed curves at pD 7 in Figures 17, 20, and 22, and reflect the extent of binding of the glycyl carboxyl group of glutathione by these metal ions. It can be seen that the order of decreasing Δ values is $\text{Pb}^{2+} > \text{Cd}^{2+} > \text{Zn}^{2+}$, the same as the relative order of the formation constants of the complexes of these metal ions with acetylglycine and the carboxyl group of polyglycine peptides (15,31). These carboxyl interactions are very weak as evidenced by the small Δ values, which are all less than 0.3 ppm. Binding of zinc to the carboxyl groups of glutathione has not been previously detected in pH titration experiments (19-22), presumably because the formation constants are so small.

Conclusions

^{13}C chemical shift data indicate that the metal ions zinc, cadmium, lead and mercury bind to the potential coordination sites of glutathione with a high degree of specificity. All four metal ions bind to the sulfhydryl group while only zinc and cadmium bind to the glutamyl amino group under the conditions used in this work. These results demonstrate the potential of cmr as a technique for elucidating the binding of metal ions by peptides. The technique should also be applicable to similar studies for other multidentate biological molecules.

CHAPTER VII

EXPERIMENTAL

A. CHEMICALS AND SOLUTIONS

Reduced glutathione (Nutritional Biochemicals Corp. and Terochem Laboratories) was washed with a water-ethanol solution and dried at 110° before using. Reagent grade metal nitrate salts were used as received.

The solutions were prepared in D_2O or triply distilled water under an atmosphere of nitrogen to minimize oxidation of the sulfhydryl group of glutathione. For the chemical shift vs. pD measurements, the pD of D_2O solutions, 0.30 M in glutathione and 0.15 M in metal nitrate, was adjusted with a 40% KOD solution and concentrated nitric acid and samples of about 2 ml each were withdrawn at the appropriate pD values. 1,4-dioxane was added to the solutions as an internal reference at a concentration of about 0.1 M. For making chemical shift vs. mole ratio measurements at constant pH, the requisite amount of metal nitrate was added to an H_2O solution of glutathione, the pH adjusted and a sample withdrawn. More metal nitrate was added to the solution and the same procedure followed for all samples at this pH.

B. POTENTIOMETRIC AND CMR MEASUREMENTS

All pH and pD measurements were carried out as described in Chapter IV.

The ^{13}C spectra were obtained using a Bruker HFX-90 spectrometer operating at a frequency of 22.63 MHz and equipped with a Nicolet 1085 computer. The Fourier transform mode was used with proton decoupling. When D_2O was the solvent, the deuterium resonance from the D_2O was used for the heteronuclear lock signal. When H_2O was the solvent, the ^{19}F resonance from hexafluorobenzene in a coaxial capillary was used for the lock. For each free induction decay signal, 8K data points were collected in the computer and 4K accumulations were carried out to achieve an adequate signal-to-noise ratio. The frequency range of the transformed spectra was 5000 Hz. Chemical shifts are reported in ppm relative to the resonance of internal 1,4-dioxane which is 67.4 ppm downfield from the TMS resonance. Positive chemical shifts correspond to greater shielding than in 1,4-dioxane. The chemical shift measurements are considered accurate to within 0.1 ppm. For all measurements the sample temperature was $32 \pm 2^\circ$.

BIBLIOGRAPHY

1. R. J. P. Williams, Roy. Inst. Chem. Rev., 1, 13 (1968).
2. B. L. Vallee and R. J. P. Williams, Chem. in Britain, 4, 397 (1968).
3. A. E. Dennard and R. J. P. Williams, Transition Metal Chem., 2, 115 (1967).
4. H. Sigel and D. B. McCormick, Accounts Chem. Res., 3, 201 (1970).
5. H. C. Freeman, Adv. Protein Chem., 22, 257 (1967).
6. C. B. Monk, Trans. Faraday Soc., 47, 285, 292, 297 (1951).
7. W. P. Evans and C. B. Monk, ibid., 51, 1244 (1955).
8. N. C. Li and M. C. M. Chen, J. Amer. Chem. Soc., 80, 5678 (1958).
9. H. Dobbie and W. O. Kermack, Biochem. J., 59, 246, 257 (1955).
10. R. B. Martin, M. Chamberlin and J. T. Edsall, J. Amer. Chem. Soc., 82, 495 (1960).
11. M. K. Kim and A. E. Martell, ibid., 88, 914 (1966).
12. M. K. Kim and A. E. Martell, ibid., 89, 5138 (1967)
13. R. B. Martin and J. T. Edsall, ibid., 82, 1107 (1960).
14. G. R. Lenz and A. E. Martell, Biochem., 3, 750 (1964).
15. D. L. Rabenstein and S. Libich, Inorg. Chem., 11, 2960 (1972).
16. M. K. Kim and A. E. Martell, J. Amer. Chem. Soc., 91, 872 (1969).
17. R. Mathur and R. B. Martin, J. Phys. Chem., 69, 668 (1965).
18. G. K. Pagenkopf and D. W. Margerum, J. Amer. Chem. Soc., 90, 6963 (1968).

19. N. C. Li, O. Gawron and G. Bascuas, ibid., 76, 225 (1954).
20. N. C. Li and R. A. Manning, ibid., 77, 5225 (1955).
21. R. B. Martin and J. T. Edsall, ibid., 81, 4044 (1959).
22. D. D. Perrin and A. E. Watt, Biochem. Biophys. Acta, 230, 96 (1971).
23. B. J. Fuhr and D. L. Rabenstein, J. Amer. Chem. Soc., in press.
24. W. Stricks and I. M. Kolthoff, ibid., 75, 5673 (1953).
25. D. L. Rabenstein, ibid., 95, 2797 (1973).
26. R. B. Martin and J. T. Edsall, Bull. Soc. Chim. Biol., 40, 1763 (1958)
27. M. Christl and J. D. Roberts, J. Amer. Chem. Soc., 94, 4565 (1972).
28. W. J. Horsley and H. Sternlicht, ibid., 90, 3738 (1968).
29. G. Jung, E. Breitmaier, W. Voelter, T. Keller, and C. Tanzer, Angew. Chem. Internat. Edit., 9, 894 (1970).
30. G. Jung, E. Breitmaier and W. Voelter, Eur. J. Biochem., 24, 438 (1972).
31. D. L. Rabenstein, Can. J. Chem., 50, 1036 (1972).
32. A. Berger, A. Loewenstein and S. Meiboom, J. Amer. Chem. Soc., 81, 62 (1959).
33. P. J. Morris and R. B. Martin, Inorg. Chem., 10, 964 (1971).
34. J. D. Bell, H. C. Freeman, A. M. Wood, R. Driver, and W. R. Walker, Chem. Comm., 1441 (1959).
35. A. E. Martell and M. Calvin, "Chemistry of the Metal Chelate Compounds," Prentice Hall, New York, 1952, p. 134.

36. W. L. Koltun, M. Fried and F. R. N. Gurd, J. Amer. Chem. Soc., 82, 233 (1960).
37. E. W. Wilson, Jr. and R. B. Martin, Inorg. Chem., 9, 528 (1970).
38. M. Ihnat and R. Bersohm, Biochem., 9, 4555 (1970).
39. D. L. Rabenstein and M. T. Fairhurst, unpublished results.
40. I. M. Klotz, J. M. Urquhart and H. A. Friess, J. Amer. Chem. Soc., 74, 5537 (1952).
41. L. G. Sillen and A. E. Martell, "Stability Constants of Metal Ion Complexes," Special Publication No. 17, The Chemical Society, London, 1964.

B30087